INTRACELLULAR TRAFFICKING OF INFLUENZA HEMAGGLUTININ AND MEMBERS OF THE LOW DENSITY LIPOPROTEIN RECEPTOR FAMILY

APPROVED BY SUPERVISORY COMMITTEE

Mark Lehrman, Ph.D.

Richard Anderson, Ph.D.

Helmut Kramer, Ph.D.

Michael Roth, Ph.D.

DEDICATION

Dedicated to my husband, Greg, my parents, Lucille and Carmine,
my sister, Jennifer, my brother, Paul, and my grandfather, Vincent Esposito.

INTRACELLULAR TRAFFICKING OF INFLUENZA HEMAGGLUTININ AND MEMBERS OF THE LOW DENSITY LIPOPROTEIN RECEPTOR FAMILY

by

RENEE DANIELLE TALL

DISSERTATION

Presented to the Faculty of the Graduate School of Biomedical Sciences

The University of Texas Southwestern Medical Center at Dallas

In Partial Fulfillment of the Requirements

For the Degree of

DOCTOR OF PHILOSOPHY

The University of Texas Southwestern Medical Center at Dallas

Dallas, Texas

November, 2004

ACKNOWLEDGEMENTS

I would like to thank my mentor, Dr. Michael Roth, for providing an environment of countless scientific discussions where ideas are limitless. His breadth of knowledge of the literature has been extremely helpful to my research. My committee members, Dr. Mark Lehrman, Dr. Helmut Kramer, and Dr. Richard Anderson have been very helpful with their suggestions.

Dr. David Padron-Perez has been unimaginably helpful to me with his time and advice. Maria Kosfiszer has provided the lab with excellent technical assistance and a positive attitude.

My parents, Lucille and Carmine Esposito, taught me to believe in myself. I am grateful for all of the love and support they have given and continue to provide me. I thank my sister, Jennifer, my brother, Paul, my grandparents, Victoria, Valentino, Emily and Vincent for their love.

I am especially grateful to my husband, Dr. Gregory Tall, for his unending love and advice throughout my graduate school experience. Greg's parents, Mary and Gordon Tall, have been a great addition to my life.

INTRACELLULAR TRAFFICKING OF INFLUENZA HEMAGGLUTININ AND LOW DENSITY LIPOPROTEIN RECEPTOR FAMILY MEMBERS

Publication No._____

Renee Danielle Tall, Ph.D.

The University of Texas Southwestern Medical Center at Dallas, 2004

Supervising Professor: Michael Roth, Ph.D. Professor, Department of Biochemistry; Associate Dean of Graduate School

Polarized epithelial cells usually line body cavities, providing a barrier between two dissimilar environments. Distinct apical and basolateral membrane surfaces are maintained by sorting proteins in the biosynthetic and endocytic pathways. Influenza hemagglutinin is sorted to the apical membrane in polarized epithelial cells by a mechanism mediated by an association with lipid microdomains known as lipid rafts. Lipid rafts and their associated proteins are operationally defined by their resistance to detergent solubilization at cold temperatures. By systematic mutagenesis of the transmembrane domain of hemagglutinin, I show that ten consecutive amino acids are required to confer resistance to detergent

extraction. Although some of the hemagglutinin transmembrane mutants were sorted apically without incorporation into detergent-resistant membranes, I determined that these mutants were transiently associated with lipid rafts. A small fraction of hemagglutinin co-precipitates with MAL/VIP17, a protein required for apical transport. The hemagglutinin and MAL that co-precipitated were contained in a detergent-resistant vesicle in an orientation consistent with a transport intermediate, suggesting that MAL might sort hemagglutinin into apical vesicles in the Golgi. However, the time course of the association of hemagglutinin and MAL in the biosynthetic pathway indicate that the two proteins do not associate until the majority of the HA reached the cell surface. Both the timing and limited extent of co-precipitation suggest that MAL may not sort hemagglutinin into apical vesicles in the biosynthetic pathway.

Megalin, a member of the low density lipoprotein family of receptors, is sorted apically in polarized epithelial cells via a sorting signal present in its cytosolic domain. I show that the cytosolic domain of megalin associates with sorting nexin 17, a protein that interacts with all core members of the low density lipoprotein receptor family. Although sorting nexin 17 may not sort megalin apically in the biosynthetic pathway, I show that overexpression of sorting nexin 17 increases the rate of low density lipoprotein receptor recycling to the plasma membrane. The increase in recycling does not affect the expression of low density lipoprotein receptor at the cell surface, suggesting that sorting nexin 17 decreases the cycling time of the receptor.

TABLE OF CONTENTS

Acknowledgements iii
Abstract v
Prior Publications ix
List of Figures x
List of Abbreviations xi

CHAPTER ONE: Introduction and Literature Review 15
Cells Sort Proteins to Establish and Maintain Spatial Asymmetry 15
Basolateral Sorting Signals 19
Apical Sorting 23
Lipid Sorting and Membrane Asymmetry in Polarized Epithelial Cells 23
Lipid Rafts and Caveolae 27
Detergent Resistance Operationally Defines Lipid Rafts 30
The Transmembrane Domain of Influenza Hemagglutinin Contains an Apical Sorting Signal 32
Myelin and Lymphocyte Protein Is Required for Apical Trafficking of HA 35
The Apical Sorting Signal for Megalin is Located in its Cytosolic Domain 38
NPXY in the Cytoplasmic Domains of LDLR Family Members Interacts with Clathrin-Associated Internalization Machinery 41
Several LDLR Family Members are Recycled in the Endocytic Pathway 45
Sorting Nexins Regulate Multiple Aspects of the Endocytic Recycling Pathway 50

CHAPTER TWO: Materials and Methods 57
Cell Culture 57
Antibodies 57
Materials 58
Adenovirus Construction 58
Site-directed Mutagenesis of the Transmembrane Domain of HA 59
Sorting Assay 60
Detergent Insolubility Assay 62
Fluorescence Recovery After Photobleaching 64
Flotation and MAL and HA Co-immunoprecipitation Experiments 64
Co-immunoprecipitation of HA and MAL After Endocytosis from the Plasma Membrane 67
Sorting Nexin 17 Cloning 67
Yeast Two-Hybrid Bait Constructs 68
Yeast Two Hybrid Screen 69
Megalin Co-immunoprecipitation Experiments 70
Indirect Immunofluorescence 71
Recycling Assay 72
LDLR Degradation Assay 73
Short Interfering RNA Transfection and Quantitative PCR 74

Cell Surface Protein Measurement 76
Transferrin Internalization Assay 77

CHAPTER THREE: Features Required for Hemagglutinin Sorting are Different from those Required for Interaction with MAL 78
INTRODUCTION 78
RESULTS 81
Mutagenesis of the HA Transmembrane Domain 81
Ten Consecutive Amino Acids in the Transmembrane Domain of HA are Required for HA to be Isolated in DRMs 85
HA Requires at Least 11 Wild-Type Amino Acids in the Transmembrane Domain to be Sorted to the Apical Surface 90
FRAP in Conjunction with Raft Immobilization Detects Transient Associations with Lipid Rafts 93
Overexpression of MAL Does not Improve HA DRM Association 97
HA Associated with MAL Is Enclosed in Intact Vesicles 98
The Vesicles That Contain HA and MAL Do Not Have Characteristics of Golgi-derived Transport Intermediates 104
Association of HA and MAL is Undetectable in Plasma Membrane Derived Vesicles 106

CHAPTER FOUR: Sorting Nexin 17 Regulates Intracellular Trafficking of Low Density Lipoprotein Family Members 108
INTRODUCTION 108
RESULTS 110
A Yeast Two Hybrid Screen with the Cytoplasmic Tail of Megalin Identifies Several Novel Interactions 110
Megalin Associates with SNX17 and GIPC 115
SNX17 Localizes to Sorting Endosomes 119
Overexpression of SNX17 Increases the Recycling Rate of LDLR 121
SNX17 Affects LDLR Protein Expression 127
SNX17 does not Affect LDLR Cell Surface Expression 132
Transferrin Receptor Recycling and Internalization is Unaffected by SNX17 Overexpression 134

CHAPTER FIVE: Discussion 136
Eleven Amino Acids in the Transmembrane Domain of HA are Required for Apical Sorting and DRM Association 136
MAL and HA do not Associate in Apical Vesicles Derived from the TGN 138
The First NPXY Sequence in the Cytoplasmic Domain of Megalin is Required for an Association with Sorting Nexin 17 143

Bibliography 150
Vitae 178

PRIOR PUBLICATIONS

Tall, R.D. and M.G. Roth. 2004. Sorting Nexin 17 Regulates Intracellular Trafficking of Low Density Lipoprotein Receptor Family Members. *In Preparation*.

Tall, R.D., M.A. Alonso, and M.G. Roth. 2003. Features of influenza HA required for apical sorting differ from those required for association with DRMs or MAL. *Traffic*. 4:838-849.

Shvartsman, D.E., M. Kotler, **R.D. Tall**, M.G. Roth, and Y.I. Henis. 2003. Differently anchored influenza hemagglutinin mutants display distinct interaction dynamics with mutual rafts. *Journal of Cell Biology*. 163:879-888.

Stewart, M.Q., **R.D. Esposito**, J. Gowani, and J.M. Goodman. 2001. Alcohol oxidase and dihydroxyacetone synthase, the abundant peroxisomal proteins of methylotrophic yeasts, assemble in different cellular compartments. *Journal of Cell Science*. 114(Pt 15):2863-2868.

ABSTRACT

Tall, R.D. and M.G. Roth. 2002. Apical Sorting Determinants of Influenza Hemagglutinin. *Molecular Biology of the Cell*. 13(Supplement):90a.

LIST OF FIGURES

Figure 1. Protein Sorting in Polarized Epithelial Cells 17

Figure 2. The cytoplasmic domains of megalin and LRP share similar sequence motifs ... 40

Figure 3. Endocytic recycling 46

Figure 4. Amino acid sequences of the TM segments of HAs from 15 serotypes 82

Figure 5. TM sequences of HA mutants in which wild type amino acids are systematically replaced into the background of TM 4.0 83

Figure 6. Conserved amino acids that would reside in the exoplasmic leaflet of the bilayer are located on the external and internal surfaces of the HA trimer 84

Figure 7. HA transmembrane mutants are transported to the plasma membrane 85

Figure 8. Ten consecutive amino acids in the transmembrane domain of HA are required to confer a detergent-resistant phenotype 86

Figure 9. HA expression does not affect the percentage of protein associated with DRMs 87

Figure 10. DRM association occurs prior to localization at the plasma membrane 88

Figure 11. Ten consecutive amino acids in the transmembrane domain of HA are required for flotation on a density gradient 89

Figure 12. Most of the amino acids of HA that would reside in the outer leaflet are required to target HA to the apical membrane 91

Figure 13. Several non-ionic detergents used to infer lipid raft incorporation have markedly different effects on the solubility of HA 93

Figure 14. Cholesterol depletion increases the rate of lateral diffusion of HA mutants that partition into DRMs 94

Figure 15. Cross-linking and FRAP demonstrates a transient association with lipid rafts.. 96

Figure 16. Overexpression of MAL does not improve wild-type HA or HA TM 11.0 flotation on density gradients 98

Figure 17. Co-precipitation of HA and MAL is not reciprocal 100

Figure 18. MAL-associated HA is enclosed in intact vesicles 102

Figure 19. HA co-precipitates with myc-MAL only after an interval when most of the HA has reached the plasma membrane 105

Figure 20. Association of HA and MAL subsequent to internalization from the plasma membrane is undetectable 106

Figure 21. Megalin bait fusion constructs are expressed in L40 yeast 111

Figure 22. The tail of megalin interacts with signaling and scaffolding proteins 112

Figure 23. Megalin co-precipitates with SNX17 and GIPC..... 116

Figure 24. Tyrosine$_{80}$ of the cytoplasmic tail of megalin is required for interaction with SNX17 in the yeast two-hybrid system 118

Figure 25. SNX17 Co-localizes with sorting endosomes 120

Figure 26. SNX17 overexpression increases the rate of LDLR release from endosomes. 122

Figure 27. Overexpression of SNX17 in the presence of leupeptin increases the rate of LDLR recycling to the plasma membrane 123

Figure 28. LDLR matures slightly faster in cells overexpressing SNX17..... 124

Figure 29. The rate of LDLR degradation at early time points is not significantly affected by SNX17 overexpression 126

Figure 30. SNX17 overexpression causes a reduction in LDLR protein expression 128

Figure 31. SNX17 overexpression causes LDLR targeting to the lysosome 129

Figure 32. Targeted reduction of SNX17 increases LDLR expression 131

Figure 33. SNX17 overexpression does not affect LDLR cell surface expression 123

Figure 34. Transferrin receptor recycling is unaffected by SNX17 overepression 134

Figure 35. Transferrin internalization is not affected by SNX17 overexpression..... 135

Figure 36. Proposed mechanism of MAL effect on apical sorting..... 142

Figure 37. Proposed model for regulation of LDLR trafficking by SNX17 147

LIST OF ABBREVIATIONS

A□PP	Amyloid Beta Precursor Protein
AP	Adaptor Protein
ARH	Autosomal Recessive Hypercholesterolemia
BAR	Bin/Amphiphysin/Rvs
BSA	Bovine Serum Albumin
CAPON	Carboxy terminal PDZ domain ligand of neuronal Nitric Oxide synthase
Dab2	Disabled-2
DMEM	Dulbecco's Modified Eagle's Media
DNA	Deoxyribonucleic Acid
DRM	Detergent Resistant Membrane
EB-1	E2a-Pbx1-associated protein
EGF	Epidermal Growth Factor
EGFR	Epidermal Growth Factor Receptor
ER	Endoplasmic Reticulum
ERC	Endocytic Recycling Compartment
FACS	Fluorescence Activated Cell Sorting
FERM	protein 4.1/Ezrin/Radixin/Moesin
FBS	Fetal Bovine Serum
FRAP	Fluorescence Recovery After Photobleaching
GalCer	Galactosylceramide

GIPC	G alpha interacting protein (GAIP) Interacting Protein Carboxy terminus
GlcCer	Glucosylceramide
GPI	Glycosyl-phosphatidylinositol
HA	Hemagglutinin
IB	Immunoblot
kDa	kilo Dalton
LDLR	Low Density Lipoprotein Receptor
LRP	Low Density Lipoprotein Receptor Related Protein
l_o	liquid-ordered
MAL	Myelin and Lymphocyte protein
MAGI-2	Membrane-Associated Guanylate Kinase 2
MDCK	Madin Darby Canine Kidney
MIN	Minute
MPR	Mannose-6 Phosphate Receptor
MVE	Multi-vesicular Endosome
PC	Phosphatidylcholine
PCR	Polymerase Chain Reaction
PDZ	Postsynaptic density 95/*Drosophila* discs-large/Zona occludens 1
PE	Phosphatidylethanolamine
PFU	Plaque-forming unit
PLAP	Placental Alkaline Phosphatase
PS	Phosphatidylserine

PSD-95	Postsynaptic Density 95
PTB	Phosphotyrosine-binding
PX	phagocyte oxidase homology
RNA	Ribonucleic Acid
S-SCAM	Synaptic Scaffolding Molecule
SAP102	Synapse-Associated Protein 102
SDS-PAGE	Sodium Dodecyl Sulfate Polyacrylamide Gel Electrophoresis
SEM	Standard Error of the Mean
SEMCAP-1	semaF Cytoplasmic Domain Associated Protein 1
SH3	src homology 3
siRNA	short interfering Ribonucleic Acid
SM	Sphingomyelin
SMS1	Sphingomyelin Synthase 1
SNX	Sorting Nexin
Tac	Interleukin 2 Receptor, alpha subunit
TfR	Transferrin Receptor
TGN	*trans* Golgi Network
T_m	Melting Temperature
TM	Transmembrane
TX-100	Triton X-100
VPS	Vacuolar Protein Sorting
VSVG	Vesicular Stomatis Virus G protein

CHAPTER ONE

INTRODUCTION AND LITERATURE REVIEW

Cells Sort Proteins to Establish and Maintain Spatial Asymmetry

A substantial number of proteins and lipids are transported through the endocytic and secretory pathways. The speed and volume at which these molecules are trafficked requires tight regulation to maintain unique protein and lipid compositions in the plasma membrane and other membranous organelles. All eukaryotic cells exhibit some degree of spatial asymmetry. Hippocampal neurons differentially traffick proteins to the axon and dendritic surfaces of the plasma membrane, which allows the cell to engage in directional neurotransmission signaling (Mattson, 1999). Retinal pigmented epithelial cells deliver specific proteins to the apical plasma membrane in order to exchange signaling molecules with adjacent rod photoreceptor cells (Nicolaissen et al., 1982). Polarized epithelial cells form a monolayer that lines the body cavities and acts as a barrier between two dissimilar environments. For polarized epithelial cells to function as barrier cells, it is of extreme importance to establish and maintain a unique protein and lipid composition at the apical and basolateral membrane surfaces. The distinct apical and basolateral membranes are separated by zonula occludens (tight junctions) that prevent protein and lipid diffusion across the monolayer (Diamond, 1977; van Meer and Simons, 1986). The apical membrane faces the lumen of the cavity, while the basolateral surface is adjacent to the extracellular matrix and blood supply (Rodriguez-Boulan, 1983). Polarized epithelial cells, mainly Madin Darby canine kidney (MDCK) cells, are the most widely used model system to examine sorting

because proteins and lipids delivered to the apical or basolateral membrane can be independently examined. In culture, MDCK cells, which resemble cells in the distal tubule region of the kidney, reproducibly exhibit the same characteristics as polarized epithelial cells *in vivo* (Herzlinger et al., 1982; Rodriguez-Boulan, 1983).

Lipid and protein sorting in polarized and non-polarized cells can occur in the biosynthetic or endocytic pathways. In the biosynthetic pathway, exocytic proteins are translocated into the endoplasmic reticulum (ER), where they are folded and glycosylated, prior to transport to the Golgi network in COPII-coated vesicles (reviewed in (Kirchhausen, 2000; Swanton and Bulleid, 2003)). The proteins are trafficked through multiple cisternae of the Golgi, where glycosylated proteins receive additional oligosaccharide modifications, *en route* to the *trans* Golgi network (TGN) (Palade, 1975). In the TGN, proteins and lipids are sorted into vesicles that are destined for the plasma membrane, lysosome, or other endocytic compartments (Griffiths and Simons, 1986).

For MDCK cells, there is considerable data indicating that many apical and basolateral proteins are transported directly in the biosynthetic pathway to the appropriate membrane in separate vesicles (Figure 1) (Keller et al., 2001; Wandinger-Ness et al., 1990). Some proteins, including polyimmunoglobulin receptor (pIgR) (Figure 1) and possibly some glycosyl-phosphatidylinositol (GPI)-anchored proteins, are transported directly from the TGN to the basolateral membrane prior to transcytosis to the apical membrane (Mostov and Deitcher, 1986; Polishchuk et al., 2004). There is also evidence that some glycosylated proteins can transcytose from the apical to the basolateral membrane and vice versa (Brandli et al., 1990). In contrast to MDCK cells, which sort most proteins through the biosynthetic

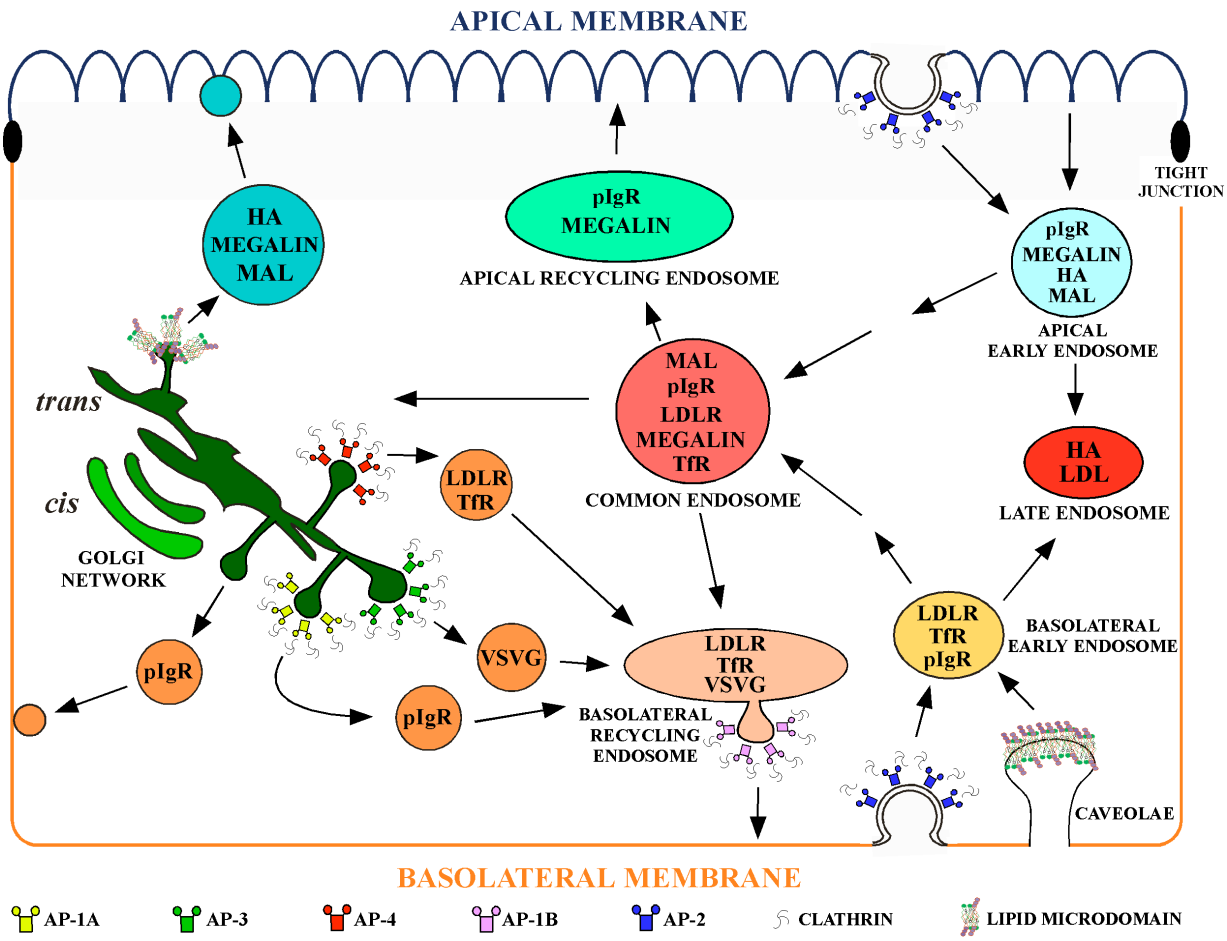

Figure 1. Protein Sorting in Polarized Epithelial Cells. Hemagglutinin (HA), megalin, and myelin and lymphocyte protein (MAL) are transported from the TGN to the apical membrane in vesicles that are distinct from those that transport basolateral proteins. Low density lipoprotein receptor (LDLR), transferrin receptor (TfR), and vesicular stomatitis virus G protein (VSVG) are transported to the basolateral membrane. Polyimmunoglobulin receptor (pIgR) is indirectly sorted to the apical membrane from the basolateral membrane by a transcytotic pathway. The model represents data from several sources as discussed in the text. None of the proteins are sorted to a specific membrane surface with one hundred percent efficiency. The model illustrates the proposed major pathway for each of the membrane proteins.

pathways, polarized hepatocytes sort most proteins through the endocytic pathway (Rodriguez-Boulan and Nelson, 1989). The apical and basolateral pathways in hepatocytes and epithelial cells share common endosomes, where sorting to the specific pathway occurs (Parton et al., 1989). These common endosomes are distinct from apical and basolateral recycling endosomes (Figure 1) (Wang et al., 2000). Because polarized epithelial cells sort proteins biosynthetically and through endocytic recycling, a hierarchy of sorting signals is required. The presence of a basolateral signal usually dominates a weaker apical signal (Bello et al., 2001; Lazarovits and Roth, 1988). An apparent basolateral targeting signal may be recognized by components of the biosynthetic sorting or endocytic machinery. Thus, the subcellular localization of the protein and the structures or sequences surrounding the basolateral or apical targeting signal may affect protein sorting (Lin et al., 1997). Whether a protein is sorted apically or basolaterally may also depend on cell type. Some proteins which are sorted basolaterally in MDCK cells are sorted to the apical surface in polarized Fisher rat thryroid or LLC-PK1 proximal tubule cells (Roush et al., 1998; Zurzolo et al., 1993).

Defects in the cargo or sorting machinery of polarized sorting pathways can lead to disease (reviewed in (Stein et al., 2002). A mutation in low density lipoprotein receptor (LDLR) that causes the protein to be mis-sorted to the apical surface results in defective LDL clearance, which is manifested as familial hypercholersterolemia (Koivisto et al., 2001). Carboxy-terminal deletions or mutations of cystic fibrosis conductance regulator that do not allow this protein to be trafficked to the apical surface result in cystic fibrosis (Moyer et al., 1999).

Basolateral Sorting Signals

Several different basolateral targeting signals have been identified, including PDZ domains and sequences containing NPXY, YXXΦ (where Φ is a bulky hydrophophic amino acid), or di-leucine (Mostov et al., 2000; Rodriguez-Boulan et al., 2004; Shelly et al., 2003)). The two predominant basolateral targeting sequences are located in the cytoplasmic domain of transmembrane proteins and contain characteristic tyrosine or di-leucine motifs (Hunziker and Fumey, 1994; Matter et al., 1992; Thomas and Roth, 1994). Mutation of di-leucine in the cytoplasmic domain of nucleotide pyrophosphatase mis-directs the protein to the apical surface (Bello et al., 2001). Insertion of a tyrosine in the cytoplasmic tail of the apical protein hemagglutinin (HA) mis-sorts HA to the basolateral membrane in MDCK cells (Lazarovits and Roth, 1988; Naim and Roth, 1994). These experiments suggest that the basolateral targeting signal is dominant over a weak apical sorting sequence.

Tyrosine-containing basolateral signals are usually found in a YXXΦ sequence and have been shown to interact directly with clathrin-associated adaptor proteins (Ohno et al., 1995). Adaptor proteins bind directly to clathrin and facilitate vesicle budding from the TGN, plasma membrane, or other organelles in the endocytic pathway. Adaptor protein 1 (AP-1) is a complex comprised of two large subunits (γ1 and β), a medium subunit (μ1 or μ1B), and a small subunit (σ1) (reviewed in (Robinson and Bonifacino, 2001). Basolateral targeting of tyrosine signals is primarily regulated by the μ1B subunit of the clathrin adaptor protein 1B (AP-1B). Polarized porcine proximal tubule epithelial cells (LLC-PK1) lack endogenous μ1B and mis-sort LDLR to the apical surface (Folsch et al., 1999). Stable transfection of μ1B in LLC-PK1 cells corrects LDLR sorting to the basolateral surface,

suggesting that μ1B recognizes the basolateral sorting signal in LDLR and targets the receptor to the basolateral plasma membrane (Folsch et al., 1999). AP-1B was originally thought to actively sort tyrosine-containing basolateral proteins at the TGN. However, polarized cells that do not express endogenous AP-1B can sort basolateral proteins to the correct membrane. In addition, AP-1B co-localizes with endosome-specific markers, while the closely-related AP-1A co-localizes with Golgi markers (Folsch et al., 2003; Gan et al., 2002). An internalization-defective LDLR mutant is expressed at the basolateral membrane in LLC-PK1 cells (Gan et al., 2002), suggesting that μ1B may sort tyrosine-containing basolateral proteins from the recycling or common/sorting endosome subsequent to endocytosis, as depicted in Figure 1. AP-4 co-localizes with TGN markers and has been shown to bind to peptides containing the basolateral targeting sequences found in LDLR and transferrin receptor (TfR) (Simmen et al., 2002). It is possible that LDLR and TfR could be sorted into AP-4 vesicles at the TGN and trafficked directly to the basolateral surface or to a basolateral recycling endosome (Figure 1). AP-1B may act to retain recycled LDLR and TfR at the basolateral membrane. Endosomal and lysosomal targeting information is also contained in the YXXΦ sequence, suggesting that the position of the signal within the cytoplasmic domain and the intracellular location of the protein may determine how the protein is sorted (Bonifacino and Traub, 2003).

The delta subunit of AP-3 interacts with YXXΦ in the cytoplasmic tail of VSVG (Le Borgne and Hoflack, 1998). VSVG transport from the TGN to the plasma membrane is reduced in mouse fibroblasts lacking δ3-adaptin (Le Borgne and Hoflack, 1998), suggesting that VSVG could sort into AP-3 vesicles at the TGN (Figure 1). However, VSVG is not

found in typical clusters in the TGN of fibroblasts, which are indicative of association with clathrin-coated vesicles, and does not co-localize with β3-adaptin, as observed by electron microscopy (Polishchuk et al., 2003). Additional information is required to determine if AP-3 is involved in basolaterally sorting VSVG in polarized epithelial cells. Expression of a dominant-negative mutant of the rho-family GTPase Cdc42 inhibits basolateral delivery of VSVG in MDCK cells, suggesting that Cdc42 may also have a direct or indirect effect on basolateral targeting (Kroschewski et al., 1999).

pIgR is sorted to the basolateral membrane prior to transcytosis to the apical surface in polarized epithelial cells (Mostov and Deitcher, 1986) (Figure 1). The receptor binds to its ligand, IgA, on the basolateral surface, where it is endocytosed and trafficked to a common endosome, followed by trafficking to the apical recycling endosome on its way to the apical membrane (Apodaca et al., 1994). Once pIgR reaches the apical membrane, IgA is released and the ligand-binding domain of pIgR cleaved (Figure 1) (Musil and Baenziger, 1987). pIgR is internalized from the apical membrane by a pathway dependent on clathrin and ADP ribosylation factor 6 (Arf6) (Altschuler et al., 1999). Deletion of the cytoplasmic domain of pIgR results in direct delivery of the protein to the apical surface (Mostov et al., 1986). Although pIgR does not have a YXXΦ or di-leucine sequence in its cytoplasmic domain, it has a crucial type I β-turn, which is structurally similar to tyrosine-containing sequences (Aroeti et al., 1993). A serine residue in this type I β-turn of pIgR is required for interaction with the gamma subunit of AP-1 (Orzech et al., 1999). While mutation of the critical serine does not prevent basolateral transport, kinetics of basolateral targeting is retarded significantly (Orzech et al., 1999). This suggests that pIgR may be sorted basolaterally

through more than one mechanism (Figure 1). pIgR may be sorted in AP-1 vesicles from the TGN to a recycling endosome, where it is transported to the basolateral surface. Alternatively, pIgR could be sorted directly to the basolateral membrane in a pathway independent of AP-1.

Similar to YXXΦ, di-leucine signals are also recognized by machinery involved in basolateral, lysosomal, and endosomal sorting (Bonifacino and Traub, 2003). The specificity of the amino acid sequence or structure flanking a di-leucine signal may dictate whether the protein is recognized by the basolateral or endocytic sorting machinery. For instance, if the amino acids surrounding the di-leucine in nucleotide pyrophosphatase are removed, the protein is sorted apically, but endocytosed efficiently (Bello et al., 2001). The di-leucine signal is found in two distinct sequences, [DE]XXXXL[LI] and DXXLL, which are recognized by clathrin adaptor proteins and ADP-ribosylation factor-dependent clathrin adaptors (GGAs), respectively (Bonifacino and Traub, 2003; Puertollano et al., 2001b; Rapoport et al., 1998). The [DE]XXXXL[LI] sequence has been shown to interact with both AP-3 and the beta subunit of AP-1 (Honing et al., 1998; Rapoport et al., 1998). It is possible that basolateral proteins containing di-leucine are sorted from the TGN in AP-1 or AP-3 vesicles, although this has not been studied in polarized epithelial cells. It is also possible that GGAs could be involved in basolateral sorting.

Apical Sorting

There is no known consensus signal for apical sorting. Apical sorting determinants have been identified in the transmembrane domain, GPI anchor, and cytoplasmic domain of

various proteins (Lin et al., 1998; Lisanti et al., 1989; Takeda et al., 2003b). N- and O-linked oligosaccharides have also been suggested to act as apical sorting signals (Rodriguez-Boulan and Gonzalez, 1999). Most proteins are sorted apically through their association with highly ordered lipid microdomains called lipid rafts, that are enriched in glycosphingolipids, sphingomyelin, and cholesterol (Figure 1) (Brown and Rose, 1992; Scheiffele et al., 1997). Lipid rafts, which will be discussed in detail in a later section have been operationally defined as a membrane with resistance to extraction with non-ionic detergents at low temperature (Brown and Rose, 1992). Proteins associated with lipid rafts are resistant to solubilization by non-ionic detergents at low temperature. Although some apical proteins seem to be sorted in the absence of an observable association with detergent-resistant membranes (DRMs), this may be a result of the operational definition of a lipid raft, which will be discussed in detail (Jacob and Naim, 2001; Lisanti et al., 1989).

Lipid Sorting and Membrane Asymmetry in Polarized Epithelial Cells

Sphingolipids are enriched in the exoplasmic leaflet of the apical membrane of polarized epithelial cells, suggesting that lipids, as well as proteins, are apically sorted (Devaux, 1991; Simons and van Meer, 1988; van Meer et al., 1987). Ceramide, the backbone of glycosphingolipids and sphingomyelin (SM), consists of a sphingoid base with a long, predominantly saturated (18-20) carbon chain attached to a similarly long saturated fatty acid acyl chain at its C2 position. In SM, phosphocholine is attached to the ceramide base and for glycosphingolipids, a variety of monosaccharides provide the head groups. Unlike SM and glycosphingolipids, which are enriched in the outer leaflet plasma membrane,

the aminophospholipids phosphatidylethanolamine (PE) and phosphatidylserine (PS) are enriched in the inner leaflet of the plasma membrane (Devaux, 1991). The cytoplasmic leaflet of apical membranes is nearly identical to the inner leaflet of basolateral membranes (Simons and van Meer, 1988), intimating that lipids in the exoplasmic leaflet might influence apical sorting.

Because the sphingoid moiety of ceramide can vary in carbon chain length and degree of unsaturation, and monosaccharides can be added in many different combinations, thousands of unique glycosphingolipids can exist in the cell (Karlsson, 1970). Glycosphingolipids have been classified in two major categories depending on the addition of a glucose (glucosylceramide (GlcCer)) or galactose (galactosylceramide (GalCer)) to the C1 position of the sphingoid base (reviewed in (Degroote et al., 2004)). GalCer is predominantly found in myelin sheath cells and is one of the only sphingolipids synthesized in the ER (Schulte and Stoffel, 1993). In the ER, ceramide is randomly distributed across the two leaflets of the bilayer before it is translocated to the Golgi through a vesicular or non-vesicular pathway (Hanada et al., 2003). GlcCer is synthesized on the cytoplasmic leaflet of the *cis*-Golgi prior to translocation by the lipid translocase multidrug resistance pump to the lumenal leaflet, although the exact mechanism is not understood (Hoekstra et al., 2003). All subsequent sugar additions take place in the lumenal leaflet of the Golgi (reviewed in (Maccioni et al., 1999)).

Unlike GlcCer, which is synthesized in the cytoplasmic leaflet of the *cis*-Golgi, SM is specifically synthesized in the lumenal leaflet of the TGN prior to delivery to the apical surface (Bretscher, 1972; Huitema et al., 2004; Simons and van Meer, 1988). *In vitro*

experiments with a radioactive ceramide analog in the presence of trypsin indicate that SM does not flip-flop to the exoplasmic leaflet subsequent to synthesis in a mechanism similar to that of GlcCer (Futerman et al., 1990). For SM synthesis, ceramide synthesized in the ER is translocated to the TGN primarily by the lipid-transfer protein CERT in a non-vesicular, ATP-dependent pathway (Hanada et al., 2003). It is possible that CERT inserts ceramide directly into the lumenal leaflet of the TGN. Sphingomyelin synthase 1 (SMS1), a protein that co-localizes with the TGN marker sialytransferase, transfers a phosphorylcholine to the primary hydroxyl of ceramide to generate sphingomyelin (SM) (Huitema et al., 2004). SMS1 is predicted to span the membrane six times, with its putative active site located in the exoplasmic leaflet, suggesting that synthesis specifically occurs in the exoplasmic leaflet (Huitema et al., 2004).

Lipids can be transported from the TGN to the plasma membrane by monomeric diffusion or through a vesicular pathway. If transport occurs by monomeric diffusion to a membrane of another organelle, the lipid must be located in the cytosolic leaflet (reviewed in (Holthuis et al., 2001)). SM and GlcCer are predominantly located in the exoplasmic leaflet of the TGN and the plasma membrane. It is possible that scramblases could flip the lipids to the opposite leaflet, although this has only been demonstrated for plasma membrane aminophospholipids (Zhou et al., 1997). Thus, it seems likely that most SM and glycosphingolipids would be transported through a vesicular pathway. If vesicular lipid transport occurred in the absence of sorting, the lipids from the donor membrane would mix with the lipids of the acceptor membrane, causing homogenous lipid distribution in all cellular membranes.

In order to establish and maintain lipid asymmetry, lipids may be sorted by a few possible mechanisms, including direct interaction with a protein carrier, exclusion from entrance into a particular pathway, or retention in a specific organelle. SM is enriched in an increasing gradient from the TGN to the plasma membrane (Huitema et al., 2004) and preferentially excluded from the retrograde COPI-coated vesicles transporting proteins and lipids from the TGN to intra-Golgi cisternae and the ER (Brugger et al., 2000; van Meer, 1998). Cholesterol synthesized in the ER also has an increasing gradient across the secretory pathway, where it is enriched in the plasma membrane (Liscum and Munn, 1999). The association of cholesterol and sphingolipids in the exoplasmic leaflet forms a liquid ordered domain, generating a phase separation from other unsaturated lipids, which creates a lipid raft. The details of this association will be discussed in the next section. Specific enrichment of lipid rafts in the exoplasmic leaflet may dictate the curvature of the membrane. Gerrit van Meer and others have postulated that the liquid ordered domains in the TGN consisting of SM and cholesterol cause thick bilayers that are not conducive to vesicle formation (Holthuis et al., 2001). They suggest that proteins and lipids associated with these lipid rafts are excluded from the basolateral pathway and accumulate in the TGN. Basolateral proteins are specifically removed from the TGN by the mechanisms discussed in an earlier section, and Golgi-resident proteins are incorporated into COPI vesicles which recycle back to the *cis*-Golgi. The remaining proteins associated with lipid rafts would aggregate into a large post-Golgi container that is sorted to the apical membrane.

Several observations support the hypothesis that apical sorting from the TGN requires association with liquid ordered domains. Apical cargo, such as GPI-anchored proteins and

HA, are incorporated into detergent-resistant membranes (DRMs) at the TGN (Brown and Rose, 1992; Skibbens et al., 1989). In addition, proteins with longer transmembrane domains (23 amino acids) have a higher affinity for DRMs and are sorted to the plasma membrane, while proteins with shorter transmembrane domains (17 amino acids) are retained in the Golgi (McIntosh et al., 2003; Munro, 1995). Caveolin-1 mutants that have a reduced affinity for DRMs are also retained in the Golgi (Ren et al., 2004). Proteins with shorter transmembrane domains and caveolin-1 mutants are thought to associate more readily with retrograde vesicles because of their reduced DRM association, causing them to spend more time in the Golgi cisternae. While the sorting by exclusion model is very appealing, it could result in protein mis-targeting to the apical membrane if a non-raft protein is sandwiched between two lipid rafts.

Lipid Rafts and Caveolae

Lipid rafts are membrane microdomains enriched in glycosphingolipids, SM and cholesterol, which have been implicated in exocytosis, endocytosis, and signaling (Simons and Ikonen, 1997). The long saturated acyl chains of sphingolipids allow them to pack tightly together through hydrogen bonding, yielding a higher melting temperature (T_m) and higher order than other unsaturated, kinked phospholipids (reviewed in (Edidin, 2003)). Cholesterol has a flat, rigid molecular structure, which, through its association with acyl chains, allows it to order lipids (Almeida et al., 1993; Sankaram and Thompson, 1990). In the presence of cholesterol, high T_m lipids, such as SM, separate into a liquid-ordered (l_o) phase, forming a lipid raft that can co-exist independently of surrounding lipids that are in a

liquid-disordered state (Brown and London, 2000). The percent of l_o phospholipids in model membranes is proportional to the amount of cholesterol (Crane and Tamm, 2004), suggesting that cholesterol has a direct effect on the organizing properties of phospholipids. The concentration of cholesterol required to organize unsaturated lipids, such as phosphatidylcholine (PC) into a l_o phase is approximately 1.7 fold higher than the amount of cholesterol necessary to induce SM into a l_o state (reviewed in (Simons and Vaz, 2004)). PS and PE, which are enriched in the cytoplasmic leaflet, have been shown to associate with cholesterol, separating into a l_o phase. However, lipid rafts in the inner leaflet are less stable than those in the exoplasmic leaflet (Subczynski and Kusumi, 2003), which is attributed to the inability to cholesterol to pack as tightly with the unsaturated, bent hydrocarbons of PS and PE. Cholesterol preferentially associates with SM>PC>PS>PE, although there is disagreement whether the interaction is chemically direct (Holopainen et al., 2004; Rog and Pasenkiewicz-Gierula, 2004). One model proposes that cholesterol and phospholipids exist in a complex of 12 to 60 molecules in a ratio of 3:2 or 2:1 phospholipids per cholesterol, which effectively condenses the phospholipid, creating a l_o phase (McConnell and Radhakrishnan, 2003; Radhakrishnan et al., 2001). A second "umbrella model" suggests that instead of directly interacting with SM, cholesterol accumulates close to the polar phosphocholine head group of SM to shield itself from water (Huang and Feigenson, 1999). This proposal is corroborated by the observation that SM and cholesterol may not directly interact (Holopainen et al., 2004).

Experiments with model and cellular membranes or live cells have generated several models to explain the organization of proteins within lipid rafts. Measurement of raft size

through several different techniques indicates that the diameter can vary from 7 to 700 nm, suggesting that protein association with lipid rafts is dynamic (Anderson and Jacobson, 2002). Many proteins have been shown to interact directly with cholesterol or lipids, suggesting that the protein could be encased in a small lipid shell which has a strong affinity for pre-existing lipid rafts (Anderson and Jacobson, 2002). Lipid shells could target proteins to apical vesicles in the TGN, or caveolae or lipid rafts on the plasma membrane (Anderson and Jacobson, 2002). While lipid shells on their own may not form a separate l_o phase, they could have a propensity to associate with lipids in the l_o state. Another hypothesis proposes that proteins are associated with small unstable rafts that coalesce to form larger, more stable lipid rafts (Kusumi et al., 2004). This theory is similar to the lipid shell model, except that it suggests that proteins are dynamically associated with lipids, in contrast to lipid shells, which would presumably have a longer lifetime. In this model, large rafts in the exoplasmic leaflet could recruit smaller rafts in the inner leaflet (Kusumi et al., 2004). Coupling between the two leaflets would be assisted by interdigitation between the long acyl chains of SM and other similarly long lipids and proteins that span the bilayer. However, there is still some disagreement as to whether rafts from the outer and inner leaflets are actually coupled (Devaux and Morris, 2004).

Caveolae are flask-shaped invaginations of the membrane with a similar lipid content as lipid rafts, distinguishing them from bulk membrane lipids (Anderson, 1998). Unlike lipid rafts, which are enriched at the apical membrane of polarized epithelial cells, caveolae are enriched at the basolateral membrane (reviewed in (Parton and Richards, 2003)). Caveolae are involved in endocytosis and signal transduction and biochemically defined by their

association with caveolin (Anderson, 1998; Kurzchalia et al., 1992; Rothberg et al., 1992). Caveolin-1, a cholesterol-binding protein and component of apical transport vesicles, is required for HA apical sorting (Murata et al., 1995; Scheiffele et al., 1998; Wandinger-Ness et al., 1990). Treatment of permeabilized MDCK cells with antibodies specific to caveolin-1 significantly reduces HA apical transport, although it is unclear if HA accumulates in the TGN or if it is mis-targeted to the basolateral membrane (Scheiffele et al., 1998).

Detergent Resistance Operationally Defines Lipid Rafts

The seminal observation that resistance to detergent extraction at cold temperature operationally defines lipid rafts has enabled the characterization of lipid rafts in multiple signaling, endocytic, and sorting pathways (Brown and Rose, 1992). The GPI-anchored protein placental alkaline phosphatase (PLAP) attains the ability to resist extraction by Triton X-100 at cold temperature once it is terminally glycosylated in the TGN (Brown and Rose, 1992). Incorporation of PLAP into DRMs rich in sphingomyelin, glycosphingolipids, and cholesterol is not disrupted by high salt, suggesting that PLAP does not peripherally associate with another protein to resist detergent extraction (Brown and Rose, 1992). *In vitro* liposome experiments with increasing ratios of cholesterol:PC at 45° C indicate that there is a direct correlation between the appearance of lipids in the l_o state and resistance to detergent extract ion, suggesting that Triton does not create insoluble membranes (Schroeder et al., 1998). However, decreasing temperature in conjunction with increasing Triton promotes lipids to separate into the l_o state, as determined by calculation of the lipid order by ^{31}P-NMR, suggesting that Triton may cause lipids to form apparent lipid rafts *in vitro* (Heerklotz, 2002).

The observation that DRMs may not represent pre-existing complexes has brought into question the operational definition of a lipid raft and prompted researchers in the field to validate the hypothesis that DRMs represent a biologically-relevant membrane domain. A detergent-free method of lipid raft/caveolae enrichment through flotation on an OptiPrep gradient circumvents the possibility that detergent could induce l_o domains (Smart et al., 1995). Antibody co-patching is another alternative to detergent resistance. If two proteins are in close proximity to each other on the cell surface, labeling with a primary antibody followed by a second antibody conjugated to a fluorescent tag will cross-link the primary antibodies, causing them to cluster into a visible patch on the membrane (Harder et al., 1998; Shvartsman et al., 2003). The two antigenically-distinct raft proteins of the Japan and X:31 influenza hemagglutinin (HA) serotypes co-patch, while Japan HA does not co-patch with an HA mutant that is not associated with DRMs (Shvartsman et al., 2003). The co-patching is diminished when the cells are depleted of cholesterol, suggesting that the two proteins co-patch because they both occupy the same or nearby lipid rafts (Shvartsman et al., 2003). Co-patching alone might not be an adequate alternative to detergent resistance, since examination by electron microsopy indicates that some raft markers can co-cluster independently of other raft markers (Wilson et al., 2004). Another method to measure lipid raft association is fluorescence recovery after photobleaching (FRAP). Proteins associated with lipid rafts have a slower rate of lateral diffusion than non-raft proteins (Sheets et al., 1997; Shvartsman et al., 2003). Comparison of the lateral mobility of raft and non-raft markers by FRAP in live cells can verify the DRM phenotype. Fluorescence correlation spectroscopy can measure the diffusion of a single fluorescent particle without perturbing the

membrane (Bacia et al., 2004). In live basophilic leukemia cells, the non-raft marker dialkylcarbocyanine dye has a significantly faster diffusion rate than the raft marker cholera toxin B bound to ganglioside (Bacia et al., 2004). Fluorescence correlation spectroscopy is thought to be superior to FRAP because the method has a shorter acquisition time and does not require movement into large bleached regions, eliminating one source of potential artifacts generated in FRAP experiments (Bacia et al., 2004).

The Transmembrane Domain of Influenza Hemagglutinin Contains an Apical Sorting Signal

Influenza virus hemagglutinin (HA) is a single-spanning homo-trimeric integral membrane protein that is sorted apically in polarized epithelial cells (Roth et al., 1983). The HA glycoprotein is transported directly to the apical membrane in polarized epithelial cells immediately following biosynthesis (Figure 1) (Matlin and Simons, 1984). Alanine-scanning mutagenesis of amino acids in the transmembrane (TM) domain of HA (A/Japan/305/57 serotype) revealed that the information required for apical sorting is contained in residues of the transmembrane domain that would reside in the exoplasmic leaflet of the membrane, where SM and glycosphingolipids are enriched (Lin et al., 1998). Most of the same mutations that prevent HA apical sorting also reduce association with DRMs (Lin et al., 1998). HA associates with DRMs in the Golgi with the same kinetics that it receives terminal glycosylation, and remains associated with DRMs at the apical membrane (Scheiffele et al., 1997; Skibbens et al., 1989). Reduction of cholesterol in MDCK cells with lovastatin, mevalonate, and methyl-β-cyclodextrin significantly reduces the transport of HA

to the apical surface without affecting VSVG transport, suggesting that incorporation of HA into lipid rafts is required for apical transport (Keller and Simons, 1998). Circular dicroism spectroscopy experiments with a peptide of the transmembrane domain of A/Hong Kong/1968 (X:31) HA in liposomes indicate that the transmembrane of HA exists as an alpha helix in the membrane (Tatulian and Tamm, 2000). Increasing the peptide:lipid ratio increases the order of the acyl chains in the bilayer (Tatulian and Tamm, 2000), suggesting that X:31 HA could nucleate lipid rafts through interactions with its transmembrane domain. This possibility will be experimentally addressed in this study.

Association of influenza with lipid rafts may also be required for some aspects of the virus life cycle, including infection. For efficient infection, the influenza virus binds to the plasma membrane and is internalized by the endocytic machinery of the host cell. Low pH causes conformational changes in the HA trimer which allows the viral and host cell membranes to fuse, permitting entry of the viral genome into the cell (reviewed in ((Stegmann, 2000)). The extracellular domain of each HA monomer consists of two disulfide-linked subunits, HA1 and HA2 that can be cleaved at a single site by serine proteinases like *trypase Clara*, a trypsin-like enzyme in the lungs (Nayak et al., 2004). In MDCK cells, HA is cleaved by a similar endogenous serine proteinase. HA1 binds to sialic acid on the host membrane, while the N-terminal fusion peptide of HA2 inserts into the membrane, helping to drive the fusion reaction. Fusion proceeds through several intermediate steps, including formation of a stalk when the outer membranes of each bilayer fuse. Formation of the stalk is followed by hemifusion, creation of an unstable reversible fusion pore, and formation of the large irreversible fusion pore. Japan HA or HA

(A/Udorn/72) transmembrane mutants that do not associate with DRMs are not efficient at inducing membrane fusion ((Takeda et al., 2003a); J. Zimmerberg, 2001 unpublished observation). Replacement of the transmembrane domain and cytoplasmic tail of HA with a GPI anchor halts the fusion reaction at the hemifusion state (Kemble et al., 1994). These experiments suggest that the transmembrane domain of HA is necessary for fusion. However, a conflicting report indicates that replacement of the transmembrane domain and cytoplasmic tail of HA with the transmembrane domain and a truncated tail of pIgR, which does not associate with DRMs, actually accelerates the fusion rate as compared to wild-type HA (Melikyan et al., 1999). In addition, depleting cellular cholesterol with methyl-β-cyclodextrin has no effect on HA-mediated fusion (Melikyan et al., 1999). However, a point mutation of an amino acid in the transmembrane domain of HA that has been shown to be required for apical sorting significantly inhibits fusion (Melikyan et al., 1999). These conflicting experiments indicate that the fusion reaction is a more complex process than was initially understood. The mechanics of fusion may require a specific structure in the transmembrane domain, which is perturbed in the HA TM point mutant or the other HA TM mutants that do not associate with DRMs. The majority of HA fusion experiments are performed in the absence of influenza virus. It is possible that influenza internalization may require recruitment of specific endocytic components for efficient infection. It may be more advantageous for influenza to have a slower fusion reaction to allow recruitment of the necessary machinery. In the fusion pore, the HA trimer is likely arranged in a ring surrounded by lipid rafts which may act as a fence to retard lipid flux between the viral and host cell membranes, promoting fusion (J. Zimmerberg, unpublished observation). Lipid

rafts may promote a specific membrane curvature that promotes fusion, while structurally preventing lipid flux between the donor and acceptor membranes.

Lipid raft association may also affect influenza budding. Influenza virus assembles and buds from the apical surface of polarized epithelial cells into the lumen of the lungs. Influenza clusters at the surface of the plasma membrane prior to budding (Compans and Dimmock, 1969). The influenza envelope contains lipid rafts acquired from the host cell membrane, suggesting that influenza virus selectively buds from areas of the plasma membrane containing lipid rafts (Scheiffele et al., 1999). Influenza viruses containing HA mutants that do not associate with DRMs do not cluster nor bud efficiently (Takeda et al., 2003a). Conflicting data suggests that HA is not required for influenza budding, since influenza virus lacking HA buds from cells but is not infectious (Latham and Galarza, 2001). Although HA may or may not be required for budding, the data indicates that influenza virus clusters in lipid rafts at budding sites. It is possible that influenza buds at lipid rafts in order to acquire the lipids necessary for efficient viral fusion.

Myelin and Lymphocyte Protein Is Required for Apical Trafficking of HA

Myelin and lymphocyte protein (MAL/VIP17) is a 17 kDa tetra-spanning integral membrane proteolipid. MAL is expressed in myelinating Schwann cells during the late stages of myelinogenesis, mature T-cells, and developing distal tubuli of the kidney (Alonso and Weissman, 1987; Frank et al., 1999; Frank et al., 1998). Although mice lacking MAL are viable and have a normal lifespan, paranodal proteins are mistargeted, resulting in improper maintenance of axioglial contacts (Schaeren-Wiemers et al., 2004). Immunoisolation of vesicles with antibodies that recognize the carboxy terminus of VSVG or

HA identified MAL as a component of both apical and basolateral vesicles (Wandinger-Ness et al., 1990). Proteomic analysis of CHAPS-insoluble membranes from MDCK cells identified MAL as a major constituent that could be extracted with chloroform/methanol (Taylor et al., 2002; Zacchetti et al., 1995). MAL has been isolated in DRMs and is predominantly localized to the apical surface of the plasma membrane in glandular stomach epithelium and distal kidney tubuli (Frank et al., 1998; Puertollano et al., 1999).

In polarized MDCK cells, targeted reduction of endogenous MAL with antisense oligonucleotides reduces the amount of HA trafficked to the apical surface and the percentage of HA in DRMs (Cheong et al., 1999; Puertollano et al., 1999). Attenuation of MAL impairs trafficking of HA to the cell surface more than two fold in polarized and non-polarized MDCK cells and causes HA to accumulate in the Golgi (Cheong et al., 1999; Puertollano et al., 1999). MAL has been shown to associate with HA (Puertollano et al., 1999), although experiments reported in this dissertation suggest that the association is very weak or transient and may not be direct. Reduction of MAL also impairs secretion of the two apically sorted proteins thyroglobulin and gp80/clusterin, while sorting of the basolateral protein E-cadherin is unaffected (Martin-Belmonte et al., 2001; Martin-Belmonte et al., 2000). Delivery of total surface apical proteins is reduced in MDCK cells depleted of endogenous MAL, while total basolateral protein levels are unaffected (Martin-Belmonte et al., 2000). Taken together, these experiments suggest that MAL is involved in apical sorting. MAL is the most likely candidate for a sorting protein that directs HA into apical vesicles at the TGN. MAL has been shown to associate with the galactolipid sulfatide (Frank et al., 1998), and it is possible that MAL stabilizes HA in lipid rafts.

The phenotype of MAL depletion is different than the effect of depleting the basolateral sorting protein μ1B. In cells lacking μ1B, LDLR is mis-sorted to the apical membrane and does not accumulate intracellularly, while apical proteins are retained at the Golgi in cells with reduced MAL (Cheong et al., 1999; Folsch et al., 1999). It is possible that these two different phenotypes are a result of mechanistic differences in the apical and basolateral sorting pathways. As discussed in an earlier section, it has been suggested that μ1B may sort basolateral proteins from the endocytic recycling pathway and not from the TGN. LDLR may be redirected to the apical surface in cells lacking μ1B through the endocytic pathway. Apical proteins may take a more direct route to the plasma membrane during biosynthetic transport.

The subcellular localization of MAL suggests that it may not actively sort proteins from the TGN. The expression pattern of transfected MAL in MDCK or COS-7 cells is punctate throughout the cell with a concentration in the perinuclear region and partial co-localization with Golgi and ER markers (Kim and Pfeiffer, 2002; Zacchetti et al., 1995). However, when protein synthesis was blocked for 90 minutes with cyclohexamide, MAL was localized to vesicles that did not co-localize with the Golgi, suggesting that MAL does not localize to the Golgi subsequent to synthesis (Zacchetti et al., 1995). Immunoelectron micrographs of MAL in MDCK cells indicate that while 82% of MAL is associated with tubular/vesicular structures, only 0.6% of MAL is localized to the Golgi area (Puertollano et al., 2001a). Approximately 12% of MAL is located at the plasma membrane at steady state (Puertollano et al., 2001a). It is possible that MAL may apically sort proteins indirectly by recycling a necessary component of apical vesicles back to the TGN.

In this study, I intend to further characterize the relationship between HA and MAL. I will determine if the interaction between HA and MAL is required for HA to be delivered to the apical plasma membrane. In addition, I will determine if the expression level of MAL affects the percentage of HA incorporation into DRMs. The time course of the association of HA and MAL in the biosynthetic apical transport pathway will be examined to determine if MAL sorts HA at the TGN.

The Apical Sorting Signal for Megalin is Located in its Cytoplasmic Domain

Apical targeting signals have been identified in the cytoplasmic domains of several proteins (Inukai et al., 2003; Jia et al., 2003; Marzolo et al., 2003; Takeda et al., 2003b; van Balkom et al., 2004). Megalin (gp330/LRP-2), a member of the LDLR family of receptors, is localized to the apical membrane of many epithelial cells, including kidney proximal tubule cells, the linings of the retina, placenta, uterus, and intestine, Clara cells in the lung, and ependymal cells in the brain (Kounnas et al., 1994; Marzolo et al., 2003; Zheng et al., 1994). Megalin, a large (~600 kDa) single-spanning integral membrane receptor, has many extracellular ligands, including apolipoproteins B, E, and J, vitamin carrier proteins, and receptor associated protein (Herz and Bock, 2002; Muller et al., 2003). Genetic disruption of megalin causes mice to die perinatally with abnormalities in the mid- and forebrain, suggesting that megalin is required to internalize fat-soluble vitamins and cholesterol in the neuroepithelium from the amniotic fluid during development (Willnow et al., 1996). It is also possible that megalin depletion disrupts signaling of sonic hedgehog, one of the megalin extracellular ligands involved in midbrain development (Agarwala et al., 2001; McCarthy et

al., 2002). In the proximal tubule of the kidney, megalin interacts with the vitamin D-binding protein carrying inactive vitamin D_3 precursor. Kidney-specific depletion of megalin blocks uptake and conversion of vitamin D_3 precursor, suggesting that megalin is the only endocytic receptor of vitamin D_3 precursor in the kidney (Leheste et al., 2003). LDL receptor-related protein (LRP), another member of the LDLR family, is expressed at the basolateral surface of epithelial cells (Marzolo et al., 2003; Zheng et al., 1994). Like megalin, LRP is a large (~600 kDa) single-spanning integral membrane protein that shares a few of the same extracellular ligands as megalin, including apolipoprotein E and receptor associated protein.

The cytoplasmic tails of megalin and LRP contain LL and YXXϕ sequences, which have been identified as basolateral targeting signals (Figure 2) (Bonifacino and Traub, 2003; Hunziker and Fumey, 1994; Matter et al., 1992; Thomas and Roth, 1994). It is possible that the sequences or structures surrounding the di-leucine or YXXϕ determine whether the sequence acts as a basolateral targeting signal, as discussed in an earlier section. This may explain why LRP and megalin are differentially sorted despite both proteins containing apparent basolateral targeting information. It is also possible that megalin contains a dominant apical sorting determinant as well as a basolateral signal, although basolateral signals are usually dominant over apical signals. Tyrosine and di-leucine containing sequences also act as internalization signals (Bonifacino and Traub, 2003), which will be discussed in the next section. LRP and megalin may specifically interact with different proteins that sort the receptors to the basolateral or apical surface.

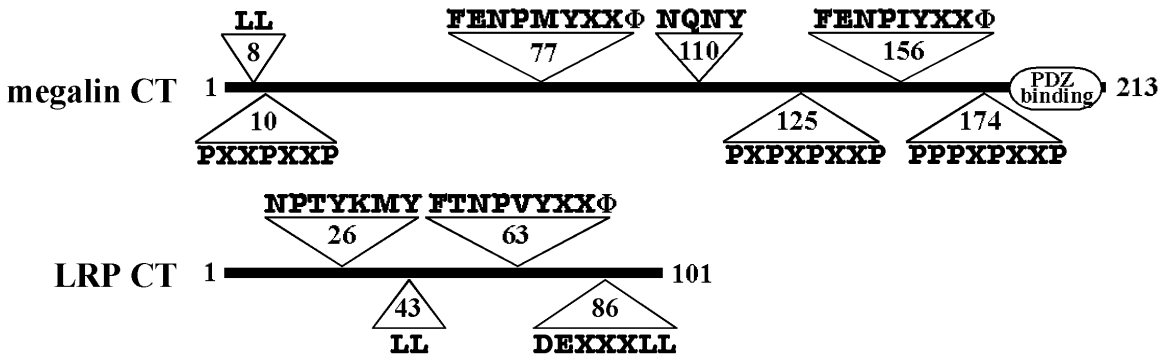

Figure 2. The cytoplasmic domains of megalin and LRP share similar sequence motifs. The 213 amino acid cytoplasmic tail of *Rattus norvegicus* megalin has three proline-rich sequences, which have been shown to bind to SH3-containing proteins. The 101 amino acid cytoplasmic domain of *Homo sapiens* LRP is also shown. Megalin contains a serine, valine, aspartic acid sequence at the extreme carboxy terminus, which has been shown to bind to PDZ domains. Both LRP and megalin contain di-leucine and YXXΦ sequences, which usually act as basolateral targeting signals. The two proteins have NPXY sequences required for internalization.

A chimera of the fourth ligand binding and transmembrane domains of megalin fused to the cytoplasmic tail of LRP is biosynthetically trafficked to the basolateral membrane of MDCK cells, where it remains at steady state (Takeda et al., 2003b). Substitution of the cytoplasmic tail of LRP with that of megalin causes the LRP chimera to be sorted apically, indicating that the cytoplasmic domain of megalin contains an apical sorting signal (Marzolo et al., 2003; Takeda et al., 2003b). Carboxy-terminal truncations of the megalin tail, sequentially removing the PDZ-binding domain (1-210), NPXYXXΦ (1-136), and NXXY (1-106) reveal that the YXXΦ and PDZ-binding domain are not required for apical sorting (Takeda et al., 2003b). However, a truncation that also removes the 30 amino acid sequence including the NXXY causes the mutant to be equally distributed on the apical and basolateral membranes, suggesting that the NXXY sequence is required for apical sorting (Takeda et al., 2003b).

When endogenous megalin and an amino-terminal truncated megalin missing the first through third ligand binding domains were extracted with 1% Triton X-100 and overlaid with a linear sucrose gradient, the proteins were buoyant, indicating that megalin may be associated with lipid rafts (Marzolo et al., 2003). However, the chimera in which the cytoplasmic domain of LRP was replaced with the megalin cytoplasmic domain does not float on linear density gradients even though it sorts apically (Marzolo et al., 2003), suggesting either that association with lipid rafts may not be required for apical sorting, or that the affinity of the chimera for lipid rafts was too low to survive the experimental conditions. Additional assays, of the type described in the earlier section, would be required to verify that the chimera is not associated with lipid rafts.

NPXY in the Cytoplasmic Domains of LDLR Family Members Interacts with Clathrin-Associated Internalization Machinery

The LDLR family of receptors share several similar structural and sequence motifs. All members of the immediate family contain epidermal growth factor (EGF) precursor homology domains and EGF repeats in their ectodomain, a single-spanning transmembrane domain, and at least one NPXY sequence in their cytoplasmic tail (Herz and Bock, 2002). Many of the LDLR family members interact with adaptor or scaffolding proteins through their cytoplasmic tail, which allows the proteins to control signaling pathways in the brain and other tissues (Herz and Bock, 2002). Extensive research with LDLR indicates that a sequence in the cytoplasmic tail, identified as NPXY, is required for clathrin-mediated internalization (Anderson et al., 1977; Chen et al., 1990; Davis et al., 1986; Lehrman et al.,

1985). Naturally-occurring internalization-defective LDLR mutants prevent LDL uptake, which can lead to hypercholesterolemia (Brown and Goldstein, 1984). NPXY may not be the entire internalization signal, as substitution of an alanine for the phenylalanine in FDNPXY reduces the internalization index of LDLR by 63% (Chen et al., 1990).

Although FDNPXY is required for internalization and basolateral sorting, the sequence is distinct from YXXΦ, a tyrosine consensus sequence that is also recognized by basolateral sorting and internalization machinery. AP-2 is a clathrin adaptor protein enriched at the plasma membrane that facilitates clathrin-coated pit internalization. X-ray crystallization studies indicate that AP-2 binds to clathrin through a LΦ[D/E]Φ[D/E] sequence in its Φ-subunit, exposing and extending the μ2 subunit of AP-2, which permits an interaction with YXXΦ sequences (Collins et al., 2002; Kirchhausen, 2002; Owen and Evans, 1998). The two tyrosine-containing sequences, YXXΦ and NPXY, bind to unique sites on the μ2 subunit of the clathrin adaptor protein AP-2, as determined *in vitro* by peptide binding to purified μ2 chain (Boll et al., 2002). Consequently, overexpression of TfR, which contains YXXΦ, does not affect internalization of epidermal growth factor receptor (EGFR), which has an NPXY sequence, although both receptors have saturable internalization kinetics (Warren et al., 1997). While overexpression of two chimeras containing YXXΦ affects internalization, overexpression of a chimera containing YXXΦ does not affect internalization of a di-leucine chimera (Marks et al., 1996).

AP-2 and clathrin-mediated LDL internalization is fast (~30 sec) and dynamic (Ehrlich et al., 2004; Keyel et al., 2004). In the absence of clathrin association, DiI-LDL molecules bound to LDLR diffuse laterally on the cell surface until LDLR contacts a pre-

existing clathrin cluster, as determined by imaging fluorescent clathrin with a spinning disk confocal microscope (Ehrlich et al., 2004). In some cases, clathrin may cluster around a static LDLR on the cell surface (Ehrlich et al., 2004). The dynamic clathrin cluster has an average lifetime of 28-32 seconds (Ehrlich et al., 2004). If it does not contact cargo in the time period, it disappears and regroups. Following cargo capture, DiI-LDL and clathrin associate for approximately 11 seconds before clathrin uncoats from the vesicle (Ehrlich et al., 2004). A subset of clathrin seems to remain associated with its cargo through the endocytic pathway, suggesting that clathrin may help sort proteins at the sorting endosome (Keyel et al., 2004).

Although FDNPXY sequences have been shown to bind directly to the μ2 subunit of AP-2 (Boll et al., 2002), depletion of AP-2 by RNA interference does not significantly affect LDL uptake in HeLa cells (Motley et al., 2003). However, attenuation of clathrin heavy chain by RNA interference almost completely blocks LDL internalization (Motley et al., 2003), confirming that clathrin is required for LDLR internalization. AP-2 depletion has a significant effect on Tf internalization, without affecting EGF endocytosis (Motley et al., 2003). These experiments suggest that EGFR and LDLR access clathrin-coated vesicles through a mechanism that does not require AP-2. Peptides containing the FDNPXY sequence bind directly to the amino terminal domain of the clathrin heavy chain, as determined by NMR (Kibbey et al., 1998). Substitution of a serine for tyrosine in the FDNPXY sequence impaired the interaction with clathrin (Kibbey et al., 1998), indicating that the association is specific.

While it is possible that LDLR could bind to clathrin *in vivo*, it is also possible that LDLR binds to alternate clathrin adaptors. Disabled-2 (Dab2) co-localizes with LDLR and clathrin and interacts with the β-subunit of AP-2 *in vitro* and *in vivo* (Mishra et al., 2002a; Morris and Cooper, 2001). The phosphotyrosine-binding (PTB) domain of Dab2 interacts with peptides containing unphosphorylated NPXY sequences *in vitro* and overexpression of the PTB domain suppresses LDL uptake (Mishra et al., 2002a; Morris and Cooper, 2001). In liposomes, Dab2 promotes clathrin-coated pit formation and conditional targeted disruption of Dab2 in mice results in a significant loss of clathrin-coated vesicles in the apical proximal tubule (Mishra et al., 2002a; Morris et al., 2002), suggesting that the protein could function as a clathrin adaptor. Megalin associates with Dab2 in the second FENPXY sequence of megalin, suggesting that Dab2 may act as a clathrin-adaptor for several LDLR family members (Oleinikov et al., 2000).

Autosomal recessive hypercholesterolemia protein (ARH) also contains a PTB domain and acts as a clathrin-adaptor protein. Patients with nonsense or frame-shift mutations in ARH do not internalize LDL in the liver and have severe hypercholesterolemia despite normal LDLR sequences (Garcia et al., 2001). ARH binds to the FDNPXY of LDLR and specifically requires an aromatic residue at the tyrosine position (He et al., 2002). ARH also associates with the amino terminal domain of clathrin heavy chain and the β-subunits of AP-1 and AP-2, intimating that ARH could bridge LDLR to clathrin (He et al., 2002; Mishra et al., 2002b). Lymphocytes isolated from a patient with a null ARH mutation have impaired LDL internalization despite >20 fold increase in LDLR at the plasma membrane (Michaely et al., 2004). Despite the large increase in LDLR at the cell surface, the number of LDLRs/μm

of membrane in clathrin-coated pits is approximately the same as control cells, although LDLR associated with these pits is not internalized (Michaely et al., 2004). In addition, LDL binding to the receptor is only increased approximately two fold because most of the LDLR outside of coated pits does not bind LDL (Michaely et al., 2004). These experiments suggest that ARH stabilizes LDLR in coated pits possibly by facilitating association of LDLR with another component of the coated pit, permitting internalization. In addition, ARH may impose structural changes to LDLR that allow the receptor to bind LDL. Megalin co-localizes with ARH in early and recycling endosomes and stable expression of ARH in MDCK cells, which no not express detectable ARH, stimulates uptake of the megalin ligand ^{125}I-lactoferrin (Nagai et al., 2003). Taken together, these experiments indicate that ARH is required for LDLR endocytosis and may be an alternate clathrin adaptor for several LDLR family members. ARH may act alone or in concert with another adaptor protein, such as AP-2 or Dab2, to promote efficient endocytosis.

Several LDLR Family Members are Recycled in the Endocytic Pathway

The endocytic recycling pathway, which traverses several organelles, is a complex mechanism of protein trafficking back to the plasma membrane following endocytosis (Figure 3) (reviewed in (Maxfield and McGraw, 2004)). LDLR is recycled every 12 minutes for a total of approximately 150 times in its lifetime (Brown et al., 1982). There is also some evidence indicating that LRP and megalin are recycled (Melman et al., 2002; Nagai et al., 2003). LDLR is rapidly (~11-30 sec) internalized by clathrin coated pits which lose their clathrin coat following budding (Ehrlich et al., 2004). LDLR and TfR can be internalized in

the absence or presence of their ligands. (reviewed in (Goldstein et al., 1985)). Although the majority of EGFR is internalized in the presence of its ligand and degraded in the lysosome,

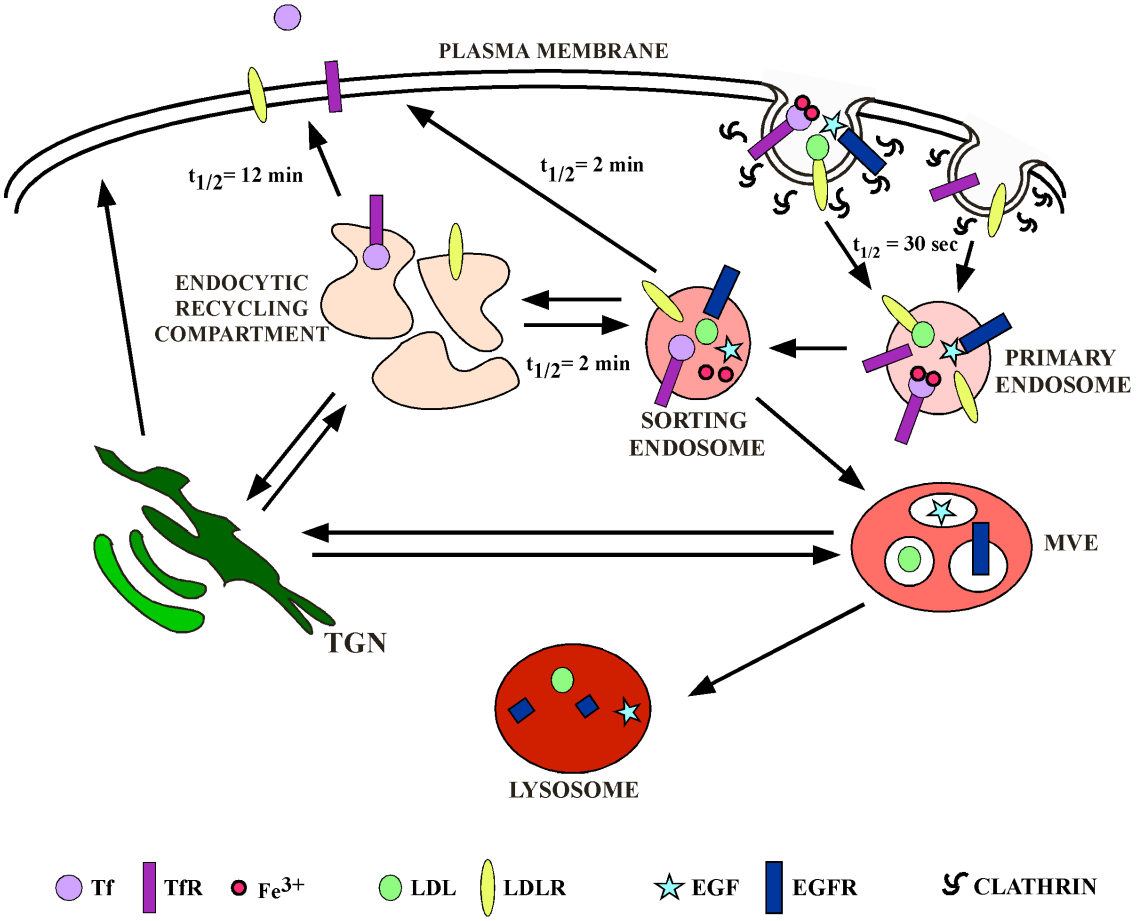

Figure 3. Endocytic recycling. LDLR, TfR, and EGFR are internalized through a clathrin-mediated mechanism, which is proceeded by shedding of the clathrin coat and fusion of the primary endosome with the sorting endosome. In the sorting endosome, LDL, free iron, and EGF are uncoupled from their binding partners before they are trafficked to the endocytic recycling compartment, the plasma membrane, or lysosomal degradation pathway. EGF, EGFR, and LDL are transported to the lysosome, where they are degraded. Tf bound to its receptor, and LDLR are recycled to the plasma membrane. The pinks to red colors represent a high (pH 6.5) to low (pH 5.5) pH gradient through the endosomal pathway. The $t_{1/2}$ values vary by cell type. This model was adapted from (Maxfield and McGraw, 2004) and represents the most predominant pathway for each receptor and ligand. MVE, multi-vesicular endosome

a small fraction of EGFR is recycled to the plasma membrane (reviewed in (Wiley and Burke, 2001)). The primary endosomes containing their respective cargo fuse with the sorting endosome in a process mediated by rab5 and SNARES (Bonifacino and Glick, 2004; Gorvel et al., 1991; Maxfield and McGraw, 2004; Rothman, 1994). Low pH (<6.0) in the sorting endosome causes LDL, EGF, and free iron to dissociate from their respective partners (Figure 3)(Brown et al., 1983; Tycko and Maxfield, 1982).

The sorting endosome, enriched in rab5, early endosome antigen 1 (EEA1), and rab4, is a dynamic organelle, also referred to as the early endosome, that only permits fusion with primary endosomes for 5 minutes before it proceeds to mature into the multi-vesicular endosome (MVE) (also referred to as the late endosome) (Maxfield and McGraw, 2004). Prior to maturation of the sorting endosome, LDLR and TfR are transported directly to the cell surface or to the endocytic recycling compartment (ERC) (Dunn and Maxfield, 1992; Dunn et al., 1989; Mayor et al., 1993). Experiments with DiI-LDL and rhodamine-Tf in CHO cells indicate that the two ligands are transported to the sorting endosome within the first two minutes of internalization, where LDL continues to accumulate for an additional 8-10 minutes before it is transported to the lysosomal pathway (Dunn et al., 1989). Tf accumulates in the sorting endosome for two minutes before it is trafficked to the perinuclear recycling endosome or the cell surface (Dunn et al., 1989; Mayor et al., 1993).

The small GTPase rab4 may be involved in budding recycling vesicles from the sorting endosome (Pagano et al., 2004; van der Sluijs et al., 1992). *In vitro* generation of recycling vesicles in permeabilized non-polarized MDCK cells is dependent on rab4 and AP-1 (Pagano et al., 2004). Antibody depletion of rab5, AP-2, and AP-3 from the cytosol has no

effect on the formation of recycling vesicles (Pagano et al., 2004). Overexpression of rab4 results in increased localization of TfR to the plasma membrane at steady state, while a dominant-negative rab4 mutant causes 80% of TfR to accumulate intracellularly (van der Sluijs et al., 1992). Interestingly, overexpression of rab4 does not allow dissociation of iron from Tf, and intracellular TfR is predominantly in the ERC (van der Sluijs et al., 1992). These experiments suggest the possibility that rab4 may be specifically involved in generating recycling vesicles that fuse with the ERC or plasma membrane.

TfR and LDLR are recycled from the sorting endosome to the plasma membrane in a fast (2 minute half-time) or slow (9-12 minute half-time) pathway (Figure 3) (Hao and Maxfield, 2000). Experiments with fluorescent sphingomyelin (C_6NBD-SM), which co-localizes with Cy5-Tf and DiI-LDL, indicate that approximately half of the lipid was sorted to the ERC from the sorting endosome, while the other half was transported directly to the plasma membrane. Although rab4 may be involved in transport from the sorting endosome to the ERC, it is unclear how proteins are sorted into the recycling pathway from the sorting endosome and what determines whether the protein is recycled through the fast or slow pathway. C_6NBD-SM and rhodamine-Tf are internalized and recycled in CHO cells with almost identical kinetics, suggesting that TfR is transported with the bulk flow of lipids (Mayor et al., 1993). However, treatment with bafilomycin A has a smaller effect on bulk membrane recycling than TfR recycling, intimating that the two pathways could be distinct (Presley et al., 1997). Removal of nearly the entire cytoplasmic domain of TfR does not have an appreciable effect on TfR recycling (Jing et al., 1990), indicating that TfR does not associate with a sorting protein via its tail. Taken together, these results suggest that TfR

does not have an active sorting mechanism, which is very surprising, given the enormous quantity of proteins and lipids that traverse through the sorting endosome. It is possible that, similar to the proposed sorting mechanism of apical proteins in the TGN, recycled proteins are sorted by exclusion from the late endosomal pathway. However, a few proteins have been identified with sequences required for recycling (Cao et al., 1999; Gage et al., 2001; Vargas and Von Zastrow, 2004). The G-protein coupled dopamine receptor has a 23 amino acid sequence in the proximal region of its cytoplasmic domain that, when inserted into the tail of the normally degraded δ opioid receptor, is sufficient to cause ligand-stimulated recycling (Vargas and Von Zastrow, 2004). Beta-2 adrenergic receptor has a PDZ-binding sequence in the extreme carboxy terminus of its cytoplasmic domain that is required for recycling and sufficient for recycling the δ opioid receptor (Gage et al., 2001). These experiments suggest that dopamine and beta-2 adrenergic receptors are recycled by an active sorting mechanism.

The ERC is comprised of a number of tubules which may be organized in a *cis* and *trans* configuration, similar to the Golgi network (Maxfield and McGraw, 2004). Once proteins are trafficked to the recycling endosome, it is unclear if a second mechanism exists to sort proteins to the plasma membrane. Exit from the ERC is the rate-limiting step in the endocytic recycling pathway (Figure 3) (Maxfield and McGraw, 2004). Rab11, which is enriched in the ERC, may be involved in trafficking proteins into or out of the ERC. Overexpression of a constitutively-active rab11 mutant causes Tf accumulation in the ERC, whereas overexpression of a dominant negative rab11 mutant results in a diffuse punctate pattern of Tf, which co-localizes with EEA1, a marker of sorting endosomes (Pasqualato et

al., 2004; Ullrich et al., 1996). These results suggest that rab11 could participate in the fusion of recycling vesicles to the ERC, although the molecular mechanism of the involvement of rab11 in recycling has not been determined.

Sorting Nexins Regulate Multiple Aspects of the Endocytic Recycling Pathway

Although the rab proteins seem to regulate some aspects of endocytic recycling, the mechanism by which the LDLR family is recycled is not completely understood. LDLR family members associate with sorting nexin 17 (SNX17) (Burden et al., 2004a; Stockinger et al., 2002b), a member of a family of proteins which has been shown to regulate several endocytic pathways (reviewed in (Worby and Dixon, 2002)). It is possible that sorting nexins may traffick proteins by specifically binding to certain receptors. There are approximately 27 known sorting nexins and many of the SNX proteins have specificity for a certain protein or family of proteins. The SNX family is characterized by the inclusion of a phagocyte oxidase homology (PX) domain, a conserved sequence required for binding to phosphoinositides (Worby and Dixon, 2002). The SNX-PX domain is distinct from the PX domains of other proteins, including phospholipase D 1 and 2, phosphatidylinositol 3-kinase, and the $p40^{phox}$ and $p47^{phox}$ subunits of NADPH oxidase superoxidase generating complex (Teasdale et al., 2001; Worby and Dixon, 2002). SNX-PX domains have more than 50% amino acid similarities and cluster apart from other PX domains in a phylogenetic tree (Teasdale et al., 2001; Worby and Dixon, 2002). The crystal structures of the PX domains of $p40^{phox}$, $p47^{phox}$, and Grd19p, the yeast SNX3 ortholog, indicate that these structurally-similar domains all consist of a three-stranded β-sheet and three α-helices (Bravo et al., 2001;

Karathanassis et al., 2002; Zhou et al., 2003). $p40^{phox}$ and Grd19p have a structurally-similar basic PI(3)P-binding pocket (Bravo et al., 2001; Zhou et al., 2003). Both of these PX domains preferentially bind PI(3)P, although a torsional change of the arginine in the binding pocket could accommodate a phosphate at the 4-hydroxy position (Zhou et al., 2003). Binding to a phosphoinositide with a phosphate at the 5-hydroxy position is prevented by steric hindrance (Zhou et al., 2003). The PX domain of $p47^{phox}$ has a structurally-similar binding site as the basic pocket of $p40^{phox}$ and Grd19p, which can bind PI(3)P or PI(3,4)P (Karathanassis et al., 2002). In addition, $p47^{phox}$ contains a unique second basic pocket, which is thought to bind to lipids with a small polar head group, such as phosphatidic acid (Karathanassis et al., 2002). Prediction of the secondary structure of the SNX-PX domains indicates a structural similarity to the $p40^{phox}$ PX domain (Worby and Dixon, 2002).

Phosphoinositides and their various kinases are important regulators of membrane trafficking and signaling pathways (reviewed in (Roth, 2004)). Enrichment of phosphoinositides in specific organelles could provide a molecular address for SNX localization. PI(4,5)P2 is enriched in the inner leaflet of the plasma membrane, while PI(3)P and PI(3,5)P2 are localized to the sorting endosome and multi-vesicular body of the lysosomal pathway, respectively (Roth, 2004). While most sorting nexins are localized to a particular organelle, removal of the SNX-PX domain abrogates membrane association and results in a diffuse cytoplasmic pattern (Burden et al., 2004a; Choi et al., 2004; Cozier et al., 2002).

SNX1 is the most extensively studied member of the sorting nexin family. The mammalian protein was originally identified through a yeast two-hybrid screen with the

tyrosine kinase domain of EGFR (Kurten et al., 1996). Forty-fold overexpression of SNX1 in CV-1 cells enhances ligand-induced downregulation of EGFR, suggesting that SNX1 could be involved in targeting EGFR to the lysosome (Kurten et al., 1996). Autonomous expression of the PX domain of SNX1 acts in a dominant-negative mechanism to attenuate ligand-stimulated EGFR downregulation, presumably by sequestering EGFR from transport into the lysosomal pathway (Zhong et al., 2002). SNX1 has a subcellular localization that partially overlaps with both the sorting endosome marker EEA1 and tubular endosomes, which could be the endocytic recycling compartment or MVEs (Gullapalli et al., 2004; Zhong et al., 2002). Recombinant SNX1 binds to PI(3)P and PI(3,5)P in sucrose-loaded liposomes, two lipids that are enriched in the sorting endosome and MVE, respectively. Taken together, the data suggests that SNX1 could be involved in targeting EGFR from the sorting endosome or MVE to the lysosomal pathway.

Similar to SNX1, overexpression of SNX2 causes an increase in ligand-induced EGFR downregulation, suggesting that the two proteins may have redundant functions (Gullapalli et al., 2004). SNX1 and SNX2 form hetero- and homo-oligomers through their coiled-coil domains and are partially localized to organelles positive for EEA1 (Gullapalli et al., 2004; Zhong et al., 2002). While targeted disruption of either SNX1 or SNX2 in mice yields no apparent phenotype, attenuation of both proteins is embryonic lethal (Schwarz et al., 2002). Reduction of SNX1, SNX2, or a combination of both by RNA interference does not have an appreciable effect on ligand-induced EGFR downregulation as compared to control cells (Carlton et al., 2004; Gullapalli et al., 2004). These data suggest that SNX1 and SNX2 may not be directly involved in targeting EGFR to the lysosome. However, SNX1

and SNX2 depletion was not completely efficient, as 20% of the protein was still expressed under the conditions in this assay (Gullapalli et al., 2004). It is possible that SNX1 and SNX2 are not limiting to the sorting mechanism and a small quantity is sufficient to promote trafficking of EGFR to the lysosome.

The yeast SNX1 ortholog, vacuolar protein sorting protein 5 (Vps5p), is part of a retromer complex that recycles proteins from the prevacuolar compartment, an organelle analogous to the mammalian MVE, to the TGN (Cooper and Stevens, 1996; Horazdovsky et al., 1997; Seaman et al., 1997; Seaman et al., 1998). In yeast, Vps10p sorts its cargo from the TGN to the prevacuolar compartment, where the cargo is released to be delivered to the vacuole, an organelle equivalent to the mammalian lysosome. The retromer complex, consisting of Vps35p, Vps29p, Vps26p, Vps5p, and Vps17p, binds to the cytoplasmic domain of Vps10p, recycling the protein back to the TGN from the prevacuolar compartment (Seaman et al., 1997). Vps5p and Vps17p associate through coiled-coil domains, and together they are thought to act as a scaffold for the assembly of components required for vesicle budding (Horazdovsky et al., 1997; Seaman and Williams, 2002).

In mammals, a mechanism analogous to the yeast retromer retrieves mannose 6-phosphate receptor (MPR) from the MVE and recycles it back to the TGN (Arighi et al., 2004; Bonifacino and Glick, 2004). Similar to Vps5p, SNX1 associates with the mammalian retromer complex comprised of hVps35, hVps26, and hVps29 (Gullapalli et al., 2004). It is possible that SNX2 is also part of the retromer, although a direct interaction has not been determined (Gullapalli et al., 2004). hVps26, one of the mammalian retromer proteins, co-localizes with MPR in MVEs and other endosomal tubules that are devoid of the lysosomal

marker LAMP-1 (Arighi et al., 2004). Interestingly, hVps26 is also in endosomes positive for Tf (Arighi et al., 2004), which would suggest that the retromer may also be localized to the sorting endosome or ERC. Attenuation of hVps26 expression by RNA interference results in decreased MPR at steady state, suggesting that MPR is sorted to the lysosome in the absence of retromer retrieval (Arighi et al., 2004).

The retromer complex has also been implicated in the transcytosis of pIgR from the basolateral to the apical membrane in polarized epithelial cells (Verges et al., 2004). pIgR associates with hVps35, and hVps35 depletion with antisense oligonucleotides results in a 15-25% decrease in transcytosis (Verges et al., 2004). These experiments suggest that the retromer complex, which includes SNX1, may have multiple functions. From the sorting endosome, SNX1 may regulate trafficking of EGFR to the MVE, MPR to the TGN, and pIgR to the recycling endosome. It is possible that SNX1 functions in a mechanism analogous to Vps5p, where it acts as a scaffold for budding components. The three coiled-coil domains in the last 200 amino acids of SNX1, have been characterized as a Bin/Amphiphysin/Rvs (BAR) domain (Carlton et al., 2004; Habermann, 2004). BAR domains have been implicated in initiating membrane curvature and there is data that suggests that SNX1 may promote budding from endosomes (Carlton et al., 2004). It is also possible that depletion of the retromer affects a pathway that is common to EGFR, pIgR, and MPR.

Sorting Nexin 17, a 56 kDa membrane-associated protein, has been implicated in trafficking LDLR and P-selectin (Burden et al., 2004a; Stockinger et al., 2002b; Williams et al., 2004). The secretory granule membrane protein P-selectin, is internalized and directed to the sorting endosome with kinetics similar to LDLR (Straley and Green, 2000). However, P-

selectin is sorted from the sorting endosome to the MVE and onto the TGN, where it is recycled back to the plasma membrane (Straley and Green, 2000). This endocytic recycling pathway differs from LDLR, which is recycled back to the plasma membrane through the recycling endosome (Figure 3). SNX17 co-localizes with the sorting endosome markers EEA1 and rab4, and associates with P-selectin and all core members of the LDLR family except megalin (Florian et al., 2001; Stockinger et al., 2002b). Deletion mutants that remove the PX domain of SNX17 or treatment with wortmannin, a PI(3)kinase inhibitor, result in a diffuse cytosolic localization of the protein, suggesting that the PX domain directs SNX17 to a specific subcellular location (Williams et al., 2004). Mutation of the asparagine, proline, or tyrosine of the NPXY sequence in the cytoplasmic tail of LDLR abrogates the interaction of SNX17 and LDLR in the yeast two-hybrid system, intimating that SNX17 interacts with the NPXY sequence of LDLR (Burden et al., 2004a). Overexpression of SNX17 induces a two-fold increase in the internalization index of ^{125}I-LDL after 5 hours of uptake, suggesting that SNX17 regulates LDLR internalization (Stockinger et al., 2002b). However, Anne Soutar and colleagues were unable to duplicate this result (Burden et al., 2004a). Overexpression of SNX17 causes an increase in internalization, higher cell surface expression, and less lysosomal targeting of P-selectin (Williams et al., 2004). The interpretation of these results is that SNX17 functions in the internalization pathway. However, it is also possible that SNX17 functions in the recycling pathway. A faster recycling rate would cause less P-selectin or LDLR to be directed into the lysosomal pathway and cause more expression at the cell surface if internalization was unaffected. Recycling from the endocytic recycling compartment to the plasma membrane is the rate-limiting step in LDLR endocytic cycling

(Figure 3). It is possible that an increase in recycling would be accompanied by an apparent increase in internalization because more receptors per time would be internalized if the rate of delivery to the plasma membrane were increased.

In this study, I intend to ascertain the effects of SNX17 expression on LDLR recycling. I will determine if TfR internalization and recycling is affected by SNX17 overexpression to investigate whether the effects of SNX17 overexpression are limited to LDLR or affect the entire endocytic recycling pathway.

CHAPTER TWO

MATERIALS AND METHODS

Cell Culture

The D5 clonal line of MDCK cells (Williams et al., 2004) cos-1, and 293 cells were maintained in Dulbecco's modified Eagle's medium (DMEM) and 10% fetal bovine serum (Invitrogen, Carlsbad, CA or Gemini, Woodland, CA). HeLa cells were maintained in DMEM plus 10 mM HEPES, pH 7.1, 1 mM sodium pyruvate, and 10% fetal bovine serum (Gemini). For experiments on plates or 3.0 μm Transwell filters (Costar), cells were detached by trypsinization, counted, and seeded with the same number of cells for each respective experiment.

Antibodies

Polyclonal serum from a rabbit immunized with A/Japan/305 virus glycoproteins or monoclonal Fc.125 (from T. Braciale, U. Virginia) was used for immunoblot and immunoprecipitation experiments. Epitope-tagged MAL was immunoprecipitated with monoclonal antibody 9E10 specific for a c-myc epitope. Monoclonal antibody to β-COP was a gift from T. Kreis (Geneva). Antibody to caveolin-1 was from Transduction Labs (BD Biosciences-Pharmingen, San Diego). Monoclonal antibody to LDLR (HL-1 2.3 mg/ml) was a gift from the laboratory of Michael Brown and Joseph Goldstein. Transferrin receptor monoclonal antibody was purchased from Transduction Laboratories. SNX17 polyclonal antibody was purchased from Protein Tech Group. Transfected SNX17 was detected with a monoclonal or polyclonal antibody that specifically recognizes the HA epitope (HA.11

Covance, Berkeley, CA). Expression of yeast two hybrid bait constructs was verified by immunoblotting with LexA antibody (N-19 Santa Cruz). Polyclonal megalin antibody (Meg 19) was a gift from the laboratory of Joachim Herz (UTSW).

Materials

Proteins were labeled with Easy Tag Express-^{35}S Protein Labeling Mix (PerkinElmer Life Sciences, Boston). Proteins on immunoblots were detected by enhanced chemiluminescence (Western Lightining, PerkinElmer Life Sciences or Supersignal West Fempto, Pierce) that was recorded on film and quantified by densitometry (Molecular Dynamics, Sunnyvale, CA). Radioactive proteins were quantified by phosphor imaging on a Typhoon (Molecular Dynamics). Restriction enzymes were from Roche (Indianapolis) unless otherwise indicated. All other chemicals were purchased from Sigma (St. Louis, MO) unless otherwise noted.

Adenovirus Construction

Recombinant adenoviruses were generated using the AdEasy system essentially as described (He et al., 1998). PCR was used to generate an *Xho*I or *Not*I restriction site immediately adjacent to the stop codon of HA. HA was subcloned from pCB6HA (He et al., 1998), using the *Bgl*II site upstream of the start codon of HA and the newly-generated *Xho*I or *Not*I restriction sites, into pShuttle-CMV (a gift from the Vogelstein laboratory, Johns Hopkins Oncology Center). Human MAL was subcloned from myc-hMAL pSR (a gift from Miguel Alonso, Spain) by creating a Bgl*II* site immediately upstream of the myc

epitope and a Not*I* restriction site downstream of the stop codon. pShuttle-CMV containing the appropriate insert was linearized with *Pme*I (NEB, Beverly, MA) and subsequently cotransfected with pAdeasy-1 (a gift from the Vogelstein laboratory) into BJ5183 *E. coli* to create a recombinant adenovirus plasmid. 10 μg of the recombinant plasmid was linearized with *PacI* and transfected into 293 cells (American Tissue Culture Collection) using the calcium phosphate technique. The viruses were passaged three times to increase the titer to an appropriate concentration. Virus was collected after approximately 30% of the cells in three confluent 15 cm plates exhibited cytopathogenic effects. Cells were scraped, centrifuged, and concentrated into 10 ml of supernatant. The cells were lysed by four rapid freeze thaw cycles with vigorous vortexing and the cell debris was removed. For experiments with SNX17, control Japan HA and HA-SNX17 were purified on a cesium chloride gradient. Viral titer was determined in 293 cells using an end-point dilution assay.

Site-directed Mutagenesis of the Transmembrane Domain of HA

The HA sequence in plasmid pkSVEHA was mutated by megaprimer mutagenesis (Brewer and Roth, 1991) to create *Bgl*II sites at the beginning and end of the coding sequence for the TM region. The sequence between the *Bgl*II sites was excised, leaving a single *Bgl*II site in place of the TM sequence. Two pairs of complementary oligonucleotides were synthesized so that when annealed together they contained GATC unpaired extensions followed by sequences encoding isoleucine and 24 leucines, in the same reading frame as the upstream HA sequences. The isoleucine was held invariant to make use of the ATC codon in the wild type HA sequence that formed part of the 5' *Bgl*II site. Plasmid pkSVEHA-*Bgl*II

was digested with *Bgl*II and ligated to the annealed oligonucleotides. Plasmids were identified encoding an HA with an Ile-Leu24 TM. The sequences encoding the HAs were subcloned into pCB6 and subsequently to pShuttle-CMV (He et al., 1998) for recombination into adenovirus. The series of mutants in which wild type TM residues were inserted back into the Ile-Leu24 TM were also made by megaprimer mutagenesis in either pkSVEHA or in pCB6HA and then subcloned into pShuttle-CMV.

Sorting Assay

1 x 10^6 MDCK cells were added to 21 mm diameter Transwell filters (Corning; Corning, NY) with 3 μm pores and cultured with frequent changes of medium for four days to establish a tight monolayer as monitored by measuring transepithelial electrical resistance with an Endohm tissue resistance measurement chamber (World Precision Instruments) and/or the ability to retain fluid in the chamber above the monolayer when fluid was removed below. The basal side of the cells was infected with 20 PFU/cell of recombinant adenovirus expressing either wild type or mutant HA. After incubating 16 h in the presence of 2.5 mM sodium butyrate, the infected cells were washed four times in phosphate-buffered saline containing 1 mM $MgCl_2$ and 0.1 mM $CaCl_2$ (PBS++) and a sorting assay was performed essentially as described (Lin et al., 1998; Matlin and Simons, 1984; Rindler et al., 1984). The washed cells were incubated in Dulbecco's modified Eagle's medium (DMEM) lacking methionine and cysteine (Invitrogen). Cells were radiolabeled from the basal surface with Easy Tag Express-^{35}S at a concentration of 2.5 mCi/ml in 140 μl for 30 min at 37° C (Lin et al., 1998). The labeled cells were chased for 60 min at 37° C in 1 ml of DMEM containing

either 10 μg/ml trypsin or 100 μg/ml soybean trypsin inhibitor added to the apical or basal compartment. The trypsin was quenched with 1 ml of DMEM containing 100 μg/ml soybean trypsin inhibitor for 15 min at 37° C, followed by an additional incubation for 30 min on ice. The cells were lysed in 1 ml of NP-40 lysis buffer (50 mM Tris-Cl pH 8.0, 1.0% NP-40, 0.1% SDS, 5 μg/ml aprotinin, and 100μg/ml soybean trypsin inhibitor) for 15 min on ice and centrifuged for 15 min at 20,000 x g at 4° C. The supernatants were immunoprecipitated with 1 μl of polyclonal antibody specific for HA and 100 μl of 10% Protein A-Sepharose (Amersham Biosciences, Uppsla Sweden) and incubated overnight with rocking at 4ºC. The beads were washed sequentially in 1 ml of NetGel (150 mM NaCl, 5 mM EDTA, 50 mM Tris pH 7.5, 0.05% NP40, 0.25% Gelatin IV (Sigma), 0.02% NaAzide) plus 0.5 M NaCl, NetGel plus 0.1% SDS, NetGel, and 10 mM Tris pH 8.0. The precipitates were resuspended in 35 μl SDS-PAGE loading buffer (125 mM Tris pH 6.8, 20% glycerol, 6% SDS, 10% BME, and 0.1% bromophenol blue), resolved by 12.5% PAGE, fixed in 10% acetic acid and 40% methanol, and analyzed by phosphor imaging (Typhoon, Molecular Dynamics). For each sample, the amount of HA accessible to trypsin on the apical, the basolateral, and both sides of the cell was measured in three separate monolayers. Cleavage of HA by endogenous proteases was measured in a fourth sample lacking trypsin. The optical density of uncleaved mature HA (the upper of two HA_0 bands, see Figure 5) and HA1 and HA2, the two cleavage products, were measured. The fraction of HA that was accessible to trypsin was calculated (HA1 + HA2)/(HA_0 + HA1 + HA2) for each sample. The resulting value was corrected for the fraction of HA cleaved to HA1 and HA2 in the sample lacking trypsin (typically <10%). The fraction of HA arriving at the apical surface was calculated as the fraction of HA cleaved

by trypsin at the apical side divided by the fraction of HA cleaved by trypsin added to both sides of the monolayer.

Detergent Insolubility Assay

1 x 10^6 MDCK cells grown on plastic dishes were infected with 10 PFU/cell of recombinant adenovirus expressing wild type or mutant HA. Infected cells were incubated for 16 h in media containing 2.5 mM sodium butyrate. For some experiments, COS-7 cells were transfected with pShuttle-CMV plasmids encoding HAs with Fugene 6 (Roche) and cultured for 24 h. For experiments to measure the effect of cholesterol depletion on DRM association, 1.25 X 10^5 COS-7 cells were plated from a subconfluent plate and transfected with wt Japan HA or HA-2A520 under the control of a CMV promoter. The cells were incubated for 24 hours, washed with serum-free DMEM, and incubated in either DMEM plus 10% fetal bovine serum, or DMEM plus 10% lipid-depleted serum (NCLPPS) (a gift from the Brown and Goldstein laboratory), 50 μM compactin, and 50 μM mevalonate for 24 hours (Brown et al., 1978; Hua et al., 1996). Cells were washed four times in phosphate-buffered saline containing 1 mM $MgCl_2$ and 0.1 mM $CaCl_2$ prior to incubation with DMEM lacking methionine and cysteine. The cells were radiolabeled with 500 μl of 0.2 mCi/ml Easy Tag Express-[^{35}S] for 30 min at 37° C, followed by a chase in DMEM for 80 min. The cells were chilled on ice for 30 min in DMEM prior to lysis in 1 ml of Triton lysis buffer (25 mM Tris-Cl pH 7.5, 150 mM NaCl, 5 mM EDTA, 1% Triton X-100, 1X protease inhibitor cocktail (Roche, Indianapolis) and 100 μg/ml soybean trypsin inhibitor) on ice for 20 min (Lin et al., 1998; Skibbens et al., 1989). The lysate was centrifuged for 5 min at 12,000 x g and 2° C in

a refrigerated microfuge. HA polyclonal antibody (1 μl), protein A Sepharose (100 μl of 10%), and a final concentration of 0.17% SDS was added to the supernatant. The pellet was resuspended with 10 strokes of a 27 gauge needle in 170 μl of solubilization buffer (50 mM Tris pH 8.8, 5 mM EDTA, 1% SDS, 1X protease inhibitor cocktail (Roche)) and incubated at 37º C for 10 min. This sample was adjusted to 1 ml with Triton lysis buffer including 1X protease inhibitor cocktail (Roche) and centrifuged for 15 min at 20,000 x g. The supernatant was removed and precipitated with 1 μl of HA polyclonal antibody and 10 μl of 10% protein A sepharose. The beads were washed sequentially in 1 ml of NetGel plus 0.5 M NaCl, NetGel plus 0.1% SDS, NetGel, and 10 mM Tris pH 8.0. The precipitates were resuspended in 35 μl SDS-PAGE loading buffer, resolved by 12.5% PAGE, fixed in 10% acetic acid and 40% methanol, and analyzed with a Typhoon scanner (Molecular Dynamics). For one of our mutant proteins, HA TM 11.2, we were not able to obtain a recombinant adenovirus. To measure the association of this protein with DRMs, it was expressed transiently in COS-1 cells. To relate the data from COS-1 cells to that obtained in MDCK cells, in every experiment with HA TM 11.2 we also transfected COS-1 cells with wild type HA and several HA mutants. The fraction of proteins that were insoluble was slightly higher in COS-1 cells than in MDCK cells, but the rank order of all mutants was the same. For simplicity of presentation, the data for HA TM 11.2 from COS-1 cells was normalized as follows: (Percent insoluble TM11.2 in COS-1) x (fraction insoluble HA wt in MDCK/fraction insoluble HA wt in COS-1).

To assure that the transmembrane mutagenesis not only affected the ability of the mutants to associate with DRMs at the plasma membrane, but also during transport from the

TGN, the cells were infected and radiolabeled as described above and incubated for 2 hours at 20° C to block transport out of the Golgi. The cells were then incubated for 0 to 60 minutes at 37° C in DMEM, followed by lysis in Triton lysis buffer and sample preparation as described above.

Fluorescence Recovery After Photobleaching

CV-1 or COS-1 cells were transfected or infected with vectors encoding X:31 HA or various Japan HA mutants. The cells were labeled with TRITC-tagged monovalent Fab' fragments alone or together with cross-linking IgGs against X31 or Japan HA. FRAP experiments were performed exactly as described in Shvartsman et al, 2003. For experiments that measured FRAP in the presence of immobilized raft markers, the cells were incubated with rabbit α-X31 antibodies, and patched with goat anti-rabbit Alexa 594.

Flotation and MAL and HA Co-immunoprecipitation Experiments

1 x 10^7 MDCK cells were infected with 5-10 PFU/cell of recombinant adenovirus encoding wild type or mutant Japan HA or myc-tagged hMAL or co-infected with both viruses for 16-18 h in medium containing 2.5 mM Na butyrate. We found that the extent to which proteins were insoluble in 1.0% Triton X-100 in the cold was influenced by the ratio of Triton lysis buffer to the cells. To standardize conditions, 3 x 10^7 uninfected MDCK cells were dissolved in 1 ml Triton lysis buffer, and added to the 1 x 10^7 infected cells. Density gradients were prepared essentially as described (Brown and Rose, 1992; Millan et al., 1997). The lysates were passed several times through a 22 gauge needle and adjusted to 40% (w/w)

sucrose in TNE (25 mM Tris-Cl pH 7.5, 150 mM NaCl, 5 mM EDTA) in a total volume of 4 ml. The dense fraction was overlaid with 1 ml of 35% (w/w) sucrose in TNE followed by 7.5 ml of a 30-5% (w/w) linear sucrose gradient in TNE. The density was determined by refractive index. The gradients were centrifuged to equilibrium at 200,000 x g for 16 h at 2º C, and 1 ml fractions were collected from the top. Twenty μl from each fraction was resolved by SDS-PAGE, immobilized on nitrocellulose, and immunoblotted with HA, myc, β-cop, or caveolin-1 antibody. β-cop and caveolin-1 were used as negative and positive markers for DRMs. For co-immunoprecipitation experiments, the buoyant fractions (fractions 3-6) and the dense fractions (fractions 9-12) were pooled separately and 450 μl from each pool was adjusted to 1 ml with Triton lysis buffer plus 1X protease inhibitor cocktail. Monoclonal antibodies specific for HA (FC.125) (100 μl) or myc (9E10) (100 μl) and Protein A Sepharose was added to each 1 ml fraction. After a 12-16 h incubation at 4º C, the immunoprecipitates were washed three times with 1 ml of Triton lysis buffer, resuspended in 35 μl of PAGE loading buffer, resolved by 12.5% PAGE, immobilized on nitrocellulose, and immunoblotted with polyclonal HA and monoclonal myc (9E10) antibodies and relative quantification of the protein bands was determined with a densitometer (Molecular Dynamics).

To determine if the HA associated with myc-tagged hMAL was enclosed in an intact vesicle, the material immunoprecipitated with myc antibody from fractions containing light membranes was washed once in Triton lysis buffer, once in TNE and resuspended in TNE containing 20 μg/ml of trypsin in the presence or absence of 0.1% SDS. After 30 min incubation at room temperature, the trypsin was denatured with SDS-PAGE loading buffer

and the samples were resolved by PAGE. The proteins were immobilized on nitrocellulose and immunoblotted with polyclonal HA or monoclonal myc antibody.

For co-immunoprecipitation of HA transmembrane mutants with myc-tagged hMAL, 1 x 10^6 MDCK cells were infected with 10 PFU/cell recombinant adenovirus expressing wild-type or mutant HA or co-infected with recombinant myc-tagged hMAL adenovirus. The infected cells were incubated at 37º C for 16-18 hours in the presence of 5 mM Na Butyrate. The cells were radiolabeled as described and incubated either at 20º C for 2 hours in serum-free DMEM followed by 0-180 minutes at 37º C in serum-free DMEM, or incubated for 100 minutes at 37º C in serum-free DMEM immediately following radiolabel. The samples were lysed in 1 ml Triton lysis buffer for 10 minutes at 37º C, followed by centrifugation for 15 minutes at 20,000 x g. 420 μl of the supernatant was incubated in either monoclonal HA or myc antibody and protein A sepharose for 16-18 hours at 4º C. The samples were washed 3 times in Triton lysis buffer, and resuspended in 35 μl of SDS-PAGE loading buffer. 1.5 μl of the samples immunoprecipitated with anti-HA and 15 μl of the samples precipitated with anti-myc were resolved by PAGE and analyzed with a Typhoon. For quantification of the amount of HA that co-precipitated with myc-tagged MAL, the percentage of HA that precipitated with anti-myc from cells expressing hMAL was corrected by subtracting the small fraction of HA that precipitated with anti-myc in the absence of hMAL.

Co-immunoprecipitation of HA and MAL After Endocytosis from the Plasma Membrane

1 x 10^6 MDCK cells were infected with 10 PFU/cell of recombinant wild-type or mutant Japan HA and/or myc-hMAL adenovirus for 16 to 18 hours at 37° C in media containing 2.5 mM sodium butyrate. The cells were washed in PBS++, followed by incubation with PBS++ containing 0.5 mg/ml (1.12 mM) EZ Link™ Sulfo-NHS-Biotin (Pierce) twice for 5 minutes and once for 15 minutes on ice to label cell surface proteins. The cells were allowed to internalize the biotinylated proteins for 0 or 60 minutes at 37° C in serum-free DMEM containing 100 μg/ml soybean trypsin inhibitor prior to lysis in 1 ml of TX-100 lysis buffer containing 1x protease inhibitor cocktail for 20 minutes at 37° C. The lysates were centrifuged at 20,000 x g for 15 minutes at 4° C. The supernatant was divided into two 450 μl aliquots and immunoprecipitated with monoclonal HA (FC.125) or myc (9E10) antibody, 100 μl 10% protein A sepharose (AmershamPharmacia), and 350 μl TX-100 lysis buffer overnight at 4° C with rocking. The immunoprecipitates were washed three times in Triton X-100 lysis buffer, resuspended in 35 μl SDS-PAGE buffer, resolved by 12.5% PAGE, immobilized on nitrocellulose, and blotted with Neutravidin-HRP (Pierce) to detect biotinylated protein in the immunoprecipitates. Blots were analyzed by densitometry (Molecular Dynamics).

Sorting Nexin 17 Cloning

cDNA was made from RNA isolated from whole rat brains (a gift from Gregory Tall) using random decamers and oligo(dT) primers (Ambion). A Not*I* site was added upstream of the start codon of SNX17 and an Xba*I* site was added downstream of the stop codon by PCR.

To add an HA epitope tag to the amino terminus of SNX17, a primer with a Kozak sequence and Bgl*II* upstream of ATG and primer T7 were used to subclone the triple HA epitope from pSM491 (a gift from Bruce Horazdovsky). The PCR product was digested with Bgl*II* and Kpn*I* and ligated into the pCB6 vector to produce pCB6 N-HA epitope. SNX17 was inserted into the pCB6 N-HA epitope vector. SNX17 adenovirus was made by subcloning the SNX17 from pCB6 N-HA into pShuttle-CMV via digestion at the Bgl*II* and Xba*I* sites. Adenovirus recombination was performed as described in the HA adenovirus construction section of Materials and Methods.

Yeast Two-Hybrid Bait Constructs

cDNA was made using oligo(dT) and random hexamers (Ambion) from RNA isolated from whole rat brains (a gift from Gregory Tall). A primer containing a start site immediately before the first histidine in the cytoplasmic tail of megalin (213 amino acids) and a BamH*I* restriction site (5'meg BamHI 5'CTTGTGATCCCATGCACTACAGGAAAACTGGCTCC) , together with a primer generating a Sal*I* site downstream of the natural stop codon (3'meg SalI 5'GCTGGGTCGACTATACGTCGGAATCTTCTT) were used to clone rat megalin into pVJL11 (megCT pVJL11). MegCT pVJL11 was transformed into L40 yeast (MATa *his3*Δ200, *trp1-901*, *leu2-3,112*, *ade2*, LYS2::(lexAop)$_4$-HIS3, URA3::(lexAop)$_8$-lacZ) using lithium acetate. Expression of the construct was verified by immunoblot of the total yeast lysate with LexA antibody (Santa Cruz). The LexA-MegCT fusion construct was expressed at the predicted molecular weight of 46 kDa. Truncations of the megalin tail were made by

the addition of a stop codon and Sal*I* site at amino acids 106, 155, or 193. A bait construct consisting of the apical sorting signal of the megalin tail (amino acids 106 to 139 of the tail (megAS)) was generated by PCR using primers adding a start codon and BamH*I* restriction site at amino acid 106 of the tail and a stop codon and Sal*I* site at amino acid 139.

Substitution of an alanine at $Tyrosine_{80}$ of the megalin tail was made by megaprimer mutagenesis (Millan et al., 1997). Primers 5'meg BamHI and megCT Y80A (5'GTGTTGTCCTTGGCTGCTGCCATTGGGTTTTCAAATATCACAGGC) were used to amplify the template megCT pVJL11. The PCR product was used as a megaprimer together with 3'meg SalI on the template megCT pVJL11 to create megY80A. megY80A was inserted into the BamH*I* and Sal*I* sites of pVJL11.

To confirm protein expression, spheroplasts of L40 yeast expressing the bait constructs were lysed with glass beads and SDS-PAGE buffer. The lysates were resolved by 12.5% PAGE, immobilized on nitrocellulose and immunoblotted with LexA antibody.

Yeast Two Hybrid Screen

A library of polyA rat brain cDNA fused to theVP16 DNA activation domain (AB849; a gift from the laboratory of Thomas Sudhof) was transformed into yeast expressing the 213 amino acid cytoplasmic tail of megalin fused to the LexA DNA binding domain. The transformed yeast were plated on media lacking tryptophan, leucine, and histidine to select yeast that were prototrophic for all three amino acids. Yeast isolates were resuspended in 100 μl of sterile water and 10 μl was patched onto plates lacking tryptophan, leucine, and histidine for 55 hours at 30° C. The patches were lifted onto 137 mm Hybond C-extra

membranes (AmershamPharmacia) and freeze fractured essentially as described (Fields and Song, 1989; Hama et al., 1999). β-galactosidase released from the yeast and bound to the nitrocellulose was detected by incubation at 30ºC for 9 minutes to 1 hour in Z buffer (60 mM Na_2HPO_4, 40 mM NaH_2PO_4, 10 mM KCl, 1 mM $MgSO_4$) containing 0.7 mg/ml X-gal (Roche). Approximately 180 colonies were scored as positive in the screen by prototrophy for histidine and visible blue color in the colorimetric β-galactosidase assay. Positive colonies were grown overnight in 10 ml of media lacking leucine, resuspended in 1 ml 10 μM DTT, 100 mM Tris pH 9.4, and incubated for 10 minutes at room temperature before centrifugation. Spheroplasts were made by resuspending the yeast pellet in 1 M sorbitol, 100 mM sodium citrate, 1% β-mercaptoethanol, and 60 mM EDTA. The yeast were incubated for 30 minutes at 30ºC and centrifuged. The spheroplasts were resuspended in 200 μl NETS (100 μM NaCl, 1 μM EDTA, 10 μM Tris pH 8.0, and 0.1% SDS) and sheared with 150-212 μm glass beads for 2 minutes. DNA was extracted with phenol:chloroform, ethanol precipited, and amplified in MC1066 *E. coli*. To select for prey constructs, the *E. coli* were replica-plated onto media lacking leucine. Prey DNA was extracted and sequenced.

Megalin Co-immunoprecipitation Experiments

5×10^5 LLC-PK1 or HeLa cells were transfected with HA-epitope tagged SNX17 or HA-epitope tagged GIPC using Lipofectamine2000 (Invitrogen). HeLa cells were used as a negative control in the experiment because they do not express a detectable level of megalin. After 4 hours at 37ºC, the media was replaced with fresh media and the cells were incubated

for an additional 22 hours at 37ºC. Cells were lysed in 700 μl TX-100 lysis buffer plus 1x protease inhibitor cocktail (Roche) for 10 minutes at 37ºC. The lysates were centrifuged at 20,000 x g for 15 minutes and the supernatant was incubated with polyclonal megalin or monoclonal HA antibody and protein A sepharose (AmershamPharmacia) at 4ºC overnight with rocking. The immunoprecipitates were washed 3 times in TX-100 lysis buffer, resuspended in 35 μl SDS-PAGE buffer, resolved by 12.5% SDS-PAGE, immobilized on nitrocellulose, and immunoblotted with monoclonal HA antibody.

Indirect Immunofluorescence

1 x 10^5 HeLa cells on No. 1 12 mm glass coverslips (Fisher Scientific) were infected with 2.5 PFU/cell of HA-SNX17 or Japan HA recombinant adenovirus for 1.5 hours at 37º C. The media was removed and replaced with fresh media for 18 hours or transfected with HA-SNX17 or Japan HA using Lipofectamine2000 (Invitrogen) for 22 hours at 37º C. The cells were washed twice in PBS++, fixed in formaldehyde for 20 minutes at room temperature with shaking, quenched with serum-free DMEM, and permeabilized in PBS++ containing 0.1% Triton X-100 for 20 minutes at room temperature. For experiments in which cell surface LDLR was measured, the cells were labeled with 4.6 μg/ml of monoclonal LDLR antibody prior to fixation with 3.7% formaldehyde and permeabilization with PBS++ containing 0.1% Triton X-100. After permeabilization, the cells were incubated with PBS++ containing 1.0% BSA for 15 minutes with shaking. The cells were labeled with monoclonal or polyclonal primary antibody diluted in PBS++ plus 1.0% BSA for 30 minutes at room

temperature, followed by labeling with a secondary goat anti-mouse or goat anti-rabbit conjugated to Alexa 488 or Alexa 568 (Molecular Probes) diluted in PBS++ plus 1.0% BSA for 30 minutes at room temperature. For experiments that measured co-localization with another protein, the primary and secondary labeling of the second protein was performed immediately after labeling the first protein of interest. The coverslips were mounted on glass slides with Aqua Poly/Mount (Polysciences, Inc).

Recycling Assay

5 x 10^5 HeLa cells were plated in 35 mm dishes and infected with 2.5 PFU/cell of recombinant HA-SNX17 or Japan HA adenovirus for 1.5 hours at 37° C. The media was removed and replaced with fresh media and incubated for 18 hours at 37° C in the presence or absence of 250 μM leupeptin (Roche). The cells were washed four times in PBS containing 0.1 mM $CaCl_2$ and 1 mM $MgCl_2$ (PBS++) and incubated twice in PBS++ containing 0.5 mg/ml (0.824 mM) EZ-Link™ Sulfo-NHS-SS-Biotin (Pierce) for 30 minutes at 37ºC. Biotinylated cells were washed in cold buffer NTC (20 mM Tris pH 8.8, 150 mM NaCl, 0.1 mM $CaCl_2$, 0.2% BSA) twice on ice and once for 5 minutes on ice (Carter et al., 1993). The cells were incubated for 0 to 30 minutes at 32° C in prewarmed buffer NTC containing 25 mM sodium 2-mercaptoethanesulfonate (MesNA) (Sigma), a cell-impermeable reducing agent used to cleave the disulfide bond in the biotin linker arm. Cells were then washed in cold buffer NTC and incubated for 20 minutes twice in buffer NTC containing 25 mM MesNA on ice. The cells were washed for 10 minutes on ice in buffer NTC containing

25 mM iodoacetic acid to quench the MesNA, followed by a wash in PBS++ or buffer NTC. TNE++ (25 mM Tris pH 7.5, 150 mM NaCl, 5 mM EDTA, 0.1% SDS, 1% Triton X-100) plus 1x protease inhibitor cocktail (Roche) was used to lyse the cells for 15 minutes on ice, followed by centrifugation for 15 minutes at 20,000 x g. Biotinylated proteins were precipitated from the supernatants using 30 μl of Immobilized Neutravidin Biotin Binding Protein (Pierce). The supernatants were washed sequentially in NetGel (150 mM NaCl, 5 mM EDTA, 50 mM Tris pH 7.5, 0.25% Gelatin IV, 0.2% sodium azide) containing 0.5M NaCl, NetGel plus 0.1% SDS, and 10 mM Tris pH 8.0. Beads were resuspended in 50 μl SDS-PAGE buffer, resolved by 10% PAGE, immobilized on nitrocellulose, and immunoblotted with monoclonal antibody recognizing LDLR (HL-1) or transferrin receptor. Immunoblots were quantified by densitometry. The percentage of internal LDLR or TfR remaining after each time point was calculated relative to the total LDLR or TfR at time zero for each condition. The values were plotted with Graphpad Prism® software and the rate constant (K) was calculated by fitting the data to a non-linear exponential decay curve.

LDLR Degradation Assay

5 x 10^5 HeLa cells were infected with 2.5 PFU/cell recombinant HA-SNX17 or Japan HA adenovirus for 1.5 hours at 37° C. The media was removed and replaced with fresh media for 18 hours at 37° C. The cells were washed in PBS++, incubated for 30 minutes at 37° C in DME^- lacking methionine and cysteine (Invitrogen), followed by labeling with 0.2 mCi/ml ^{35}S-amino acids (MP Biomedical/ICN). Labeled cells were washed twice in PBS++

on ice and incubated for 10 minutes on ice in complete media. The cells were incubated for 0 to 30 hours at 37º C in complete media, followed by washing in PBS++ on ice for 15 minutes. Lysates were prepared in 1 ml of TNE++ containing 1x protease inhibitor cocktail (Roche) and centrifuged at 20,000 x g for 15 minutes. LDLR was immunoprecipitated from the supernatants with 1 μl of anti-LDLR (HL-1) and 25 μl of Protein A/G Plus Agarose (Santa Cruz) overnight at 4º C with rocking. Immunoprecipitates were washed sequentially in NetGel containing 0.5M NaCl, NetGel plus 0.1% SDS, and 10 mM Tris pH 8.0. The beads were resuspended in 35 μl SDS-PAGE, resolved by 10% PAGE, fixed in 10% acetic acid and 40% methanol, and analyzed by phosphorimaging (Typhoon, Molecular Dynamics). The mature, 160 kDa form of the receptor was quantitated in the assay. The percentage of mature LDLR was determined relative to the highest value of mature LDLR in the time course. For cells infected with SNX17, the amount of mature LDLR was highest after 2 hours of incubation in the chase media, so the decay curve was plotted relative to the 2 hour time point. In HA-infected cells, the maximum amount of mature LDLR was observed after 3 hours of incubation in the chase media. The data was plotted with Graphpad Prism® software and the rate constant (K) was calculated by fitting to a non-linear exponential decay curve.

Short Interfering RNA Transfection and Quantitative PCR

Two pairs of short interfering RNA (siRNA) oligonucleotides were designed to deplete SNX17 in HeLa cells. The siRNA pairs were designed by Ambion's Target Finder

program (http://www.ambio.com/techlib/misc/siRNA_finder.html). The first oligonucleotide (si1) was a 21 nucleotide complementary pair directed at the sequence beginning at nucleotide 500 in the human SNX17 gene (5'AGAGGAUGGAGCCUUUUCUTT and 5'AGAAAAGGCUCCAUCCUCUTT). The second pair of oligonucleotides started at position 183 in the SNX17 gene (5'AGAAGCUUUUCUCUCUGACTT and 5'GUCCAGAGAGAAAAGCUUCUTT). The oligonucleotides were diluted to 40 μM in annealing buffer (100 mM potassium acetate, 30 mM HEPES-KOH pH7.4, 2 mM magnesium acetate) and the complementary oligonucleotides combined 1:1 to a final concentration of 20 μM for each oligonucleotide. The pairs were heated for 1 minute at 90º C, followed by incubation for 1 hour at 37º C. For transfections, 3 x 10^5 HeLa cells in 35 mM wells were plated for 2 hours in normal media. 10 μl of the annealed 20 μM siRNA pair was combined with 170 μl of OPTI-MEMI (Invitrogen). In a separate tube, 4 μl of Oligofectamine (Invitrogen) was combined with 20 μl of OPTI-MEMI for 5 minutes. The tubes were mixed for 20 minutes at room temperature before 200 μl of OPTI-MEMI was added to the mixture. The complete siRNA-Oligofectamine mix was added to cells in which the media was replaced with 600 μl OPTI-MEMI and incubated at 37 ºC overnight. The OPTI-MEMI media was replaced with normal media or media containing lipoprotein-deficient serum (a gift from the laboratory of Michael Brown and Joseph Goldstein) for an additional 30 hours.

For quantitative PCR (QPCR) experiments, RNA was harvested with RNA-STAT-60 (Tel-Test, Inc.) and cDNA generated with random hexamers (pDN6 Roche) and SuperscriptII reverse transcriptase (Invitrogen). SNX17 primers

(5'CACTATGGCTACTTGCGCTTTG and 5'ACCACCACAGGACAGTCCTTT) were generated using TaqMan Probe software. The QPCR reaction included 50 ng of cDNA, 150 nM of each primer, and 10 μl of SYBR Green PCR Master Mix (Applied Biosystems). QPCR was performed on an ABI PRISM 7000 Sequence Detection System (Applied Biosystems). SNX17 primers were validated in the linear range of the control cylophilin primers (5'GGAGATGGCACAGGAGGAA and 5'GCCCGTAGTGCTTCAGCTT) (a gift from the laboratory of Joyce Repa (UTSW)). LDLR primers (5'CAGAGGCAGAGCCTGAGTCA and 5'CGGGTGTCTCAGGCACTTAA) were a gift from the laboratory of David Mangelsdorf (UTSW). mRNA levels were normalized to the control by the comparative Ct method (User Bulletin No. 2 Perkin Elmer).

Cell Surface Protein Measurement

Cell surface proteins were measured at steady state by fluorescence-activated cell sorting (FACS). 1 x 10^5 HeLa cells were infected with 2.5 PFU/cell of recombinant HA-SNX17 or Japan HA adenovirus for 18 hours at 37° C in normal media or DMEM containing 10% lipoprotein deficient serum (a gift from the laboratory of Michael Brown and Joseph Goldstein). The cells were washed four times in PBS++, followed by an incubation for 1 hour at 4° C in PBS++ containing 1% BSA and 4.6 μg/ml of LDLR antibody (HL-1). Unbound antibody was removed by washing the cells four times in PBS++, followed by an incubation for 1 hour at 4° C in PBS++ containing 1% BSA and a 1:500 dilution of goat anti-mouse Alexa 488 secondary antibody (Molecular Probes). The cells were washed 4 times in

PBS++ and cells were detached with cell dissociation solution (Sigma) for 5 minutes at room temperature. The detached cells were resuspended in complete media, centrifuged, resuspended in PBS, and analyzed by FACS (Becton Dickinson FACSCaliber). The mean fluorescent intensity was calculated for 20,000 cells. Cells treated with lipoprotein-deficient serum to increase LDLR expression were compared to untreated cells to assure that the fluoresent intensity was specific to LDLR.

Transferrin Internalization Assay

1 x 10^5 HeLa cells were infected with 100 PFU/cell recombinant HA-SNX17 or control HA adenovirus for 16-18 hours at 37º C in normal media. Cells were washed four times in PBS containing 1 mM $MgCl_2$ and 0.1 mM $CaCl_2$ (PBS++) and incubated in DMEM for 30 minutes at 37º C. DMEM was aspirated and replaced with pre-warmed PBS++ containing 0.2% BSA and 50 μg/ml Tf conjugated to Alexa 488 (Molecular Probes) for 0 to 30 minutes at 37º C. The cells were washed on ice twice in DMEM, once in PBS++, once in PBS++ buffered to pH 5.0 with acetate for 5 minutes, and once in PBS++. The cells were detached with trypsin-EDTA for 2 minutes at room temperature and analyzed by fluorescence-activated cell sorting (FACS) (BD FacsCaliber). The average intensity of 20,000 cells for each time point was recorded.

CHAPTER THREE

FEATURES REQUIRED FOR HEMAGGLUTININ SORTING ARE DIFFERENT FROM THOSE REQUIRED FOR ASSOCIATION WITH DRMS AND MAL

INTRODUCTION

Polarized epithelial cells maintain distinct apical and basolateral surfaces by sorting membrane proteins in both the biosynthetic and endocytic pathways (Mostov et al., 2000; Simons and Ikonen, 1997; Van et al., 2000). Madin-Darby canine kidney (MDCK) cells transport glycosphingolipids (van Meer and Simons, 1988), proteins with glycolipid anchors (Brown et al., 1989; van Meer and Simons, 1988), and some transmembrane proteins (Skibbens et al., 1989) to the apical cell surface as part of a membrane that is insoluble in Triton X-100 at low temperatures. The influenza virus hemagglutinin (HA) is a transmembrane glycoprotein that becomes insoluble in Triton X-100 with the same kinetics that it receives terminal glycosylation in the Golgi (Skibbens et al., 1989), which occurs slightly before or at the time at which sorting of HA in epithelial cells is thought to occur. However, the precise relationship between the ability to enter a DRM and the ability to be sorted to the apical surface is not clear. Some apical proteins never show any indication of entering DRMs but are efficiently sorted (Casanova et al., 1991; Jacob and Naim, 2001; Skibbens et al., 1989). Thus, entering a DRM may not be necessary for all protein traffic to the apical surface. In addition, mutagenesis studies of different proteins have identified examples of sequences important for apical sorting in the cytoplasmic, TM, and luminal domains (Chuang and Sung, 1998; Jacob and Naim, 2001; Kundu et al., 1996; Lin et al.,

1998). These observations could indicate that there are multiple sorting mechanisms or even multiple pathways to the apical surface.

Eukaryotic plasma membranes have an asymmetric distribution of sphingomyelin, phosphatidylcholine, phosphatidylserine, and phosphatidylethanolamine in the lipid bilayer. Mutation of residues of the HA TM that would reside in the outer leaflet of the membrane, where glycosphingolipids and cholesterol are enriched, cause HA to be transported randomly to both surfaces or even to be predominantly sorted to the basolateral membrane (Lin et al., 1998). There is a strong correspondence between the loss of ability to partition into DRMs and defective HA sorting. However, previous studies are open to several interpretations. As one possibility, the mutations that inhibit HA sorting might disrupt a hydrophobic surface on the TM required for an interaction with lipids or a membrane protein that sorts HA into DRMs and into the apical pathway. A candidate for a protein that might interact with HA within a glycosphingolipid and cholesterol enriched membrane domain is the small, multi-spanning Myelin and Lymphocyte (MAL) membrane protein that is found in DRMs (Zacchetti et al., 1995). When MAL expression is attenuated in MDCK cells with antisense oligonucleotides, apical sorting of HA and other membrane proteins is inhibited (Cheong et al., 1999; Martin-Belmonte et al., 2000; Puertollano and Alonso, 1999).

Alternatively, mutations that disrupt sorting might affect the structure of the HA TM domain and even adjoining sequences in the HA external domain, in which case the sorting interaction might occur elsewhere in the protein. HA is a trimeric protein and there is strong conservation in the HA TM sequence among the major subtypes of influenza A viruses

(Martin-Belmonte et al., 2000). The most conserved positions include a pattern of small residues resembling several motifs that promote oligomerization of TM domains (Lazarovits et al., 1990; Zhou et al., 2001). In the previous alanine scan mutagenesis of the HA TM, all of the mutations that affected HA sorting included at least one of these conserved positions that might contribute to tertiary structure. Thus, these studies did not distinguish between short-range and long-range contributions of the HA TM domain to the processes of partitioning into DRMs and apical sorting.

To determine the minimum sequence of HA required for apical sorting, partitioning into DRMs, and interaction with MAL, I have replaced 24 of the 25 residues of the HA TM with leucines. The resulting protein, as expected, did not enter DRMs and was transported randomly to the apical and basolateral surfaces of MDCK cells. Into this mutant background, I have systematically replaced the wild type HA sequence and then measured the effects on aspects of HA transport listed above. My results indicate that the HA TM contains an interaction surface required for all three characteristics. Several mutants that did not interact with DRMs retained some ability to be sorted apically. These mutants were subsequently determined to have a transient association with lipid rafts, as measured by fluorescence recovery after photobleaching in the presence of immobilized rafts. Loss of DRM partioning also diminished the HA and MAL association.

RESULTS

Mutagenesis of the HA Transmembrane Domain

A previous alanine scan of the Japan HA TM sequence revealed that changing blocks of two or four consecutive amino acids to alanine in the region of the TM that would sit in the outer leaflet of the lipid bilayer interfered with the ability of the mutant HAs to enter DRMs or be correctly sorted in MDCK cells (Lin et al., 1998; Scheiffele et al., 1997). In contrast, changes to residues of the TM domain that would reside in the inner leaflet were not as essential for entry into DRMs or apical sorting (Lin et al., 1998). With one exception, changing any of these residues to alanine caused little change in the kinetics of HA transport to the cell surface or in the ability of the protein to fold properly. Comparison of the TM sequences of HAs from all 15 major serotypes of influenza A viruses reveals very strong conservation of residues with small side chains at several positions within the region where changes to alanines disturb HA sorting (Figure 4). In contrast, there is relatively little sequence conservation among HAs in the region of the TM domain that would sit in the inner leaflet of the bilayer. The pattern of small conserved residues resembles motifs that promote oligomerization of transmembrane helices (Dawson et al., 2002; Lin et al., 1998), presumably by allowing interchain hydrogen bonding, and these residues may stabilize the HA TM. If this is the case, then the fact that mutations of residues that reside in the outer leaflet change HA behavior more than changes to residues in the inner leaflet might simply be caused by disruption of an important structural element present in the amino terminal half of the TM domain. The effect of these changes for HA function might not be limited to or even directly involve residues residing in the hydrophobic core of the membrane but might

involve nearby residues in the external domain that are positioned to interact with lipid head groups.

Outer Leaflet																									
V	I	L	W	F	S	F	G	A	S	C	V	M	L	L	A	I	A	M	G	L	I	F	M	C	H15 duck/Australia/341/83
V	I	L	W	F	S	F	G	A	S	C	V	M	L	L	A	I	A	M	G	L	I	F	M	C	H15 Shearwater/W.Aus/2576
M	I	L	W	I	S	F	S	M	S	C	F	V	F	V	A	L	I	L	G	F	V	L	W	A	H14 Dk/Gurjev/244/82
I	I	L	W	I	S	F	S	M	S	C	F	V	F	V	A	L	I	L	G	F	V	L	W	A	H14 Dk/Gurjev/263/82
I	I	L	W	F	S	F	G	A	S	C	F	V	L	L	A	A	V	M	G	L	V	F	F	C	H10 Chick/Ger/N/49
I	I	L	W	F	S	F	G	E	S	C	F	V	L	L	A	V	V	M	G	L	V	F	F	C	H10 Mink/Sweden/84
V	I	L	W	F	S	L	G	A	S	C	F	L	L	L	A	I	A	M	G	L	V	F	M	C	H7 Chick/Vic/1/85
V	I	L	W	F	S	F	G	A	S	C	F	L	L	L	A	I	A	V	G	L	V	F	I	C	H7 FPV/Rostock/34
I	I	L	W	I	S	F	S	I	S	C	F	L	L	V	A	L	L	L	A	F	I	L	W	A	H4DK/NZ/31/76
I	I	L	W	I	S	F	S	I	S	C	F	L	L	V	A	L	L	L	A	F	I	L	W	A	H4 DK/Czech/56
W	I	L	W	I	S	F	A	I	S	C	F	L	L	C	V	V	L	L	G	F	I	M	W	A	H3 Mem/6/86
W	I	L	W	I	S	F	A	I	S	C	F	L	L	C	V	V	L	L	G	F	I	M	W	A	**H3 Hong Kong/1968 (X:31)**
W	I	L	W	I	S	F	A	I	S	C	F	L	L	C	V	V	L	L	G	F	I	M	W	A	H3 Equine/Algeria/72
A	L	S	I	Y	S	C	I	A	S	S	V	V	L	V	G	L	I	L	S	F	I	M	W	A	H13 Gull/MD/704/77
A	L	S	I	Y	S	C	I	A	S	S	V	V	L	V	G	L	I	L	A	F	I	M	W	A	H13 Whale/Maine/328/84
I	L	S	I	Y	S	S	V	A	S	S	L	V	L	L	L	M	I	I	G	G	F	I	F	G	H12 Dk/Alberta/60/76
I	L	S	I	Y	S	C	I	A	S	S	L	V	L	A	A	L	I	M	G	F	M	F	W	A	H11 Dk/Eng/56 H11
I	L	T	I	Y	S	T	V	A	S	S	L	V	L	A	M	G	F	A	A	F	L	F	W	A	H9 Chicken/Beijing/1/94
I	L	T	I	Y	S	T	V	A	S	S	L	V	L	A	M	G	F	A	A	F	L	F	W	A	H9 Turkey/Wis/66
I	L	S	I	Y	S	T	V	A	A	S	L	C	L	A	I	L	I	A	G	G	L	I	L	G	H8 Turkey/Ont/6118/68
I	L	A	I	Y	S	T	V	S	S	S	L	V	L	V	G	L	I	I	A	M	G	L	W	M	H6 Mallard /Alberta/211/85
I	I	A	I	Y	S	T	V	S	S	S	L	V	L	V	G	L	I	I	A	V	G	L	W	M	H6 Shearwater/Aus/1/72
I	L	S	I	Y	S	T	V	A	S	S	L	A	L	A	I	M	V	A	G	L	S	F	W	M	H5 Chick/Penn/1370/83
I	L	S	I	Y	S	T	V	A	S	S	L	A	L	A	I	M	I	A	G	L	S	F	W	M	H5 Chick/Scot/59
I	L	A	I	Y	A	T	V	A	G	S	L	S	L	A	I	M	M	A	G	I	S	F	W	M	H2 Berlin/3/64
I	L	A	I	Y	A	T	V	A	G	S	L	S	L	A	I	M	M	A	G	I	S	F	W	M	**H2 Japan/305/57**
I	L	A	I	Y	S	T	V	A	S	S	L	V	L	L	V	S	L	G	A	I	S	F	W	M	H1 WSN/33
I	L	A	I	Y	S	T	V	A	S	S	L	V	L	L	V	S	L	G	A	I	S	F	W	M	H1 USSR/90/77

Figure 4. Amino acid sequences of the transmembrane segments of HAs from the 15 major serotypes. The sequences can be grouped into two classes (H1-like and H3-like) by sequence relationships. The four positions that are highly conserved between the two classes are indicated by the boxes.

To determine the minimal necessary and sufficient sequence for apical sorting and isolation in DRMs, the sequence encoding the transmembrane domain of HA was replaced with sequences encoding an isoleucine followed by 24 leucines (Figure 5).

Figure 5. TM sequences of HA mutants in which wild type amino acids are systematically replaced into the background of TM 4.0. The number to the left of the decimal indicates the number of wild type residues present in the TM sequence. All sequences began with the wild type residue isoleucine for technical reasons (see Materials and Methods). The Japan HA TM sequence contains 3 leucines. The number to the right of the decimal distinguishes mutants that have the same number of wild type residues in different positions. DNAs encoding HAs with the mutant TM sequences indicated were recombined into replication defective adenovirus vectors with the exception of TM 11.2, which was expressed transiently in pShuttle-CMV. All experiments in this report that employed adenoviruses used cells infected with comparable virus titers (10 or 20 pfu/cell).

A

WT HA	ILAIYATVAGSLSLAIMMAGISFWM
2A520	ILAIYATVAAALSLAIMMAGISFWM
HA TM 4.0	ILLLLLLLLLLLLLLLLLLLLLLLL
HA TM 7.0	ILLLLALLLGSLLLLLLLLLLLLLL
HA TM 7.1	ILLLYATLLLLLLLLLLLLLLLLLL
HA TM 9.0	ILLLYATLLGSLLLLLLLLLLLLLL
HA TM 11.0	ILLLYATVAGSLLLLLLLLLLLLLL
HA TM 12.0	ILLLYATVAGSLSLLLLLLLLLLLL
HA TM 13.0	ILALYATVAGSLSLLLLLLLLLLLL

B

HA TM 11.1	ILLLLATVAGSLSLLLLLLLLLLLL
HA TM 11.2	ILLLYLTVAGSLSLLLLLLLLLLLL
HA TM 11.3	ILLLYALVAGSLSLLLLLLLLLLLL
HA TM 11.4	ILLLYATLAGSLSLLLLLLLLLLLL

A series of proteins were made in the HA TM 4.0 background in which amino acids from wild-type A/Japan/305 HA were used to substitute for the leucines in HA TM 4.0. Based on previously reported data (Lin et al., 1998) and the conservation between HA proteins of different influenza A subtypes (Figure 4), the most conserved residues were replaced first (HA TM 7.0) and then additional residues were added (Figure 5). A peptide of the transmembrane domain of the X:31 HA serotype forms an alpha helix that trimerizes when reconstituted into lipid micelles (Tatulian and Tamm, 2000). Although it is unknown where each of the amino acids in the transmembrane domain is positioned with respect to each other in trimer bundle, a helical wheel model can be constructed to project the amino acids that may reside in the internal or external surfaces of the trimer (Figure 6).

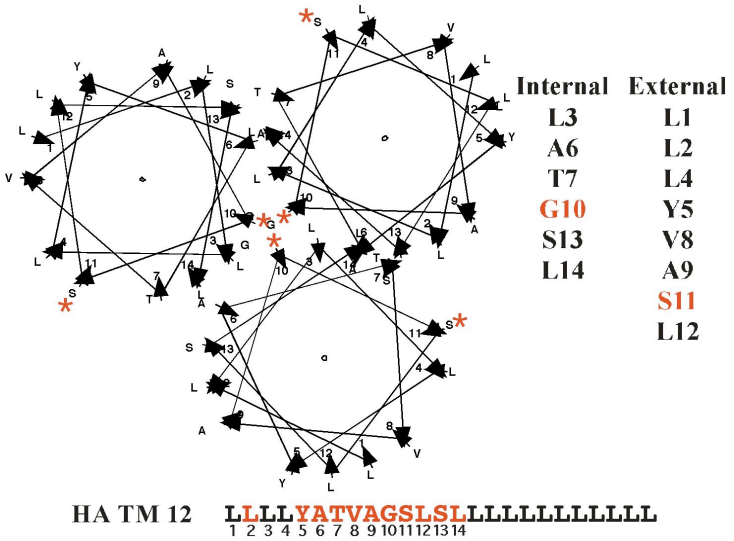

Figure 6. Conserved amino acids in the transmembrane domain of HA 12.0 that would reside in the exoplasmic leaflet of the bilayer are located on the external and internal surfaces of the HA trimer. Helical wheel projection of the transmembrane domain of HA TM 12.0.

The most conserved amino acids in the transmembrane domain would be located on both the external and internal surfaces of the trimer, suggesting that HA requires interaction between the alpha helices of the trimer as well as interaction with a protein or lipid that stabilizes association with lipid rafts. To determine if localization to the internal or external surface of the trimer was important for detergent resistant membrane association or apical sorting, four consecutive residues, which represent a single turn of the alpha helix, were mutated to leucine in the background of the HA TM 12.0 mutant. These mutant HA sequences were recombined into replication defective adenoviruses which were used to infect MDCK cells. All of the HA transmembrane mutant constructs were correctly folded and were transported from the ER to the plasma membrane of MDCK cells (Figure 7). Some of the mutants were not transported to plasma membrane with the same kinetics as wild-type HA. However, analysis of the sorting phenotype does not require that all of the mutants are trafficked to the

cell surface with the same efficiency. For the purpose of this study, only a detectable level of the mutant HA needs to be properly folded and transported to the cell surface in the selected period of time.

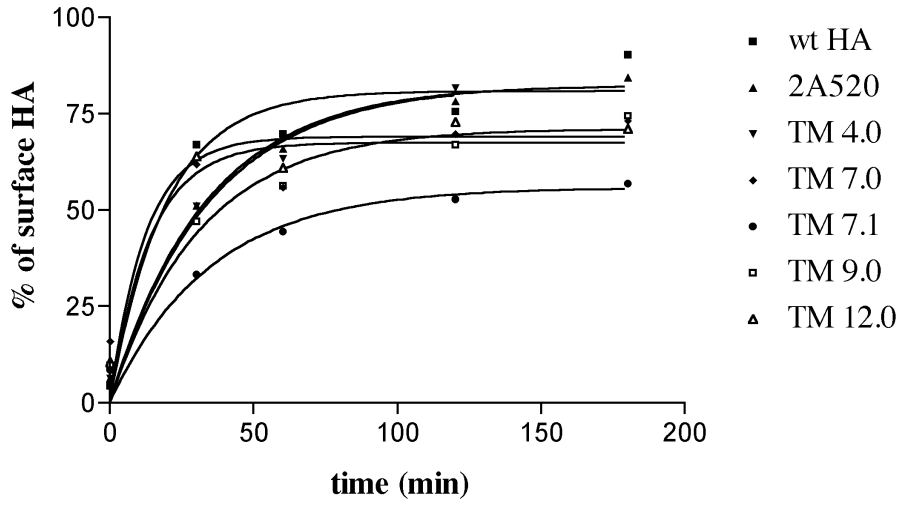

Figure 7. HA transmembrane mutants are efficiently transported to the plasma membrane. MDCK cells infected with the indicated HA mutant recombinant adenovirus were labeled with [^{35}S]-methionine and cysteine, incubated at 20ºC for 2 hours to synchronize proteins in the TGN, and chased in serum-free DMEM containing trypsin at 37ºC for the indicated times. HA was immunoprecipitatated from the lysates, resolved by 12.5% SDS-PAGE, and quantitated with a phosphorimager. The cell surface population was quantitated by measuring the percentage of HA cleaved by trypsin into HA1 and HA2.

Ten Consecutive Amino Acids in the Transmembrane Domain of HA are Required for HA to be Isolated in DRMs

To determine the minimum sequence required for HA mutants to be isolated in DRMs, MDCK cells were infected with recombinant adenovirus expressing wild type or mutant Japan HAs. After 12 to 16 h, the infected cells were metabolically labeled with [^{35}S]-

amino acids prior to incubation with serum-free DMEM for 80 min to chase the protein to the cell surface. The cells were lysed with buffer containing 1% Triton X-100 at 4° C and

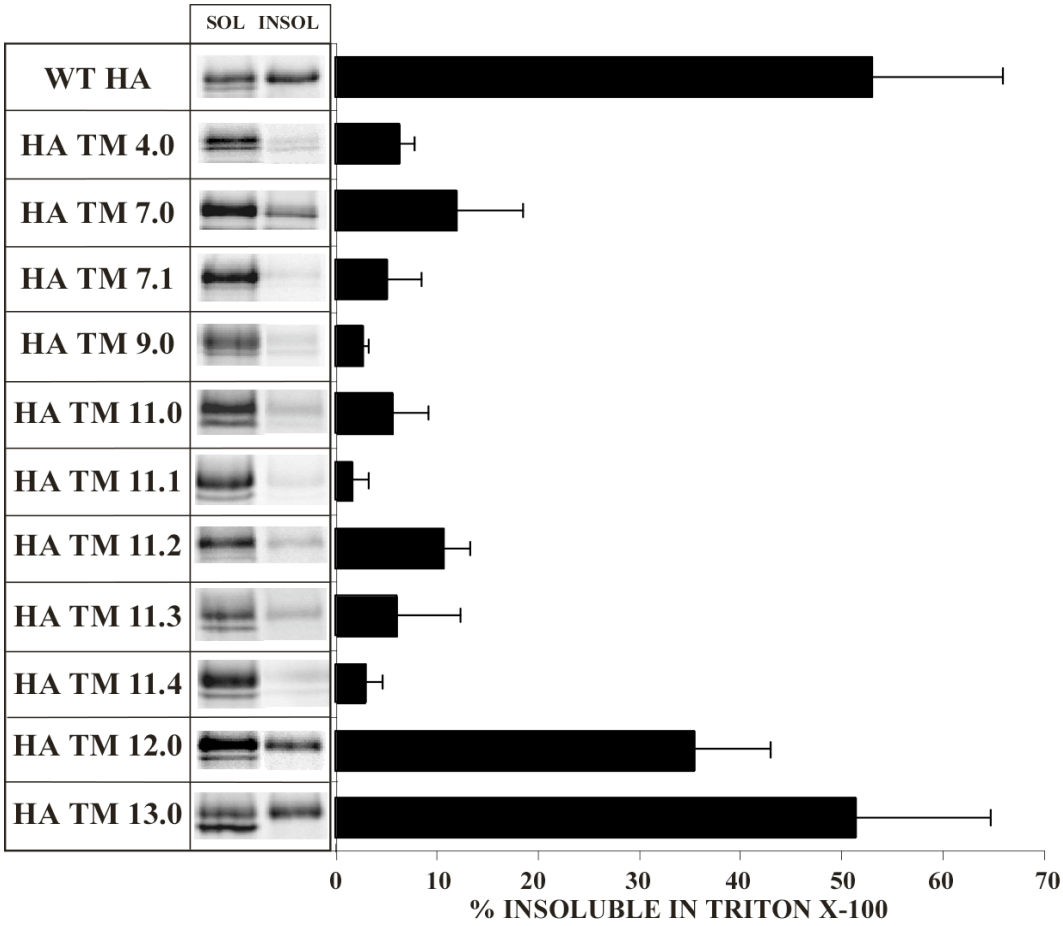

Figure 8. Ten consecutive amino acids in the transmembrane domain of HA are required to confer a detergent-resistant phenotype. Cells expressing HAs as described in the Materials and Methods chapter were labeled with [^{35}S]-methionine and cysteine, followed by an 80 min chase in serum-free DMEM. The cells were lysed on ice for 20 min in 1 ml of Triton lysis buffer, followed by centrifugation. The supernatant and pellet were immunoprecipitated with α-HA and protein A Sepharose. The washed immunoprecipitates were resuspended in SDS-PAGE loading buffer and electrophoresed on 12.5% SDS-PAGE. The samples were analyzed with a phosphor imager. For each protein, the averages of 3 to 10 replicates of the experiment are shown on the graph. Error bars are the standard deviation.

centrifuged to separate the soluble and insoluble fractions. The wild type HA was approximately 55% insoluble in cold Triton X-100, while HA TM 4.0 was almost completely soluble (Figure 8). To regain significant ability to be isolated in DRMs in this assay, HA required restoration of ten consecutive wild type amino acids into HA TM 4.0 to produce HA TM 12.0 (Figure 8). Changing even a single amino acid of this minimal sequence back to leucine significantly impaired the ability of the mutant to be insoluble in Triton X-100 (TM 11.1 – TM 11.4). Expression levels of HA did not significantly impact the ability of the protein to be incorporated into DRMs (Figure 9).

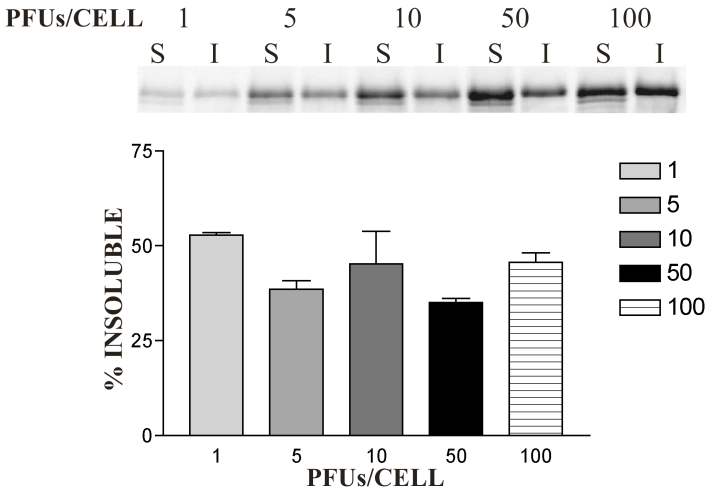

Figure 9. HA expression does not affect the percentage of protein associated with DRMs. MDCK cells were infected with the indicated PFU per cell of wt HA adenovirus as described in Methods. The cells were radiolabeled with [^{35}S]- methionine and cysteine, followed by an 80 minute incubation in serum-free DMEM at 37ºC. HA was immunoprecipitated, resolved by 12.5% SDS-PAGE, and quantitated with a phosphorimager.

To determine if the lack of association with DRMs observed for the TM 11 mutants also extended to the proteins in the Golgi and during transport from the TGN, the proteins were radiolabeled and synchronized at the exit of the TGN with a 20ºC block for 2 hours.

HA TM 12.0 retained essentially the same phenotype of DRM association during transport as at the plasma membrane (Figure 10). HA TM 11.0 in the Golgi and during transport to the plasma membrane showed no association with DRMs.

Figure 10. DRM association occurs prior to localization at the plasma membrane. Cells expressing HA TM 11.0 or TM 12.0 were radiolabeled as described in Methods, followed by incubation for 2 hours at 20° C to block the protein in the TGN. The proteins were released by incubation for 0-60 minutes at 37° C, lysed, immunoprecipitated with α-HA, and quantitated with a phosphorimager. The error bars on the graph represent the SEM.

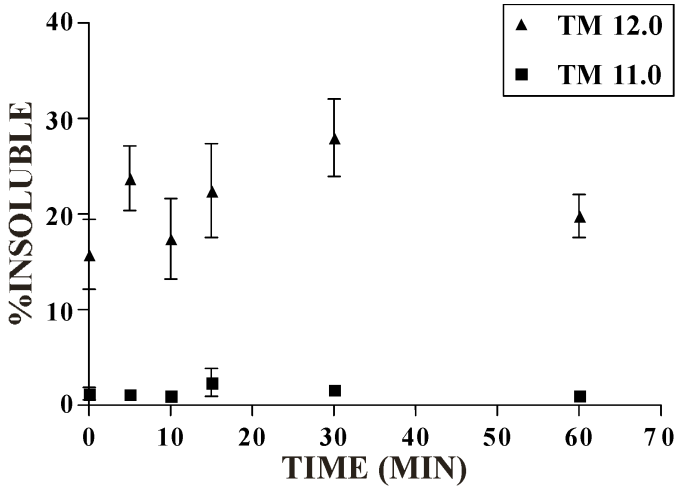

If detergent insoluble proteins are in DRMs, they will float with the membranes during centrifugation on density gradients (Brown and Rose, 1992). Approximately 24% of wild type HA floats with light membranes to positions in a sucrose gradient that also contain both MAL and caveolin-1, two markers for DRMs (Figure 11). Only 0.6% of HA TM 4.0 floated to those positions in a density gradient (Figure 11). HA TM 12.0, which contained the minimum sequence capable of exhibiting insolubility to Triton X-100 in the differential centrifugation assay also floated on a density gradient.

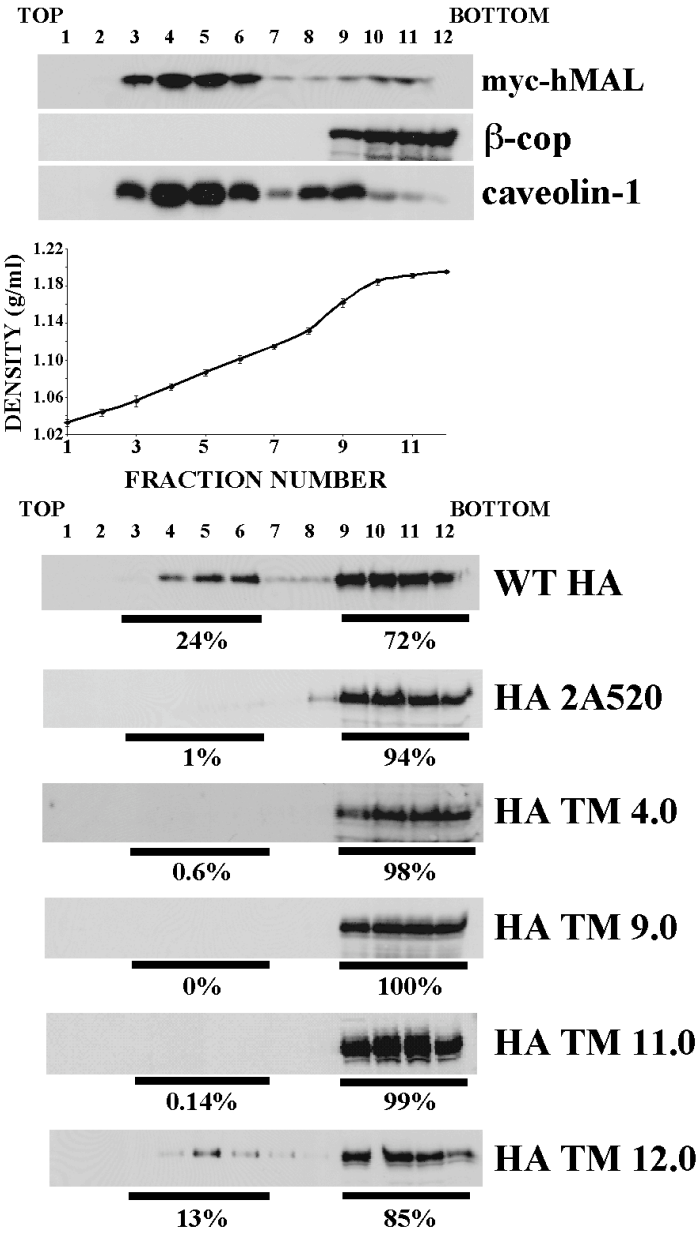

Figure 11. Ten consecutive amino acids in the transmembrane domain of HA are required for flotation on a density gradient. MDCK cells were infected with recombinant adenovirus for 18 h and lysed in cold Triton lysis buffer on ice. The lysates were adjusted to 40% (w/w) sucrose and overlaid with a 35% sucrose cushion, followed by overlay with a linear 30-5% sucrose gradient. The gradients were centrifuged to equilibrium and fractionated into 1 ml aliquots. A sample from each fraction was denatured in SDS-PAGE loading buffer, electrophoresed, and immunoblotted with α-HA, α-myc, α-β-cop, or α-caveolin. HA 2A520 is a previously described mutant that is sorted mainly to the basolateral surface of MDCK cells and does not enter DRMs (Lin *et al.*, 1998) Protein bands were analyzed with a densitometer. The exposure of the immunoblot for mutant TM 11.0 was increased relative to the other proteins to increase the chance of detecting any small fraction that might have floated with DRMs.

Although they differed by a single amino acid, mutants HA TM 11.1, 11.2, 11.3 and 11.4 (Figure 5) were unable to resist detergent extraction as compared to HA TM 12.0. If, as is likely, the HA TM domain adopts an alpha helix in the membrane, loss of one wild type

residue at every position in one turn of the helix had this effect. This means that not only residues that might face the interior of a bundle of three alpha helices, but also residues that face out into the lipid bilayer are required for partitioning into DRMs, and even a single change in this outer surface substantially reduces the interaction.

HA Requires at Least 11 Wild-Type Amino Acids in the Transmembrane Domain to be Sorted to the Apical Surface.

MDCK cells in confluent monolayers on Transwell filters were infected with recombinant adenoviruses. The cells were subjected to the pulse-chase protocol described in Materials and Methods to determine the proportion of HA that was delivered to the apical or basolateral surface. An example of such an experiment, which measures HA at the cell surface by its accessibility to trypsin included in the chase medium, is shown in Figure 12. Wild-type Japan HA was preferentially sorted to the apical surface (Figure 12), as previously observed (Lin et al., 1998; Matlin and Simons, 1984; Rindler et al., 1984). HA TM 4.0 was randomly transported to both the apical and basolateral surfaces (Figure 12), indicating that wild-type transmembrane sequences are required for directional transport. Essentially no sorting of HA mutants was observed until wild type amino acids from positions 5 to 12 were added back into the TM 4.0 sequence (TM 11.0). Adding the small residues alanine 3 and serine 13 to this sequence restored sorting of the mutant HA almost to that of HA wild type. For technical reasons, all the proteins had a wild type isoleucine at position 1, and position 2 is a leucine in the wild type sequence. Position 4 is an isoleucine in the wild type sequence

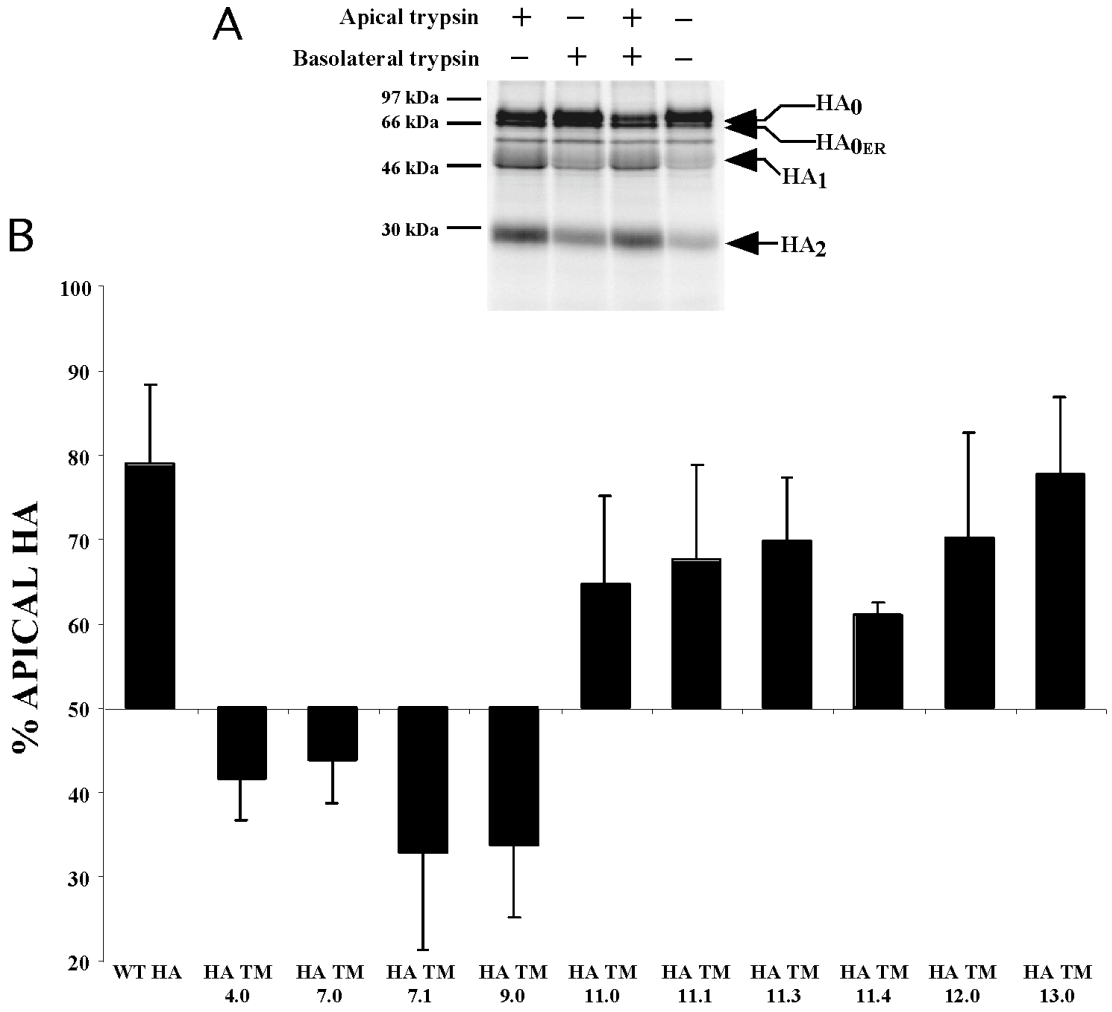

Figure 12. Most of the amino acids of HA that would reside in the outer leaflet are required to target HA to the apical membrane. (A) MDCK cells grown to confluency on filters were infected with recombinant adenovirus expressing Japan HA as described in Materials and Methods. The cells were labeled with [^{35}S]-methionine and cysteine, followed by a 60 min chase in the presence of 10 μg/ml trypsin added to the apical or basolateral surface. Following trypsin inhibition, the cells were lysed and HA immunoprecipitated with -HA and protein A Sepharose. The immunoprecipitates were washed and resolved by SDS-PAGE and analyzed with a phosphor imager. (B) Apical sorting was determined by calculating the percentage of total HA that was cleaved into HA1 and HA2 in the presence of trypsin added to the apical or basolateral compartments. For each protein, the averages of 3 to 4 replicates of the experiment are shown on the graph with error bars indicating standard deviations.

that one would expect to be substituted well by leucine. Therefore, to restore HA sorting to near wild type levels requires essentially the entire region of the protein that would reside in the outer leaflet, from positions 1 to 13.

To determine if side chains that form the outer surface of the HA TM are required for apical sorting, the mutants TM 11.1, TM 11.3 and TM 11.4 were tested in the sorting assay. In contrast to the effect of these mutations on partitioning into DRMs, individually changing the wild type residues to leucine at positions from 5 to 8 in the TM 12.0 background had insignificant effects on apical sorting (Figure 12). If the ability of HA to be isolated in DRMs accurately reflects the ability of HA to partition into lipid rafts, then stable integration into rafts is not required for apical transport. Alternatively, these mutations might have caused a reduction of affinity of HA for lipid rafts which is small or insignificant *in vivo* but large enough to allow HA to be extracted from DRMs *in vitro*. To examine the possibility that Triton X-100 is not the best choice of detergent to measure raft association, we extracted cells with 1% CHAPS, Brij 97 or Brij 98, detergents that have been reported to discriminate between raft and non-raft proteins (Figure 13) (Lin et al., 1998; Schuck et al., 2003). HA TM 4.0, which is not sorted apically or exhibits any ability to interact with lipid rafts *in vivo* (see following pages), was between 40 and 50% insoluble in CHAPS and Brij 98 respectively, whereas HA wild type was more than 90% insoluble in both detergents. Both wild type HA and HA TM 4.0 were completely soluble in Brij 97 (Figure 13). Therefore, these other detergents were inferior to Triton X-100 in their ability to identify proteins that behave like lipid raft-associated proteins *in vivo*.

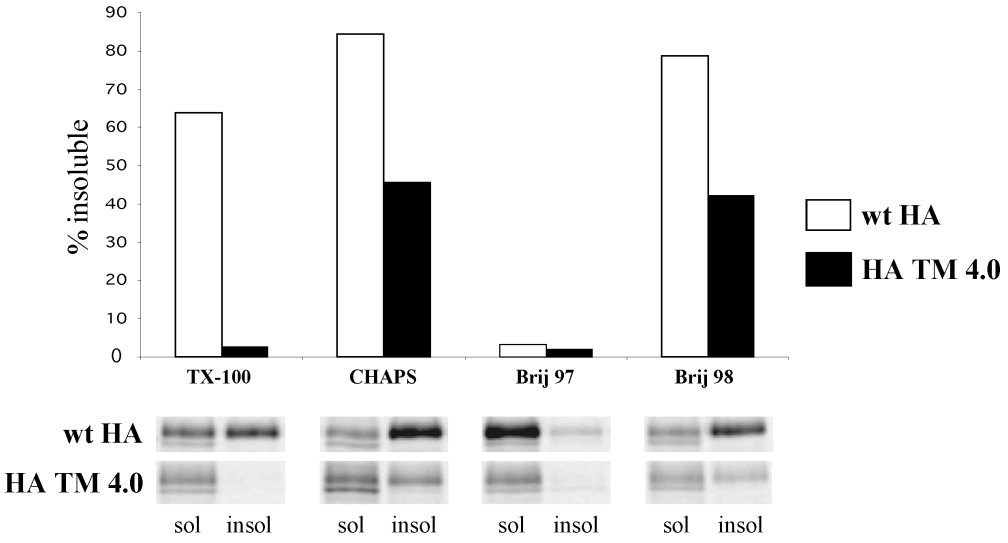

Figure 13. Several non-ionic detergents used to infer lipid raft incorporation have markedly different effects on the solubility of HA. MDCK cells were infected with wt HA or HA TM 4.0 adenovirus as described in methods. Infected cells were labeled with [^{35}S]-amino acids, followed by an incubation in serum-free DMEM for 80 minutes at 37ºC. The cells were lysed in TX-100 lysis buffer and centrifuged. The supernatant and pellet were immunoprecipitated with α-HA, resolved by SDS-PAGE, and quantitated with a phosphorimager.

FRAP in Conjunction with Raft Immobilization Detects Transient Associations with Lipid Rafts

Several methods have been used to detect lipid raft microdomains *in vivo* (Dietrich et al., 2002; Harder et al., 1998; Kenworthy et al., 2000; Wilson et al., 2004). However, these methods have limitations in detecting proteins that are only transiently incorporated into lipid rafts. In order to determine if the lack of HA TM 11.0 association with DRMs *in vitro* was due to a weak or transient association with lipid rafts, we collaborated with the laboratory of Yoav Henis to develop an *in vivo* assay to measure lipid raft association. The rate of lateral

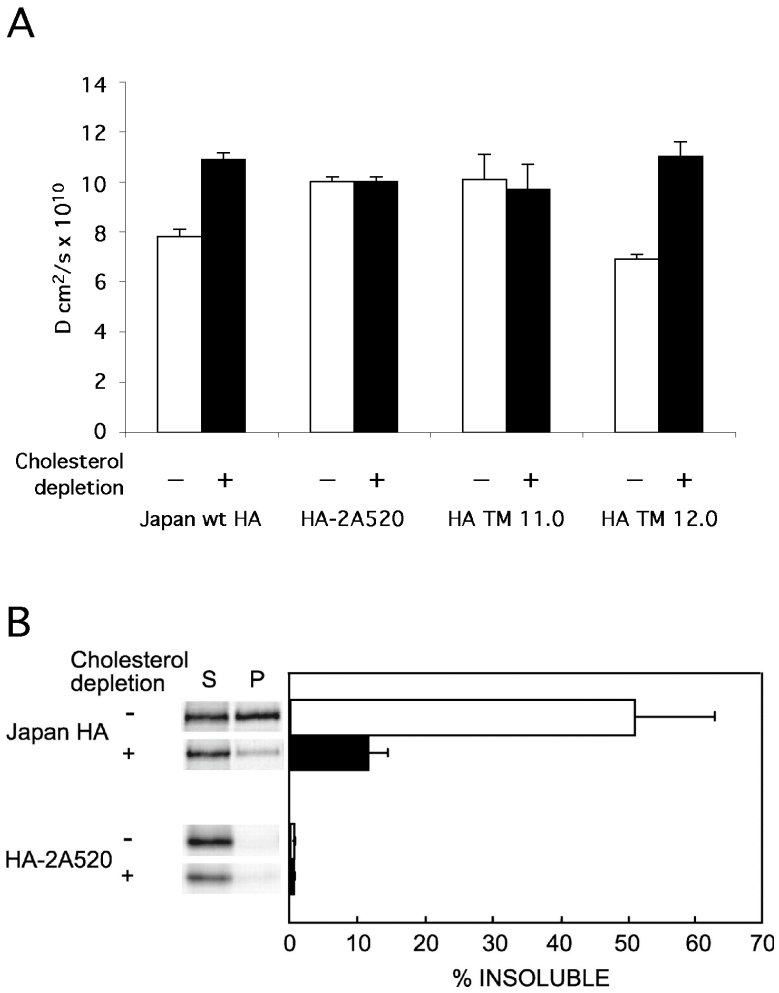

Figure 14. Cholesterol depletion increases the rate of lateral diffusion of HA mutants that partition into DRMs. CV-1 or COS-1 cells were infected with the indicated recombinant SV40 virus expressing wt HA or HA2A520 for a total of 36 hr or transiently transfected with HA TM 11.0 or HA TM 12.0 for 38 hours. The cells were biosynthetically depleted of cholesterol as described in Materials and Methods or incubated in normal media for 18-20 hr of the total infection or transfection time. (A) Cell surface HAs were labeled with monovalent α-HA TRITC-Fab' and the lateral diffusion rate was quantitated following photobleaching as described in Shvartsman et al., 2003. D of HA 2A520 in untreated cells was significantly higher than the D value of wild-type HA ($P < 0.01$). D value of TM 11.0 was significantly higher than D of TM 12.0 ($P < 0.001$) (B) Cells were labeled with [^{35}S]-amino acids for 30 minutes followed by a chase for 80 minutes in DMEM. The labeled cells were lysed in Triton lysis buffer, centrifuged, and the soluble and insoluble fractions were immunoprecipitated with α-HA and protein A-sepharose. The immunoprecipitates were resolved by SDS-PAGE, and quantitated by phosphor imaging. The error bars are the standard deviations from 3-5 independent experiments.

diffusion across the plasma membrane in intact cells can be measured by fluorescence recovery after photobleaching (FRAP). Wild type Japan HA had a slower lateral diffusion than HA2A520, a transmembrane mutant that does not associate with DRMs and is not apically sorted (Figure 14) (Lin et al., 1998; Shvartsman et al., 2003). When cholesterol was biosynthetically depleted from cells treated with mevalonate and compactin in lipoprotein-deficient serum (Hua et al., 1996), the lateral diffusion rate of wild type Japan HA mobility increased, while the lateral mobility of HA2A520 was unaffected (Figure 14). Correspondingly, the lateral diffusion rate of HA TM 12.0 was increased with cholesterol depletion, while lateral mobility of HA TM 11.0 was unchanged with cholesterol depletion. This result is consistent with the negative effect that cholesterol depletion had on the ability of wild type HA to be isolated in DRMs, suggesting that the rate of lateral diffusion of HA is retarded by association with lipid rafts. However, if a protein is only transiently associated with a lipid raft, and given that rafts themselves have measurable mobility within membranes (Pralle et al., 2000), it may be difficult to quantifiably distinguish the average lateral mobility of a raft protein from a non-raft protein. In this case, cholesterol depletion would have an undetectable effect on the lateral diffusion rate.

To enable identification of proteins transiently associated with lipid rafts, a raft-associated protein was immobilized and the lateral diffusion rate of several HA mutants were monitored in the presence of the immobilized rafts (Shvartsman et al., 2003). HA X:31 BHA-PI, a GPI-anchored HA mutant that is associated with lipid rafts and is antigenically distinct from Japan HA (Kemble et al., 1994), was immobilized by crosslinking the cell surface population with a double layer of IgGs in live cells. The lateral mobility of wild-type

Japan HA was decreased two-fold in the presence of crosslinked X:31 BHA-PI, while the diffusion of HA2A520 was unaffected by immobilized rafts (Figure 15). This data is consistent with the data in Figure 14, indicating that HA2A520 does not contact mutual rafts containing X:31 BHA-PI, whereas wild-type HA does so. The lateral mobility of HA TM 11.0 was also decreased two fold in the presence of crosslinked X:31 BHA-PI (Figure 15), suggesting that HA TM 11.0 is transiently associated with lipid rafts. The FRAP assay in conjunction with immobilized raft microdomains is a more sensitive measurement of lipid raft association than *in vitro* resistance to detergent extraction.

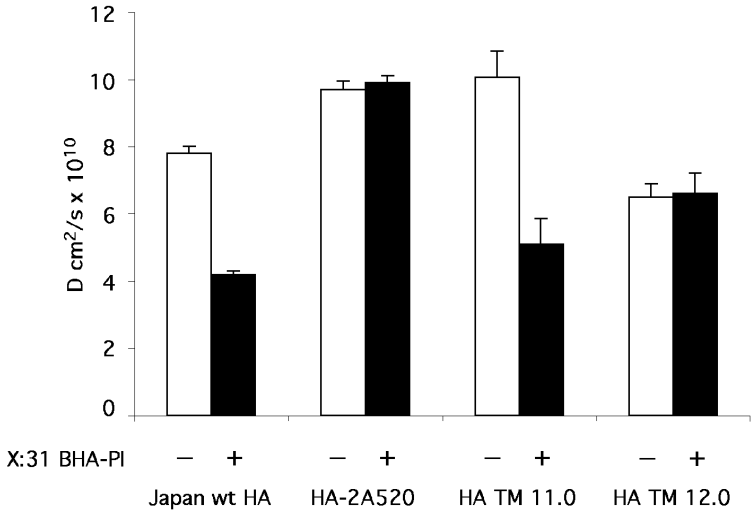

Figure 15. Cross-linking in conjuction with FRAP demonstrates a transient association with lipid rafts. CV-1 or COS-1 cells were infected with recombinant SV40 virus expressing wild-type HA or HA 2A520 or transfected with HA TM 11.0 or HA TM 12.0 for 36 hours. Alternatively, the infected or transfected cells were co-expressed with the antigenically-distinct X:31 HA. X:31 HA was immobilized on the surface of live cells by labeling with mouse α-X:31 antibody at 4° C followed by labeling with secondary antibodies conjugated to FITC. The Japan HA wild-type or mutant proteins were labeled with α-Japan rabbit TRITC-Fab'. The cells were photobleached and lateral diffusion on the plasma membrane measured as described in Shvartsman et al., 2003. Error bars represent the SEM of 20-30 measurements.

Overexpression of MAL Does not Improve HA DRM Association

One possibility for the function of the HA TM in apical sorting consistent with our data is to interact with a sorting receptor that partitions into rafts. MAL is required for apical trafficking and DRM association of HA in MDCK cells (Puertollano et al., 1999). It is possible that MAL sorts HA at the TGN by increasing the efficiency of HA incorporation into DRMs. If this is true, overexpression of MAL should increase the percentage of wild-type HA and HA TM 11.0, a mutant that is transiently associated with lipid rafts, in DRMs. MDCK cells were infected with wild-type HA or HA TM 11.0 recombinant adenovirus or co-infected with myc-MAL adenovirus, lysed in Triton buffer, adjusted to 40% (w/w) sucrose, overlaid with a 30-5% (w/w) sucrose gradient, and centrifuged to equilibrium. Co-infection with myc-MAL did not affect the percentage of wild-type HA or HA TM 11.0 in the floated fractions of the gradient (Figure 16), suggesting that MAL does not actively sort HA into DRMs. Wild-type HA DRM association is probably not saturable, since expression of 10 fold more HA does not affect the percentage of HA associated with DRMs (Figure 9). It is possible that MAL is not limiting and overexpression may not result in a higher percentage of HA incorporated into DRMs.

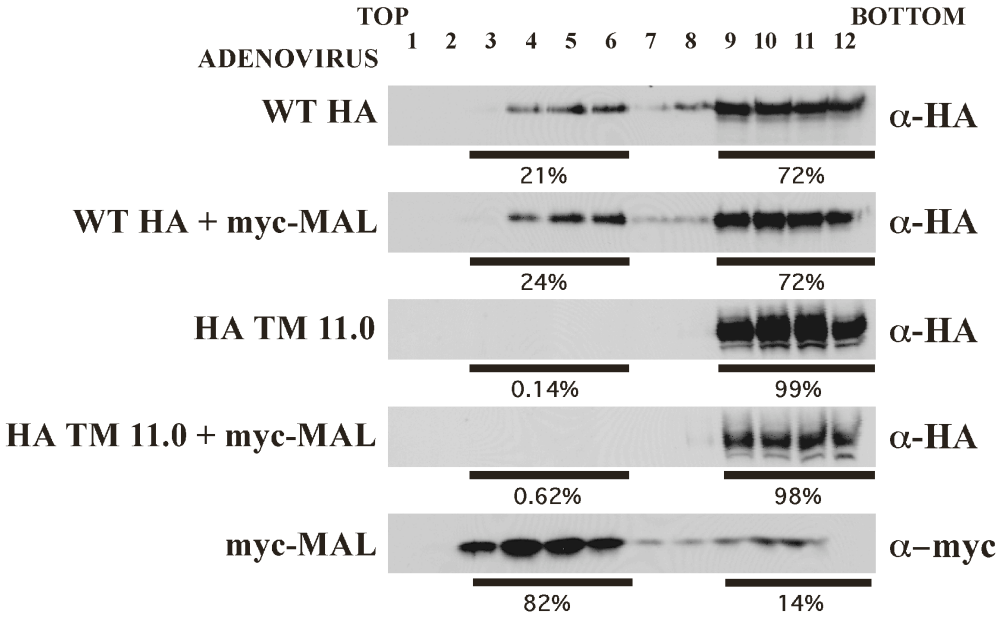

Figure 16. Overexpression of MAL does not improve wild-type HA or HA TM 11.0 flotation on density gradients. 1 x 10^7 MDCK cells were infected with wild-type HA or TM 11.0 adenovirus or co-infected with myc-MAL adenovirus for 16-18 hours. 3 x 10^7 unifected MDCK cells were solubilized with Triton lysis buffer and combined with the infected cells. The lysate was adjusted to 40% (w/w) sucrose and overlaid with 35% (w/w) sucrose, followed by 30-5% (w/w) linear sucrose gradient, and centrifuged to equilibrium. Fractions were collected from the top of the gradient and 2% of each fraction was loaded on 12.5% SDS-PAGE and immunoblotted with α-HA or α-myc.

HA Associated with MAL Is Enclosed in Intact Vesicles

When expressed together with an epitope-tagged hMAL protein, HA can be precipitated with the antibody specific for the epitope tag, indicating that HA and hMAL may interact (Puertollano et al., 1999). To determine the effect of mutations in the HA TM domain on this interaction, MDCK cells were co-infected with adenoviruses expressing hMAL tagged with a c-myc epitope at the amino terminus and adenoviruses expressing the various HA mutants. After 16 h, the cells were pulse-labeled with [^{35}S]-cysteine and methionine and chased first at 20 °C for 2 h, then at 37 °C for 80 to 125 minutes. The cells

were lysed in Triton buffer at 37° C and precipitated with either anti-myc or anti-HA. Radioactive HA co-precipitated with myc-hMAL, as has been reported previously (Puertollano et al., 1999). However, the co-precipitation was not reciprocal and no hMAL co-precipitated with HA in samples treated with anti-HA (Figure 17A). In all cases the percentage of HA co-precipitating with myc-hMAL was low and variable (2%-0.7% in different experiments). Similar experiments were performed with cells co-expressing myc-hMAL and various HA mutants, except that after labeling with radioactivity the cells were chased in normal medium long enough for the proteins to reach the plasma membrane. As a general trend in every experiment, mutations that inhibited the isolation of HA in DRMs also inhibited the co-preciptiation with hMAL (Figure 17B). TM 13.0, a mutant that associates with DRMs and sorts apically as effectively as wild type HA, co-immunoprecipitated with myc- hMAL in amounts (1.2% in Figure 17B) similar to wild type HA. Whereas, less than 0.2% of HA TM 7.1, which does not sort apically and is not detected in DRMs, co-immunoprecipitated with myc-hMAL (Figure 17B). The small amount and the variability of co-precipitating HAs limited our ability to rank the mutants with respect to their ability to co-precipitate. For instance, we observed no significant difference between HA TM 7.1, which does not sort apically and is not found in DRMs, and HA TM 11.4, which also does not partition into DRMs but does sort to some extent (Figure 17B). Although HA TM 11.4 was not tested in the *in vivo* raft immobilization with FRAP assay, there is a strong possibility that, like HA TM 11.0, HA TM 11.4 is transiently associated with lipid rafts. It is possible that MAL does not associate with HA TM mutants that are only transiently associated with lipid rafts because the association of MAL and HA occurs only when the two proteins

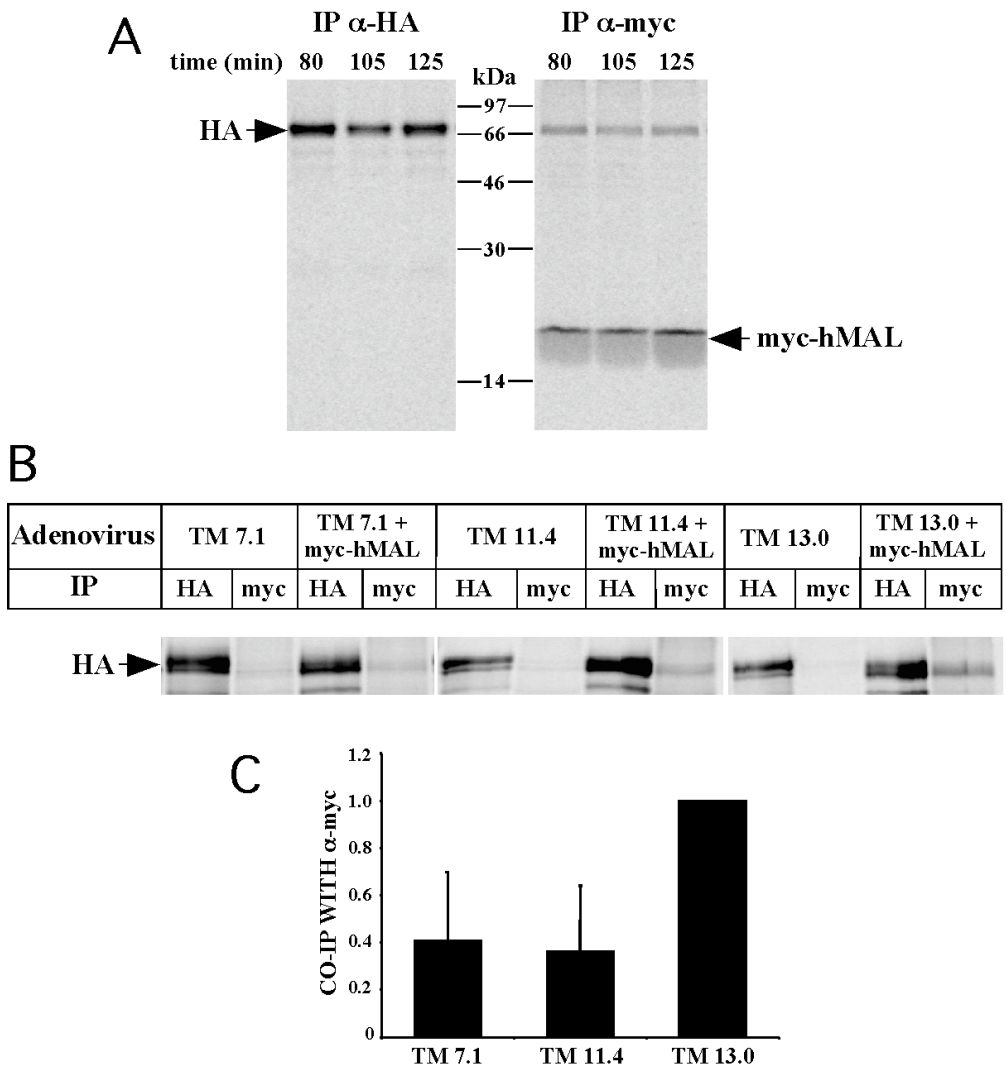

Figure 17. Co-precipitation of HA and MAL is not reciprocal. (A) MDCK cells were co-infected with recombinant adenovirus expressing wild type HA and myc-hMAL. The infected cells were labeled with [^{35}S]-amino acids, incubated for 2 hours at 20° C, and chased at 37° C for the indicated times. The cells were lysed in Triton lysis buffer for 10 minutes at 37° C, and the lysates were immunoprecipitated with monoclonal HA or myc antibody. The immunoprecipitates were resolved by SDS-PAGE and analyzed by phosphor imaging. The volume of samples immunoprecipitated with α-HA is 10% of the volume of samples immunoprecipitated with α-myc. (B) MDCK cells were infected with recombinant adenovirus expressing HA TM mutants or co-infected with myc-hMAL adenovirus. The infected cells were labeled with [^{35}S]-amino acids and chased for 100 minutes at 37° C. The cells were lysed, immunoprecipitated, and resolved by SDS-PAGE as described in A. (C) Data from three experiments similar to that shown in B are graphed. Data are normalized to that of TM 13.0. Bars indicate the standard deviation.

occupy the same raft. HA TM 11.0 might not associate with lipid rafts long enough to observe a detectable interaction with MAL. This hypothesis is also consistent with the observation that overexpression of MAL does not improve flotation of HA TM 11.0 on density gradients, suggesting that lipid raft association is not a consequence of MAL and HA interaction.

To examine the interaction between MAL and HA in the DRM fraction rather than the cell as a whole, MDCK cells were infected with wild type HA and/or epitope-tagged-MAL adenovirus and then were lysed in cold buffer containing 1% Triton X-100. The lysate was overlaid with a sucrose gradient and centrifuged to equilibrium. Fractions containing membranes that floated on the gradient (fractions 3-6) and dense fractions (fractions 9-12) containing soluble proteins were pooled separately and immunoprecipitated with monoclonal HA or myc antibody. Approximately 6% of wild type HA in the buoyant fractions (representing 1.2% of HA in the cell lysate) was immunoprecipitated with the myc antibody when tagged-MAL and HA were co-expressed (Figure 18A, second lane). HA and tagged-MAL did not associate in dense fractions, indicating that the association occurs only in DRMs (Figure 18A, lanes 3 and 4). Epitope tagged-MAL was not precipitated with monoclonal (Figure 18A, first lane) or polyclonal (data not shown) HA antibody in the buoyant or dense fractions, in spite of the fact that the polyclonal HA antibody was raised against the entire external domain of HA. The lack of reciprocal co- precipitation suggested that in the membranes containing both MAL and HA the proteins were oriented such that the epitope on MAL was exposed to the antibody and the external domain of HA was not.

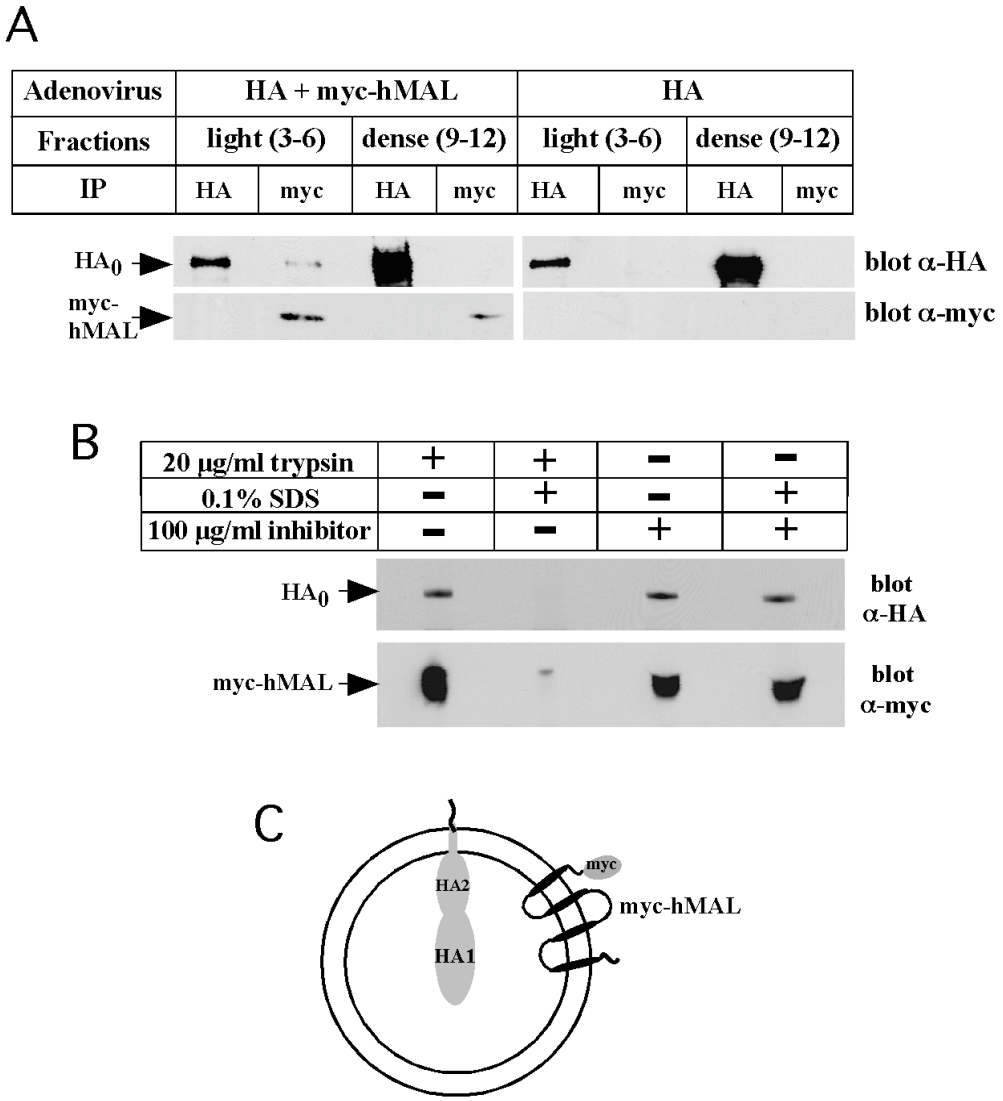

Figure 18. MAL-associated HA is enclosed in intact vesicles. MDCK cells were infected with recombinant adenovirus expressing wild type HA alone or co-infected with epitope tagged hMAL. Infected cells were lysed in cold Triton lysis buffer and overlaid with a linear sucrose gradient as described in Materials and Methods. (A) The light fractions (3-6) and dense fractions (9-12) were pooled separately and one-half of each pool was immunoprecipitated with either monoclonal α-HA or α-myc. The immunoprecipitates were immunoblotted with polyclonal anti-HA or monoclonal anti-myc. (B) The floated fractions (fractions 3-6) were immunoprecipitated with anti-myc and protein A Sepharose. The immunoprecipitates were washed once in cold Triton lysis buffer and treated with trypsin, SDS, or trypsin inhibitor in the combinations listed. The treated samples were resuspended in SDS-PAGE loading buffer, separated by PAGE, and immunoblotted with anti-HA or anti-myc. (C) The relative orientation of MAL and HA in DRM vesicles is diagrammed.

This would be the situation if, within the buoyant fraction, the only HA in association with MAL was enclosed in a vesicle with the cytosolic epitope of MAL exposed on the vesicle surface and the HA ectodomain inside (Figure 18C). The majority of membranes containing HA in this fraction, in which the ectodomain of HA was exposed to the antibody, did not contain myc-tagged MAL, as indicated by the failure of MAL to co-precipitate with HA and anti-HA.

To determine if HA pulled down with the myc antibody was in fact enclosed in an intact vesicle, 20 μg/ml trypsin in TNE was added to the anti-myc immunoprecipitates in the absence or presence of 0.1% SDS (Figure 18B). DRM membranes are solubilized by 0.1% SDS but this concentration of the detergent has no effect on the activity of trypsin or the structure of trimeric HA (Copeland et al., 1986; Doms and Helenius, 1986; Puertollano et al., 1999). In the absence of SDS, trypsin could not access HA, leaving HA uncleaved (the 10 amino acids of the HA cytoplasmic tail do not contain a lysine). In the presence of SDS, HA was cleaved by trypsin, indicating that the raft-containing vesicles were disrupted. This classic test of latency (Lazarovits et al., 1990; Rock et al., 1977) confirms that the DRMs in the light fractions that contain both MAL and HA are vesicles in which the external domain of HA is located in the lumen. It is important to note that the buoyant fraction of the gradient does not represent a uniform suspension of vesicles that are all in the same orientation. However, the vesicles in the light fractions that contain both MAL and HA are in an orientation such that the external domain of HA is positioned towards the lumen. This topology is consistent with the properties of an intracellular vesicle and opposite the topology of vesicles formed when the plasma membrane is fragmented, which tend to form with the

extracellular side exposed. Much to our surprise, a similar result was obtained when HA and MAL were co-precipitated with myc antibody from cell lysates in 1% Triton X-100 at 37° C, although the amount of co-precipitating HA was greatly reduced (data not shown). The precipitation at 37° C was non-reciprocal and the HA that co-precipitated with MAL was also inaccessible to cleavage by trypsin. These results suggest that even after lysis for 10 minutes at 37 °C, under the conditions of our experiment a fraction of DRM vesicles remain intact and HA and MAL co-precipitate because they reside in the same DRM vesicle (Figure 18C).

The Vesicles That Contain HA and MAL Do Not Have Characteristics of Golgi-derived Transport Intermediates

One candidate for the DRM vesicle containing MAL and HA would be the transport vesicle that carries HA from the TGN to the apical surface. If so, then one would expect that during a pulse-chase experiment the fraction of HA co-precipitating with antibody to myc-tagged MAL would be maximum during the period when a pulse of HA is released from the TGN and is traveling to the plasma membrane. To test this hypothesis, MDCK cells were infected with recombinant adenovirus expressing HA and/or myc-MAL for 12-16 h. The infected cells were metabolically labeled with [^{35}S]-amino acids prior to incubation for 2 h at 20º C to retain the labeled proteins in the TGN. The cells were then incubated at 37º C for time points from 0-180 minutes in serum-free media. At each time point, the cells were lysed in TNE containing 1% Triton X-100 at 37º C. The lysates were precipitated with HA or myc antibody, washed, resolved by SDS-PAGE, and analyzed with a Typhoon scanner (Figure 19A).

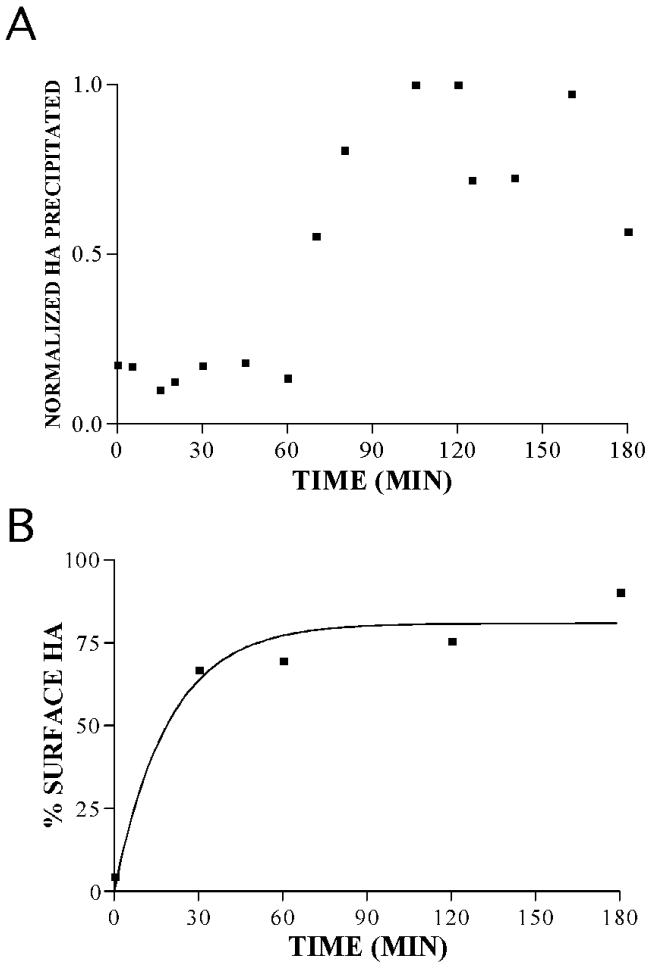

Figure 19. HA co-precipitates with myc-MAL only after an interval when most of the HA has reached the plasma membrane. (A) MDCK cells cultured on plastic were co-infected with a mixture of adenoviruses that express myc-tagged MAL and HA. After 16 h the cells were pulse-labeled with [^{35}S]-amino acids and chased for 2 h at 20° C to allow the proteins to accumulate in the TGN. The cells were shifted to 37° C and samples were collected at various intervals after the temperature shift. Samples were lysed at 37° C in Triton lysis buffer and the amount of HA that precipitated with myc antibody was determined by SDS-PAGE and phosphor imaging. (B) Samples infected with adenovirus expressing HA and pulse labeled as described above were chased after the temperature shift from 20° C to 37° C in medium containing trypsin to cleave HA that reached the cell surface into its HA1 and HA2 subunits. Samples were immunoprecipitated with antibody to HA and the amount of HA present as uncleaved HA or HA1 and HA2 subunits was quantified by PAGE and phosphor imaging. The percentage of total HA recovered that was cleaved into HA1 and HA2 is the percentage of HA having reached the cell surface. In panel A, the combined data from two experiments are shown. Panel B is representative of many experiments and consistent with previously published data (Hortin and Boime, 1981; Lin et al., 1998).

Very little HA co-precipitated with MAL until after 80 min of chase. At this period of chase, the majority of HA had reached the cell surface (Figure 19B). Thus, the association of HA and MAL that we observe in DRMs does not have the characteristics one would expect if

MAL and HA travel together in the transport intermediate that takes HA from the TGN to the plasma membrane.

Association of HA and MAL is Undetectable in Plasma Membrane Derived Vesicles

MAL and HA did not have a detectable association until at least one hour after biosynthesis. At this time, the majority of HA has been sorted to the plasma membrane, suggesting that HA and MAL may associate at the plasma membrane or during internalization. Depletion of MAL with anti-sense nucleotides has been shown to impair internalization of the polymeric Ig receptor in MDCK cells (Martin-Belmonte et al., 2003), indicating that MAL may be involved in sorting during endocytosis. Cell surface proteins of MDCK cells infected with myc-hMAL or wild type HA adenovirus were labeled with biotin at 4º C, followed by an incubation at 37º C for 0 or 60 minutes to allow internalization. HA is internalized at a rate of less than 1% per minute (Lazarovits and Roth, 1988), which should

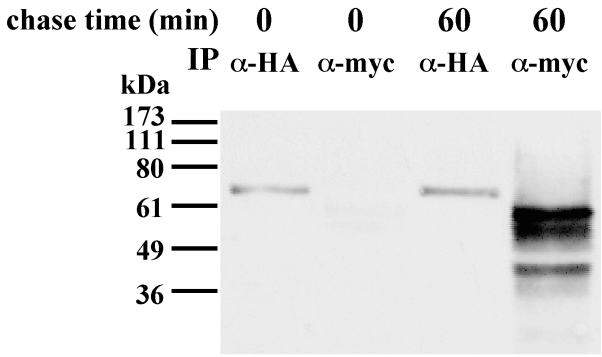

Figure 20. Association of HA and MAL subsequent to internalization from the plasma membrane is undetectable. MDCK cells were infected with recombinant myc-hMAL or wild-type HA adenovirus. After an 18 hour incubation, cell surface proteins were labeled with biotin at 4º C. The cells were allowed to internalize the labeled surface proteins for 0 or 60 min at 37º C prior to lysis and immunoprecipitation with antibody specific for HA or myc. The immunoprecipitates were blotted with neutravidin-HRP to detect biotinylated proteins in the immunoprecipitate.

allow a detectable amount of biotinylated HA inside the cell after 60 minutes. myc-hMAL did not co-precipitate with biotinylated HA that was not permitted to internalize. In addition, none of the biotinylated HA detectably co-immunoprecipitated with myc-hMAL after 60 minutes of internalization (Figure 20). These experiments suggest that MAL and HA do not have a detectable association at the cell surface or in the endocytic pathway. All of the HA and MAL co-immunoprecipitation experiments detect a maximum of 2% of the total HA specifically associated with MAL.

It is possible that HA and myc-hMAL did not have a detectable association after internalization because the low signal of biotinylated HA specifically immunoprecipitated with myc antibody is below the detection limit of the assay. Several unidentified biotinylated proteins specifically precipitated with the myc antibody 60 minutes after the cell surface proteins were internalized (Figure 20), suggesting that MAL may be involved in sorting multiple proteins during endocytosis. This data, in conjunction with the time course of HA and MAL association, suggests that MAL may not sort proteins at the TGN during biosynthetic trafficking. Instead, MAL may be involved in sorting apical proteins at the apical recycling endosome or may be required to recycle a necessary component of apical sorting vesicles from the plasma membrane to the TGN.

CHAPTER FOUR

SORTING NEXIN 17 REGULATES INTRACELLULAR TRAFFICKING OF LOW DENSITY LIPOPROTEIN RECEPTOR FAMILY MEMBERS

INTRODUCTION

Although an apical sorting consensus sequence has not been identified, many apical targeting signals are located in the transmembrane domain or GPI anchor of proteins (Brown and Rose, 1992; Lin et al., 1998; Tall et al., 2003). Recently, apical targeting signals have been identified in the cytoplasmic domain of several proteins, including megalin, a member of the LDLR family (Inukai et al., 2003; Jia et al., 2003; Marzolo et al., 2003; Takeda et al., 2003b; van Balkom et al., 2004). Replacing the tail of the basolateral protein LRP1 with the megalin cytoplasmic tail targeted the LRP chimera to the apical surface, indicating that the megalin cytoplasmic tail was necessary and sufficient for apical sorting (Marzolo et al., 2003; Takeda et al., 2003b).

In order to identify proteins that could potentially sort apical proteins from the TGN, we performed a yeast two-hybrid screen with the cytoplasmic tail of megalin. We detected many novel megalin binding partners, including several signaling and scaffolding proteins. Although we did not isolate any candidates that appeared to regulate apical sorting from the TGN, we identified a novel interaction of megalin with sorting nexin 17 (SNX17), a protein that may regulate internalization or recycling of the LDLR family members. Sorting nexins contain a characteristic phox homology (PX) domain, which is required to localize the protein to a specific organelle (Worby and Dixon, 2002). The SNX family has been shown

to regulate trafficking of various membrane receptors, including LDLR, EGFR, TfR, and platelet derived growth factor receptor (Worby and Dixon, 2002).

LDLR family members contain a NPXY sequence in their cytoplasmic domains which is required for clathrin-mediated internalization (Chen et al., 1990). SNX17 interacts with the NPXY sequence in LDLR, and overexpression of SNX17 induces an apparent two fold increase in the LDLR internalization index, suggesting that SNX17 may regulate internalization of LDLR (Burden et al., 2004a; Stockinger et al., 2002a). Unlike LDLR, which contains only one NPXY sequence, megalin contains two NPXY sequences and an NXXY sequence. We observed that SNX17 interacts with the first NPXY sequence of megalin, which may not be the sequence required for internalization. Dab2, a clathrin adaptor which has been shown to regulate internalization of megalin and LDLR, binds to the second NPXY sequence in the cytoplasmic tail of megalin (Oleinikov et al., 2000).

LDLR recycles through a fast pathway from the sorting endosome to the plasma membrane or a slower pathway that trafficks the protein through the endocytic recycling compartment (Ehrlich et al., 2004). When SNX17 was overexpressed, I observed a two-fold increase in the rate of LDLR recycling to the plasma membrane, suggesting that SNX17 decreases the cycling time of the receptor. My experiments suggest that SNX17 regulates recycling of the LDLR, possibly by directing LDLR from the sorting endosome to the plasma membrane, avoiding the endocytic recycling compartment, and increasing the recycling rate.

RESULTS

A Yeast Two Hybrid Screen with the Cytoplasmic Tail of Megalin Identifies Several Novel Interactions

A yeast two-hybrid screen was initiated to identify proteins that direct apical proteins in the biosynthetic pathway from the TGN to the correct cell surface. The megalin tail was an appropriate choice of bait because it was not membrane-associated and it is a member of the LDLR family of proteins, which, with the exception of megalin, are sorted basolaterally. Therefore, positive interactions in the yeast two-hybrid screen with megalin could be tested against the other members of the family in order to distinguish potential apical sorting proteins from proteins that bind to other LDLR family members. In addition, the apical targeting signal in the megalin tail was defined to a sequence of 31 amino acids (Takeda et al., 2003b). This information could be used to discriminate interactions that occur in other regions of the multi-domained tail of megalin from those required for apical sorting. The 213 amino acid cytoplasmic tail of megalin (megCT) or the 93 nucleotide sequence required for apical sorting (megAS) were fused at the N-terminus with the LexA DNA binding domain and protein expression verified (Figure 21).

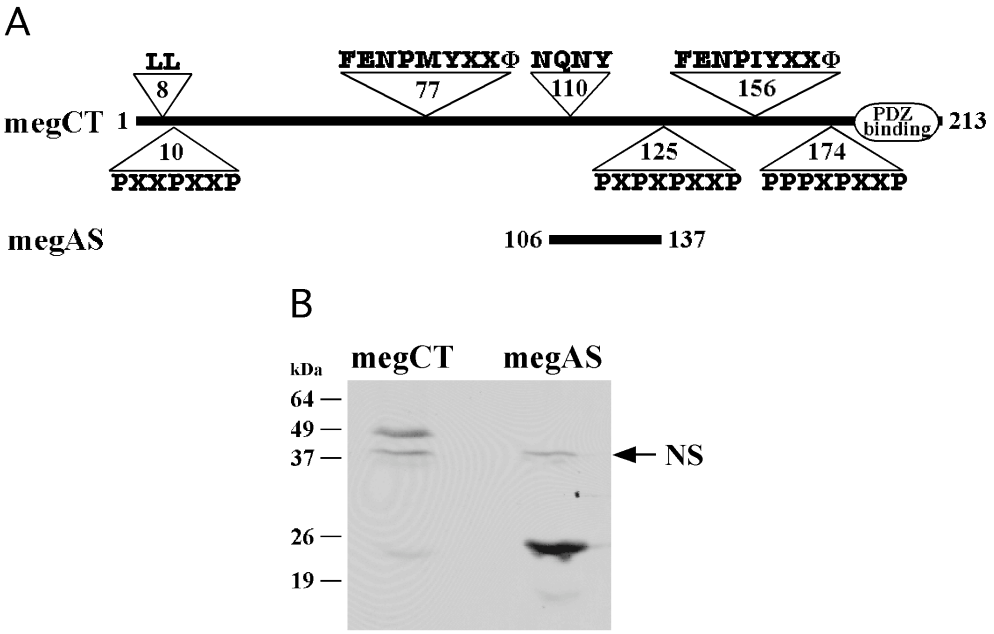

Figure 21. Megalin bait fusion constructs are expressed in L40 yeast. (A) The cytoplasmic tail of megalin contains three SH3 binding domains, two NPXY sequences, an NXXY sequence, and a PDZ binding domain. (B) Spheroplasts of L40 yeast expressing megalin bait constructs were lysed with glass beads and SDS-PAGE buffer, resolved by 12.5% PAGE, immobilized on nitrocellulose, and immunoblotted with α-LexA. MegCT was expressed at the predicted 46 kDa molecular weight and megAS was the predicted 25 kDa size. NS, non-specific band present in untransformed L40 yeast (Figure 24)

The cytoplasmic tail of megalin has many domains which could potentially act as binding sites for several classes of molecules (Figure 21). Megalin has the sequence serine, aspartic acid, valine at its extreme carboxy terminus, which acts as a Postsynaptic density 95/*Drosophila* discs-large/Zona occludens 1 (PDZ)-binding domain (Figure 21). In addition, the tail of megalin has three proline-rich motifs, which could bind to src homology 3 (SH3)-containing proteins (Morton and Campbell, 1994), and a di-leucine sequence, which has been

shown to act as a basolateral targeting sequence in other proteins (Hunziker and Fumey, 1994).

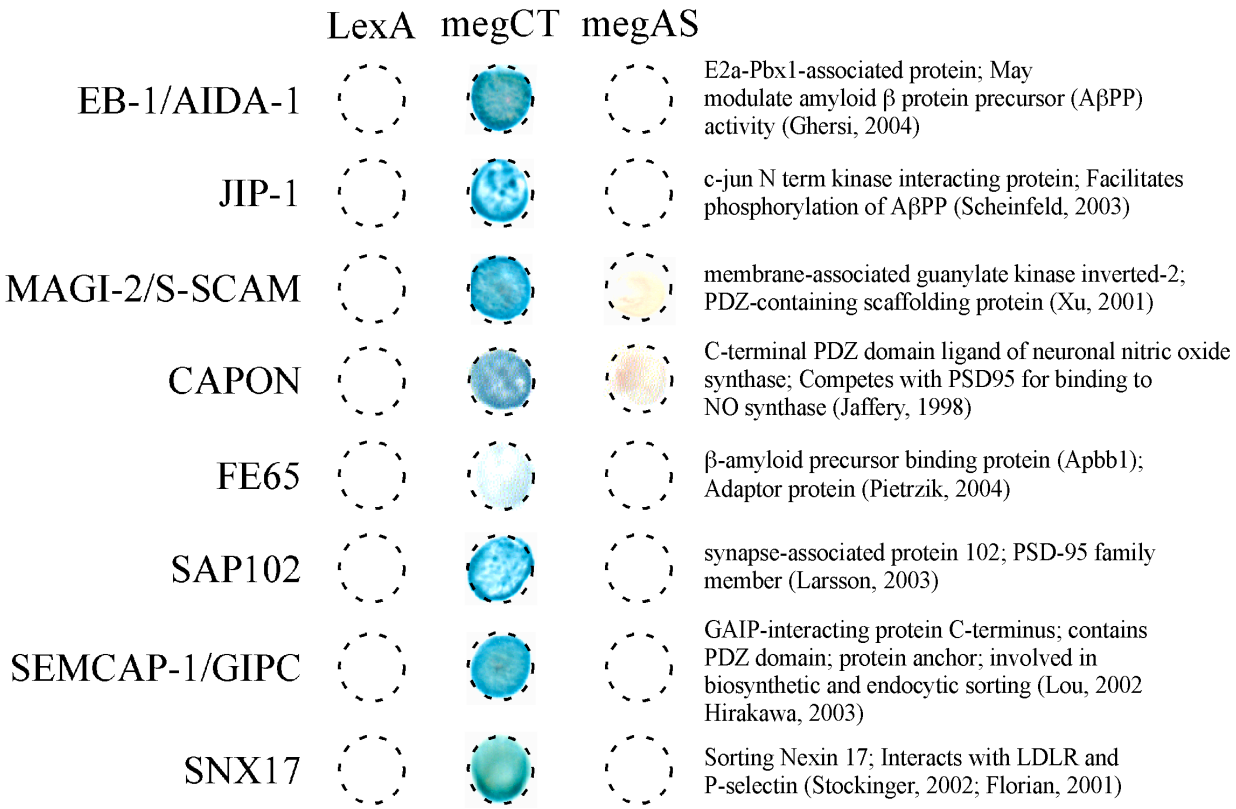

Figure 22. The cytoplasmic tail of megalin interacts with several signaling and scaffolding proteins. A LexA fusion with the 213 amino acid cytoplasmic tail of megalin (megCT) was screened against a rat brain cDNA library fused to the VP16 activation domain. The yeast were plated onto media lacking tryptophan, leucine, and histidine, lifted onto supported nitrocellulose membrane, and freeze fractured. β-galactosidase released from the yeast and bound to the nitrocellulose was detected by incubation with X-gal for 9 minutes to 1 hour, resulting in a blue color. Prey constructs from yeast that were protrotrophic for tryptophan, leucine, and histidine and activated β-galactosidase were sequenced and tested for interaction with LexA or LexA fused to the proposed apical sorting signal of megalin (megAS).

Megalin also contains two NPXY sorting sequences and an NXXY signal sequence (Figure 21). NPXY sequences in other proteins have been shown to interact with proteins that modulate clathrin-mediated internalization, including Disabled-2 (Dab2), autosomal recessive hypercholesterolemia protein (ARH), and the μ2 subunit of adaptor protein-2 (AP-2) (Boll et al., 2002; Mishra et al., 2002a; Nagai et al., 2003; Oleinikov et al., 2000). Dab2 binds to the second NPXY sequence of megalin and regulates clathrin-mediated internalization of the receptor (Oleinikov et al., 2000).

MegCT was screened against a library of rat brain cDNA fused to the VP16 DNA activation domain (a gift from the laboratory of Thomas Sudhof) and positive interactions were tested for an association with megAS, the predicted apical sorting signal of the tail (Figure 22). Some of the preys isolated in the screen had previously been shown to interact with megalin, including EB-1 (Petersen et al., 2003), SAP102 (Larsson et al., 2003), JIP-1, GIPC, and CAPON (Gotthardt et al., 2000). Megalin, EB-1, JIP-1, and FE65 may exist in a complex to modulate the activity of amyloid beta precursor protein (A□PP), a protein involved in the progression of Alzheimer's disease (Ghersi et al., 2004; Pietrzik et al., 2004; Scheinfeld et al., 2003; Trommsdorff et al., 1998). MAGI-2, SAP102, CAPON, and GIPC, which all interact with megalin in the yeast two-hybrid system (Figure 22), contain at least one PDZ domain and may bind to the extreme carboxy terminus of the megalin tail, which is not required for apical sorting (Takeda et al., 2003b). However, GIPC co-localizes with megalin in the apical region of proximal tubule epithelial cells (Lou et al., 2002), which could make GIPC a candidate for an apical sorting protein. The location of GIPC at the

plasma membrane suggests that, although it could be involved in some aspect of apical sorting, it most likely does not sort megalin as it exits the TGN.

Another novel interaction identified in the yeast two hybrid screen with the megalin tail was sorting nexin 17 (SNX17) (Figure 22), a member of a family of proteins characterized by the inclusion of a conserved phox homology (PX) domain, which has been shown to bind phosphatidylinositol phosphates (Worby and Dixon, 2002). Sorting nexins are involved in various stages of endocytosis and protein trafficking (Lundmark and Carlsson, 2003; Schwarz et al., 2002). SNX17 binds to LDLR in the first NPXY sequence (Burden et al., 2004a) and has been reported to interact with other members of the LDLR family, except megalin (Stockinger et al., 2002a). Because SNX17 binds to members of the LDLR family that are basolaterally sorted, it may not be involved in the apical sorting of megalin. However, it is possible that other members of the LDLR family contain apical sorting information that is dominated by the basolateral targeting signals in their cytoplasmic domains. The other LDLR family members do not contain an apical consensus sequence similar to that identified in the megalin cytoplasmic tail.

None of the preys that interacted with the full-length megalin tail in the yeast two-hybrid system associated with the 31 amino acid apical sorting sequence (megAS) (Figure 22). Although megAS was expressed in L40 yeast at the correct molecular weight (Figure 21), it is possible that the peptide was not folded in the same confirmation as the full-length cytoplasmic tail, which would impede its association with apical sorting proteins. It is also possible that the preys isolated in the yeast two-hybrid were not involved in sorting megalin apically.

Megalin Associates with SNX17 and GIPC

Although none of the isolated interaction partners were candidates for sorting megalin from the TGN, both GIPC and SNX17 could be involved in the trafficking the LDLR family and were interesting proteins to investigate. The smallest SNX17 fragment isolated in the yeast two-hybrid screen was missing the first 72 nucleotides of the gene. The first 300 nucleotides of the gene encode a PX domain, indicating that an intact PX domain is not required for interaction with megCT. SNX17 was originally characterized as containing a FERM (protein 4.1/Ezrin/Radixin/Moesin) domain in amino acids 115-206 (Stockinger et al., 2002a). However, sequence alignment of the predicted FERM domain of SNX17 with other known FERM domains using ClustalW did not identify high similarity (not shown). Additional alignments utilizing programs developed by the laboratory of N. Grishin did not identify significant similarities between the FERM domain of SNX17 and other FERM domains (not shown). Analysis of the rat SNX17 sequence with Prodom predicts that amino acids 115-206 are a ras-binding domain (e value 2.1×10^{-6}). The smallest fragment of GIPC isolated retained the PDZ domain of the gene, which is the most likely interaction site for GIPC and megalin.

To confirm that megalin and GIPC or SNX17 associate *in vivo*, full-length SNX17 and GIPC were cloned from rat brain cDNA, tagged at the N-terminus with a triple HA epitope, and expressed in LLC-PK1 and HeLa cells (Figure 23). Megalin was specifically immunoprecipitated with polyclonal megalin antibody (a gift from the laboratory of Joachim Herz) and immunoblotted with anti-HA to detect HA-GIPC or HA-SNX17 in the immunoprecipitate. HeLa cells do not express detectable endogenous megalin and were used

as a negative control in the experiment. Approximately 16% of the total HA-SNX17 and 30% of the total HA-GIPC co-precipitated with endogenous megalin (Figure 23). A reciprocal immunoprecipitation was not performed because the megalin polyclonal antibody was not adequate for immunoblotting LLC-PK1 lysates.

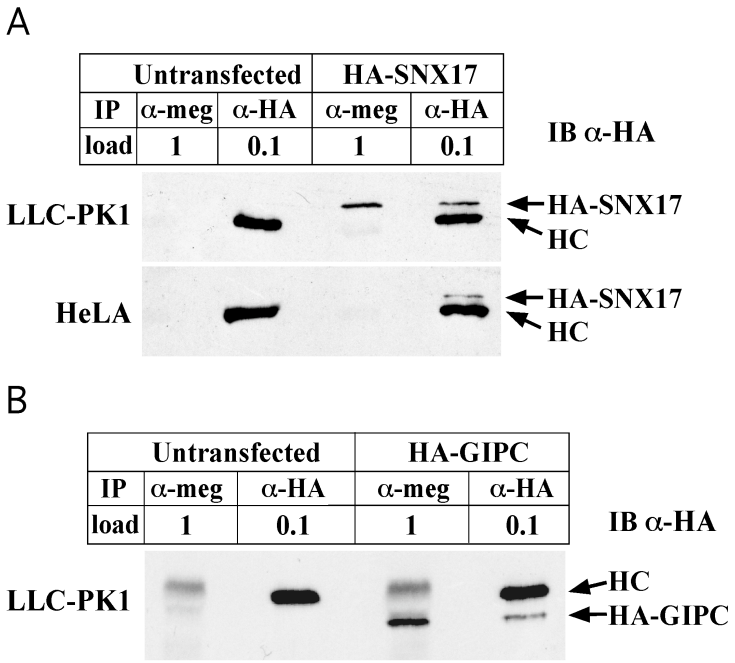

Figure 23. Megalin co-precipitates with SNX17 and GIPC. (A) Porcine kidney (LLC-PK1) or HeLa cells were transfected with HA epitope-tagged SNX17. The cells were lysed in Triton X-100 lysis buffer, centrifuged, and the supernatants were immunoprecipitated with polyclonal α-megalin or monoclonal α-HA. The immunoprecipitates were resolved by SDS-PAGE, immobilized on nitrocellulose, and immunoblotted with monoclonal α-HA. The volume of HA immunoprecipitates loaded was 10% of the volume of megalin immunoprecipitates. HeLa cells do not express a detectable level of endogenous megalin and were used as a control for non-specific binding of HA-SNX17 to the megalin antibody. (B) LLC-PK1 cells were transfected with HA epitope-tagged SNX17 and the cells were lysed, immunoprecipitated with α-HA, and immunoblotted with α-HA as described in (a). HC, IgG heavy chain

Although LDLR and megalin both have at least one NPXY signal sequence in their cytoplasmic domains, the two proteins do not share many other similar sequence or structural motifs in the tail region. SNX17 has been shown to associate with the LDLR at the NPXY sequence (Burden et al., 2004a), and experiments were performed to determine the interaction site of SNX17 and megalin (Figure 24). MegCT fused to LexA at the N-terminus was truncated to sequentially exclude the PDZ domain (meg193), the second NPXY (meg155), or the NXXY (meg106) (Figure 24). All of the megalin tail mutants were expressed at the correct size (Figure 24). Elimination of the PDZ domain or the second NPXY did not affect the interaction of megalin and SNX17 in the yeast two-hybrid system (Figure 24). A truncation that omitted the second NPXY and the NXXY sequences (meg106) disrupted the megalin and SNX17 interaction. Once it was determined that the second NPXY sequence was not required for interaction with SNX17, Tyr_{80} of the megalin tail from the first NPXY was mutated to an alanine (megY80A) and assayed for its ability to interact with SNX17-VP16. Both meg106 and megY80A lost the ability to associate with SNX17, suggesting that SNX17 could bind both the first NPXY and the NXXY sequences of megalin. An alternate possibility is that the meg106 truncation is not properly folded, causing obstruction of the first NPXY sequence, and blocking the SNX17 binding site.

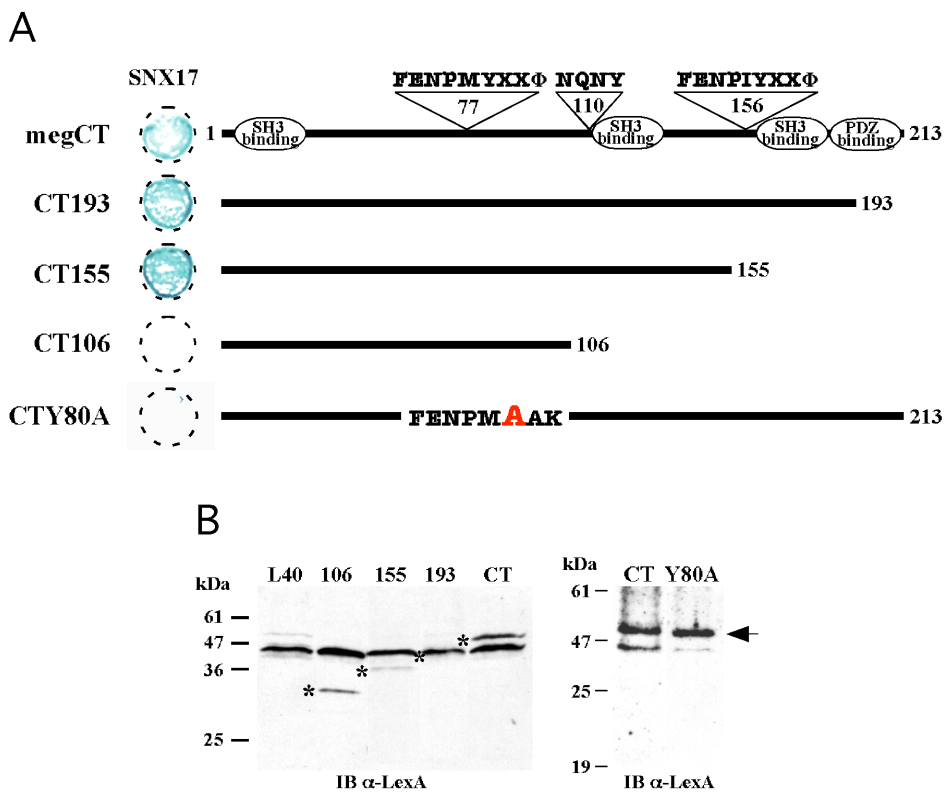

Figure 24. Tyrosine$_{80}$ of the cytoplasmic tail of megalin is required for interaction with SNX17 in the yeast two-hybrid system. (A) The 213 amino acid cytoplasmic tail of megalin was sequentially truncated from the carboxy terminus and a stop codon added. Alternately, tyrosine$_{80}$ of the megalin tail was mutated to an alanine by megaprimer mutagenesis as described in *Materials and Methods*. The truncated or mutated LexA fusion constructs were co-transformed with a partial construct of SNX17-VP16, lacking the first 72 nucleotides, into L40 yeast, and patched onto media lacking tryptophan, leucine, and histidine. Colonies were lifted onto nitrocellulose, freeze-fractured, and assayed in a colorimetric β-galactosidase assay. (B) Lysated of L40 yeast co-transformed with SNX17 and each of the megalin truncations or megY80A baits were immunoblotted with α-LexA. The specific protein band at the correct molecular weight for each sample is indicated by an asterisk or arrow.

While SNX17 had been shown to interact with other members of the LDLR family (Stockinger et al., 2002b), its association with megalin had not been observed previously. Megalin is a large ~ 600 kDa protein that is difficult to manipulate and ectopically express in cells. To avoid these problems, a chimera consisting of the external and transmembrane domains of the interleukin 2 receptor alpha subunit (Tac) fused to the cytoplasmic domain of

megalin was constructed (not shown). Unfortunately, no association between the chimera and HA-SNX17 was detected (data not shown), indicating that the chimera did not function like endogenous megalin. Therefore, the remainder of the assays were performed with endogenous LDLR because its expression is detectable in HeLa cells, which are excellent cells for gene and short interfering RNA transfections, and there are several well-established methods to measure LDLR trafficking. This choice limited the following study to the interaction between LDLR family members and SNX17 because, although GIPC has been previously shown to interact with both the megalin and LRP cytoplasmic tails, an association with LDLR was not observed (Gotthardt et al., 2000). Because the chimera of Tac fused to the megalin cytoplasmic domain failed to behave like endogenous megalin, an alternative megalin construct is required. A construct which has previously been successfully used to assay megalin sorting (Takeda et al., 2003b), containing the fourth ligand binding domain, transmembrane domain, and cytoplasmic domain of megalin, will be created to investigate the relationship between GIPC and megalin. For these reasons, GIPC was not analyzed further in this study.

SNX17 Localizes to Sorting Endosomes

Members of the sorting nexin family function in several aspects of endocytosis and recycling (Worby and Dixon, 2002). SNX17 has been shown to partially co-localize with EEA1 and rab4, two proteins enriched in the sorting endosome (Burden et al., 2004a; Williams et al., 2004). Substantial overexpression of SNX17 causes noticeable

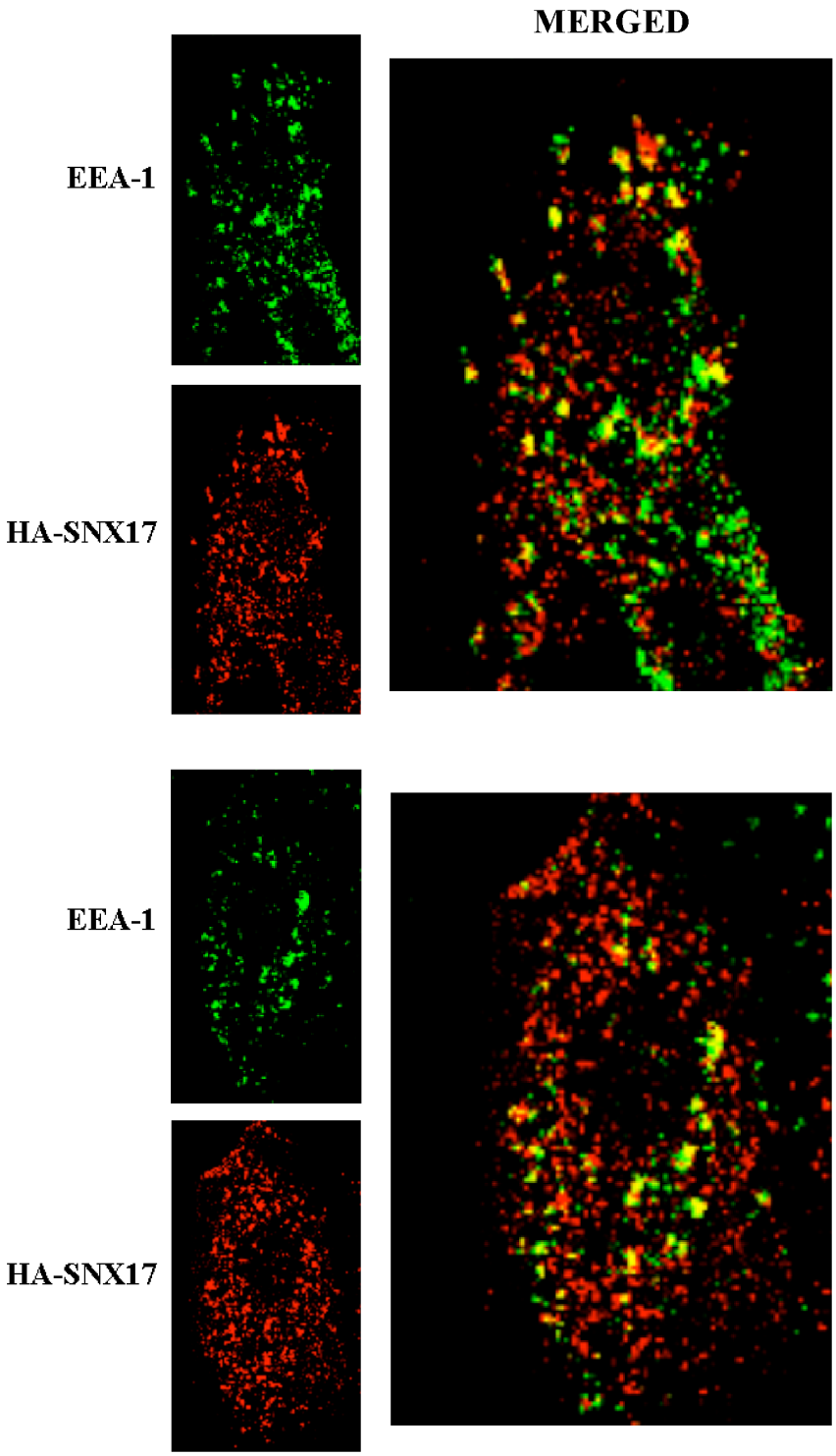

Figure 25. SNX17 is localized to sorting endosomes. 1 x 10^5 HeLa cells were infected with 2.5 PFU/cell of recombinant SNX17 tagged with an HA epitope. The cells were washed, fixed in formaldehyde and permeabilized. Cells were labeled with mouse monoclonal α-EEA1 or rabbit polyclonal α-HA followed by secondary labeling with goat α-mouse Alexa-488 and goat α-rabbit Alexa 568. The images were taken with a 63x objective on a Zeiss confocal microscope. The merged image is 2 fold magnified from the single-color images.

morphological changes to the cells (data not shown) (Burden et al., 2004a). To preclude artifacts caused by secondary effects of massive SNX17 overexpression, various titers of HA-SNX17 adenovirus were tested to attain a low level of ectopic SNX17 expression in the highest percentage of cells. 2.5 PFU/cell of adenovirus infected approximately 70% of the HeLa cells with a level of HA-SNX17 that did not produce morphological changes to the cell (Figure 25). Under these conditions, we observed that SNX17 partially co-localizes with EEA1, a marker for sorting endosomes, which is consistent with previous observations. Infection with 2.5 PFU/cell of recombinant HA-SNX17 adenovirus resulted in an approximate 2.5 fold increase in SNX17 expression when compared to endogenous levels as determined by immunoblot (data not shown).

Overexpression of SNX17 Increases the Recycling Rate of LDLR

The localization of SNX17 suggests that the protein may function in recycling LDLR to the cell surface. HeLa cells were infected with 2.5 PFU/cell of recombinant HA-SNX17 or control HA adenovirus for 16 to 18 hours. All cell surface proteins with an exposed lysine were labeled with EZ-Link-Sulfo-NHS-SS-Biotin (Pierce) for 1 hour to accumulate labeled plasma membrane proteins inside the cells (Figure 26). The cells were incubated for 0 to 30 minutes in the presence of the cell-impermeable reducing agent MesNA to cleave the disulfide bond linking biotin to proteins at the cell surface. Removing biotin from all labeled proteins that were trafficked to the plasma membrane in the specified time period allowed measurement of the recycling rate of the labeled protein. At various intervals, the cells were lysed and biotinylated proteins precipitated with neutra-avidin beads. The beads were

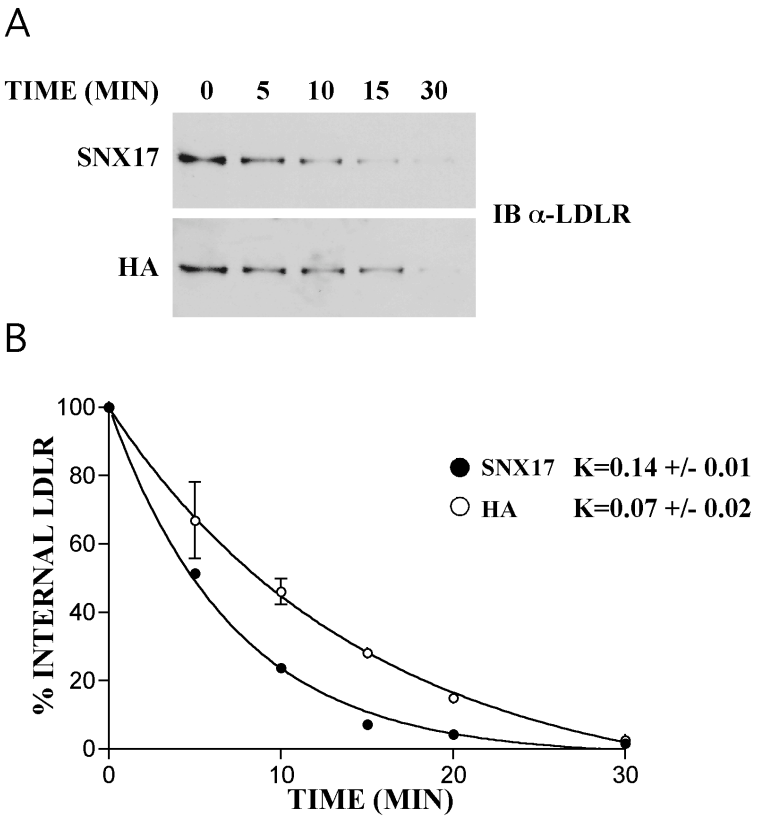

Figure 26. SNX17 overexpression increases the rate of LDLR release from endosomes. (A) HeLa cells were infected with 2.5 PFU/cell of recombinant HA or SNX17 adenovirus, labeled with NHS-SS-Biotin for 1 hour at 37° C, followed by incubation for 0 to 30 minutes at 32° C in PBS containing 25 mM MesNa, which cleaves the biotin, releasing it from the surface proteins. The cells were lysed in buffer containing 1% Triton X-100 and 0.1% SDS, as described in *Materials and Methods*, precipitated with neutravidin beads, resolved by SDS-PAGE, immobilized on nitrocellulose, and immunoblotted with α-LDLR. (B) The protein bands were analyzed by densitometry and the percentage of internal LDLR was quantitated relative to the total internal LDLR at time zero. The rate constant (K) was determined with Prism software by fitting the data to a non-linear, exponential decay curve. The error bars are the SEM from two independent experiments. IB, immunoblot.

resuspended in SDS-PAGE buffer, resolved by PAGE, and immunoblotted with monoclonal LDLR antibody. The rate of LDLR recycling was increased two-fold in cells overexpressing SNX17 as compared to control cells (Figure 26).

SNX1 partially co-localizes with EEA1 in a subcellular distribution similar to SNX17 (Haft et al., 1998). Overexpression of SNX1 causes an increase in EGFR degradation due to an increase in the rate of EGFR trafficking to the lysosome (Kurten et al., 1996). It is

possible that SNX17 could sort LDLR to the lysosome in a mechanism similar to that of SNX1. The recycling assay measured loss of biotinylated LDLR over a 30 minute time course, which inferred recycling of LDLR to the plasma membrane. However, the labeled LDLR signal could have also decreased as a result of an increase in lysosomal trafficking. Therefore, the experiment was repeated with the inclusion of 250 μM of the lysosomal inhibitor leupeptin (Roche) in the media during the 18 hour adenovirus infection (Figure 27). The addition of leupeptin to the assay did not affect the two-fold increase in LDLR recycling

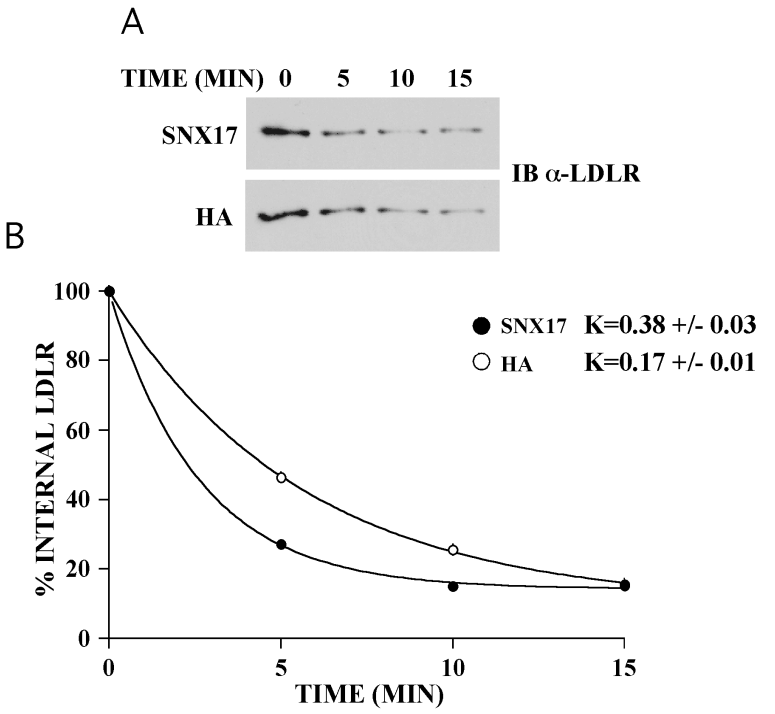

Figure 27. Overexpression of SNX17 in the presence of leupeptin increases the rate of LDLR recycling to the plasma membrane. (A) HeLa cells were infected with recombinant SNX17 or HA adenovirus in the presence of leupeptin and incubated with Sulfo-NHS-SS-Biotin for 1 hour at 37º C to accumulate labeled membrane proteins inside the cells. The labeled cells were incubated at 32º C for 0 to 15 minutes in the presence of MesNa to cleave external biotin, followed by lysis in buffer containing 1% Triton X-100 and 0.1% SDS, and precipitation with neutra-avidin beads. The precipitates were resolved by SDS-PAGE, immobilized on nitrocellulose, and immunoblotted with α-LDLR. (B) Protein bands were quantitated by densitometry and the percentage of internal LDLR was calculated relative to the total internal LDLR at time zero for each condition. The data was plotted using Graphpad Prism and the rate constant (K) calculated by fitting to a non-linear exponential decay curve.

in cells overexpressing SNX17 (Figure 27), suggesting that SNX17 overexpression increases the rate of LDLR recycling to the plasma membrane.

To rule out the possibility that SNX17 could sort LDLR to the lysosome, an experiment was performed to measure the effect of SNX17 overexpression on the rate of LDLR degradation. HeLa cells were infected with 2.5 PFU/cell of recombinant HA-SNX17 or control HA adenovirus for 16-18 hours in normal media. The cells were labeled with

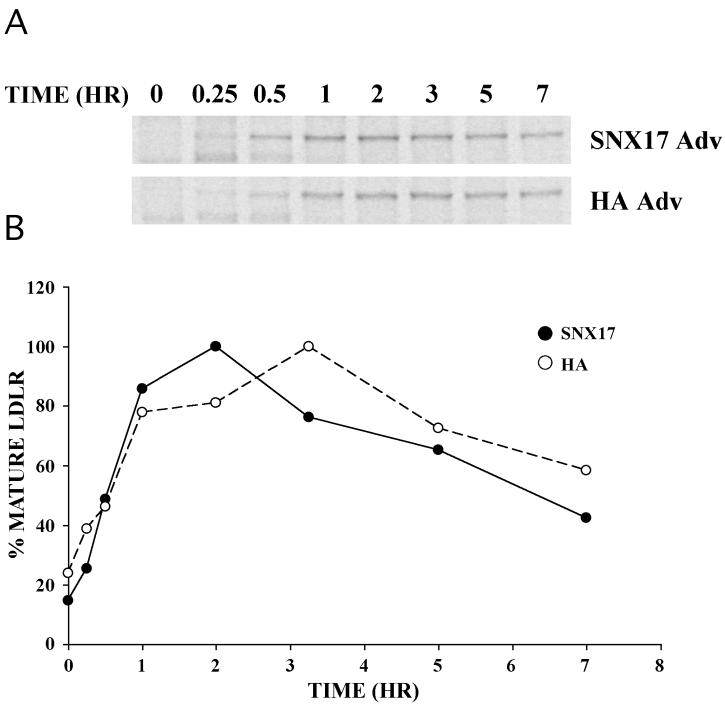

Figure 28. LDLR matures slightly faster in cells overexpressing SNX17. (A) HeLa cells were infected with 2.5 PFU/cell of HA-SNX17 or control HA adenovirus for 16 to 18 hours. The infected cells were labeled with ^{35}S-amino acids for 15 minutes followed by incubation in normal media for 0 to 7 hours. After the indicated chase time, the cells were lysed, immunoprecipitated with α-LDLR, resolved by SDS-PAGE, and analyzed by phosphor imaging. (B) The percentage of mature LDLR was calculated relative to the highest level of LDLR for each condition. The graph represents the average of two independent experiments.

[^{35}S]-amino acids for 15 minutes, followed by a chase in normal media for 0 to 28 hours. Labeled cells were lysed, immunoprecipitated with monoclonal LDLR antibody, resolved by SDS-PAGE, and analyzed by phosphor imaging (Figure 28). In the early (15 minute to 3 hour) time points, LDLR was post-translationally modified to the mature, 160 kDa apparent molecular weight. When SNX17 was overexpressed, the appearance of mature LDLR was slightly faster than in control cells (Figure 28). In cells overexpressing SNX17, the amount of mature LDLR peaked after 2 hours of chase. For the control cells, the amount of mature LDLR peaked after 3 hours of chase. However, when the data in the 0-3 hour chase period was fitted to a non-linear regression exponential association curve (Graphpad Prism®), the rate constant for LDLR maturation in cells overexpressing SNX17 was not significantly different than in control cells (1.23 +/- 0.26 for SNX17 overexpression and 1.59 +/- 0.66 in control cells).

The first time point in the degradation curve was the time at which the highest value of LDLR was observed for each expression condition (2 hours for SNX17 overexpression and 3 hours for control cells) (Figure 28). The data was fitted to a non-linear regression exponential decay curve (Graphpad Prism®) and the rate constant (K) calculated (Figure 29). In cells overepressing SNX17, the rate of LDLR degradation was not significantly different from the control cells, which is most likely attributed to similar degradation rates in the linear range of the curve. However, the difference in the plateau of LDLR for each expression condition was approximately 2 fold (19.25 +/- 3.9 for SNX17 overexpression and 35.45 +/- 3.2 for control cells) (Figure 29).

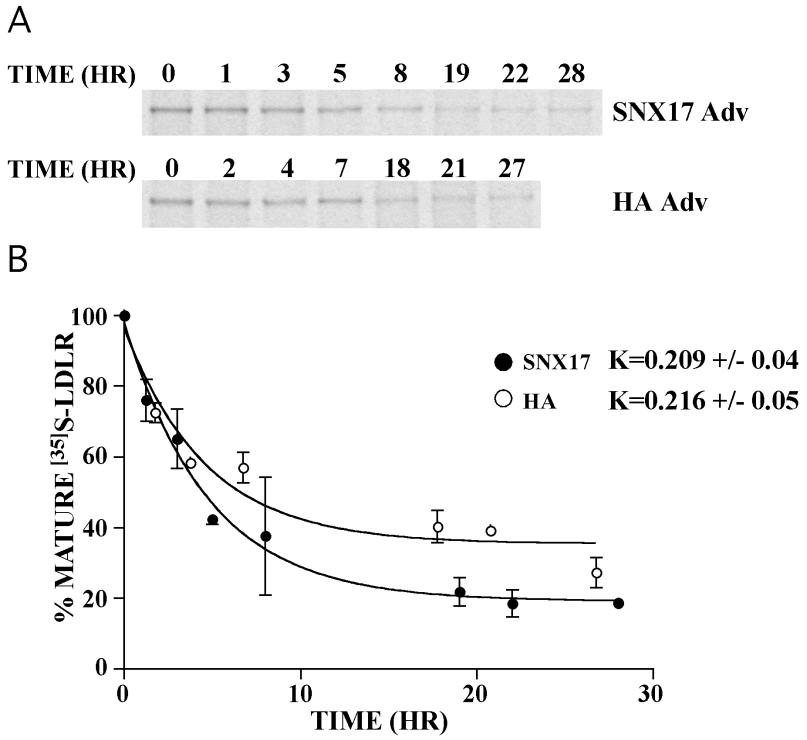

Figure 29. The rate of LDLR degradation at early time points is not significantly affected by SNX17 overexpression. (A) HeLa cells were infected with recombinant HA or SNX17 adenovirus for 18 hours followed by incubation in methionine and cysteine-deficient media for 30 minutes. The cells were labled with ^{35}S-amino acids for 15 minutes and chased in normal media for 0 to 28 hours. After the chase period, the cells were lysed in TNE buffer containing Triton X-100 and 0.1% SDS, and immunoprecipitated with α-LDLR. The immunoprecipitates were washed, resuspended in SDS-PAGE buffer, resolved by PAGE, fixed, and analyzed with a Typhoon scanner. The zero time point represents the time in the chase period when the mature LDLR was at the highest level. (B) The percentage of mature 160 kDa LDLR was calculated relative to the highest value of LDLR during the chase period. The data was plotted with Graphpad Prism® and the rate constant (K) calculated by fitting to a non-linear exponential decay curve. The error bars represent the SEM of two independent experiments.

It is possible that increased rate of LDLR recycling to the plasma membrane caused by SNX17 overexpression indirectly causes more LDLR targeting to the lysosome.

Following internalization, the bulk of LDLR is in the sorting endosome, from which it is recycled through either a fast (~2 minute) pathway directly to the plasma membrane or a slower (~14 minute) pathway through the endocytic recycling compartment on its way to the plasma membrane (Figure 3)(Maxfield and McGraw, 2004). A very small fraction (~3.0%) of LDLR is also trafficked to the multivesicular endosome and lysosome, where it will be degraded. SNX17 may sort LDLR to the plasma membrane from the endocytic recycling compartment. Presumably, the LDLR cycling time would be decreased with SNX17 overexpression, which would place LDLR in the sorting endosome with more frequency, increasing the probability of lysosomal targeting. The increased lysosomal targeting may only be apparent after many LDLR cycles, which would explain the differences in the plateaus of the SNX17 overexpression and HA control LDLR degradation curves. SNX17 most likely does not directly target LDLR to the lysosome, as suggested by the increase in LDLR recycling to the plasma membrane with SNX17 overexpression in the presence of leupeptin.

SNX17 Affects LDLR Protein Expression

To determine if SNX17 affects LDLR expression at steady state, HeLa cells were infected with recombinant SNX17 tagged with an HA epitope or control HA adenovirus, lysed in SDS-PAGE buffer, resolved by PAGE, and immunoblotted with monoclonal LDLR antibody (Figure 30). LDLR protein expression was approximately 1.7 fold decreased in cells overexpressing SNX17 as compared to control cells. LDLR mRNA expression, assayed by quantitative PCR, was not significantly affected by SNX17 overexpression (Figure 30).

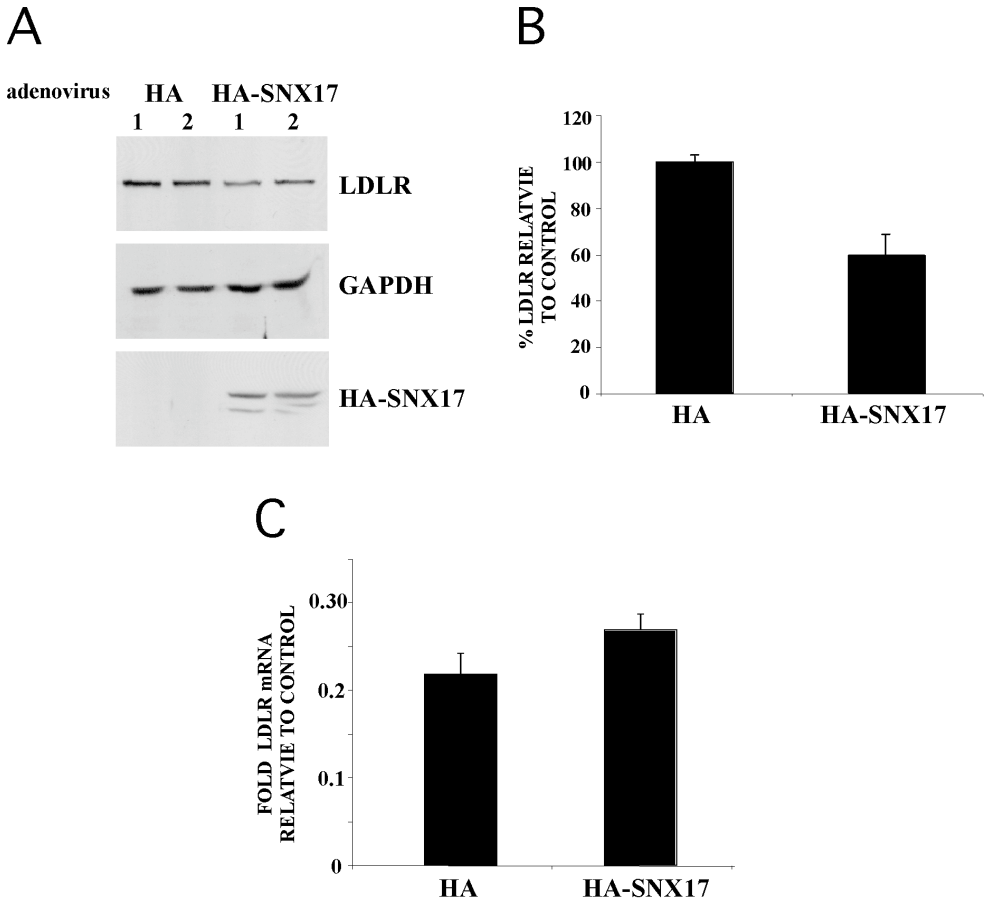

Figure 30. SNX17 overexpression causes a reduction in steady state LDLR protein levels. (A) HeLa cells were infected with 100 PFU/cell of recombinant HA-SNX17 or control HA adenovirus for 16-18 hours. The cells were lysed in SDS-PAGE buffer, resolved by 10% PAGE, and immunoblotted with -LDLR, -GAPDH, or -HA. (B) LDLR and GAPDH protein bands were analyzed by densitometry. LDLR was normalized to GAPDH and plotted relative to the control HA. The error bars represent the standard deviation from three independent experiments. (C) HeLa cells were infected with HA-SNX17 or control HA adenovirus as in (a) and RNA harvested. cDNA was generated from the harvested RNA and LDLR and cyclophilin mRNA levels were determined by quantitative PCR. LDLR was normalized to the control cyclophilin. The error bars represent the standard deviation from two independent experiments performed in triplicate. p=0.5 as determined by student's t-test

In order to observe a change in LDLR protein expression at steady state, a high titer (100 PFU/cell) of adenovirus was required. SNX17 expression may not be limiting in HeLa cells, which would require a large quantity of SNX17 to affect LDLR expression at steady state.

Decreased LDLR expression caused by SNX17 overexpression is most likely due to an indirect increase in LDLR trafficking to the lysosome as a result of the decrease in LDLR cycling time. HeLa cells were infected with recombinant HA-SNX17 or control HA adenovirus for 1.5 hours before the media was replaced with normal media or media containing 250 μM leupeptin, a lysosomal inhibitor. The cells were incubated for 18 hours,

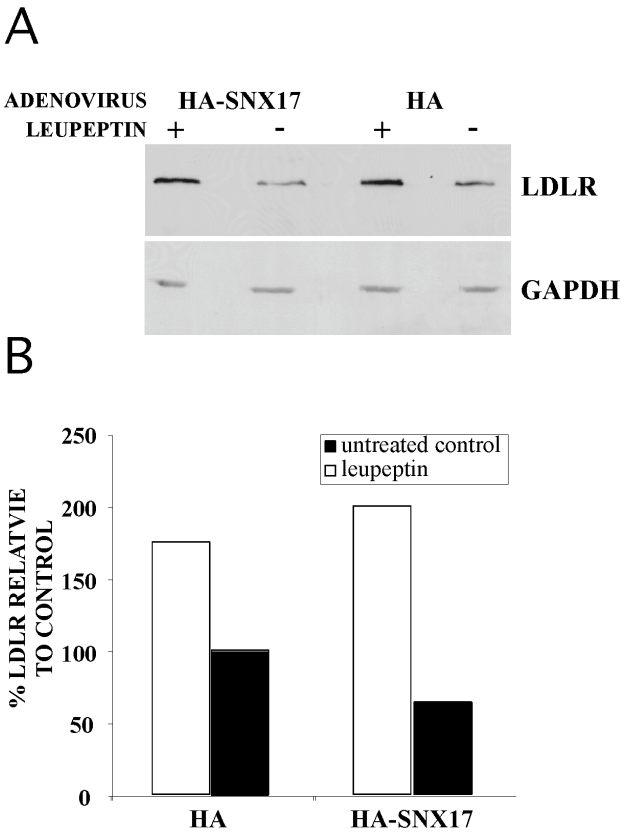

Figure 31. SNX17 overexpression causes LDLR targeting to the lysosome. (A) 5 x 10^5 HeLa cells were infected with 100 PFUs/cell of HA-SNX17 or control HA adenovirus in the presence or absence of 250 μM leupeptin for 18 hours. The cells were lysed in SDS-PAGE buffer, resolved by 10% SDS-PAGE, immobilized on nitrocellulose, and immunoblotted with α-LDLR and α-GAPDH. (B) LDLR and GAPDH protein bands were analyzed by densitometry. LDLR was normalized to GAPDH in each sample and the normalized data was plotted relative to the untreated HA control.

lysed in SDS-PAGE buffer, resolved by PAGE, immobilized on nitrocellulose, and immunoblotted with anti-LDLR and anti-GAPDH (Figure 31). The decreased LDLR expression caused by SNX17 overexpression was not observed when leupeptin was included in the assay (Figure 31), suggesting that LDLR is indirectly targeted to the lysosome with more frequency when SNX17 is overexpressed.

Short interfering RNA (siRNA) directed at endogenous SNX17 was used to observe LDLR expression under conditions in which SNX17 was depleted. Two independent pairs of siRNA oligonucleotides at position 500 (si1) or 183 (si2) in the human SNX17 gene were transfected into HeLa cells for 48 hours. SNX17 mRNA and protein expression was quantified in cells treated with si1 or si2 versus control cells. SNX17 mRNA was reduced by approximately 80% in si1-transfected cells and 70% in si2-transfected cells (Figure 32). Correspondingly, SNX17 protein expression was reduced by approximately 90% in si1-transfected cells and 75% in si2-transfected cells as compared to the control (Figure 32). LDLR protein expression was 1.7 fold increased in cells transfected with si1 and 1.5 fold increased in cells transfected with si2. The increase in LDLR manifested by directed reduction of SNX17 with two independent oligonucleotide pairs suggests that SNX17 indirectly regulates lysosomal targeting of LDLR. This data, in conjuction with decreased LDLR expression in the presence of increased SNX17 and increased LDLR recycling with SNX17 overexpression, indicates that SNX17 may regulate the total cycling time of the LDLR.

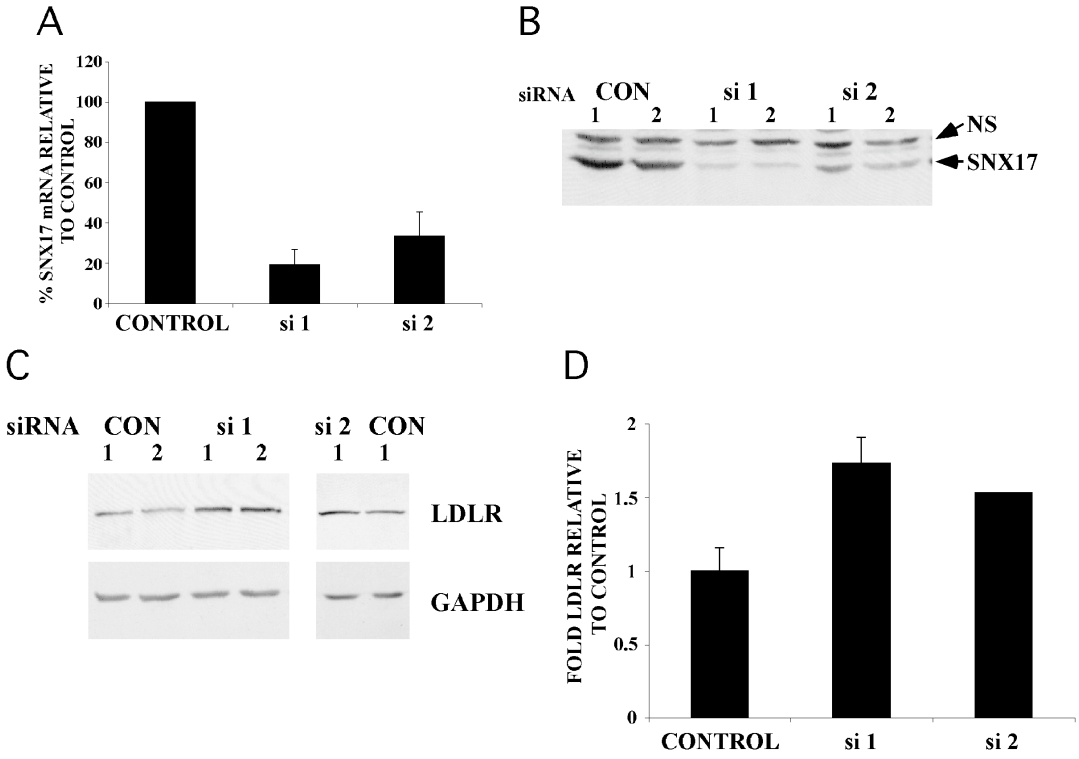

Figure 32. Targeted reduction of SNX17 increases LDLR expression. 3 x 10^5 HeLa cells were transfected with two different pairs of siRNA oligonucleotides directed at SNX17 (si1 and si2) or a control cy3-luciferase oligonucleotide pair. (A) RNA was harvested and cDNA generated. SNX17 and cyclophilin mRNA levels were determined by quantitative PCR. SNX17 was normalized to the cyclophilin and si1 and si2 were plotted relative to the control luciferase. Error bars represent the standard deviation from 2-3 experiments performed in triplicate. (B) Transfected cells were lysed in SDS-PAGE buffer, resolved by 10% PAGE, immobilized on nitrocellulose, immunoblotted with α-SNX17, and analyzed by densitometry. (C) Transfected cells were lysed in SDS-PAGE buffer, resolved by PAGE, immunobilized on nitrocellulose, and immunoblotted with α-LDLR and α-GAPDH. (D) Immunoblots in (c) were analyzed by densitometry and LDLR protein bands were normalized to GAPDH. LDLR protein expression was blottd relative to control cells. Error bars represent the standard deviation from 3 experiments performed in duplicate. CON, control cells transfected with cy3-luciferase siRNA; NS, non-specific band

SNX17 does not Affect LDLR Cell Surface Expression

The effect of SNX17 overexpression on LDLR recycling to the plasma membrane should result in an increase in the fraction of LDLR expressed at the cell surface if the internalization rate of LDLR remained the same. HeLa cells were infected with recombinant HA-SNX17 or control HA adenovirus and cell surface expression of LDLR was measured by fluorescence activated cell sorting (FACS). Surface LDLR was significantly increased (4.6 fold) in cells grown in lipoprotein-deficient serum, indicating that the antibody is specific to LDLR (Figure 33). LDLR plasma membrane expression was not affected by SNX17 overexpression (Figure 33). LDLR recycling from the endocytic recycling compartment back to the plasma membrane is the rate-limiting step in LDLR endocytosis (Maxfield and McGraw, 2004). Experiments with diI-LDL bound to LDLR have shown that LDLR diffuses laterally across the plasma membrane until it contacts a pre-existing clathrin cluster and is rapidly internalized (Ehrlich et al., 2004). SNX17 overexpression increases the rate of LDLR delivery to the plasma membrane, which would deposit more LDLR on the cell surface per unit of time. It is possible that more LDLR surface targeting allows more LDLR to contact clathrin pits, resulting in more LDLR internalized per unit time as compared to control cells. At the same time, this suggests that the endocytic cycling time for LDLR is decreased, which would allow LDLR to contact the sorting endosome with higher frequency, allowing a higher incidence of lysosomal targeting.

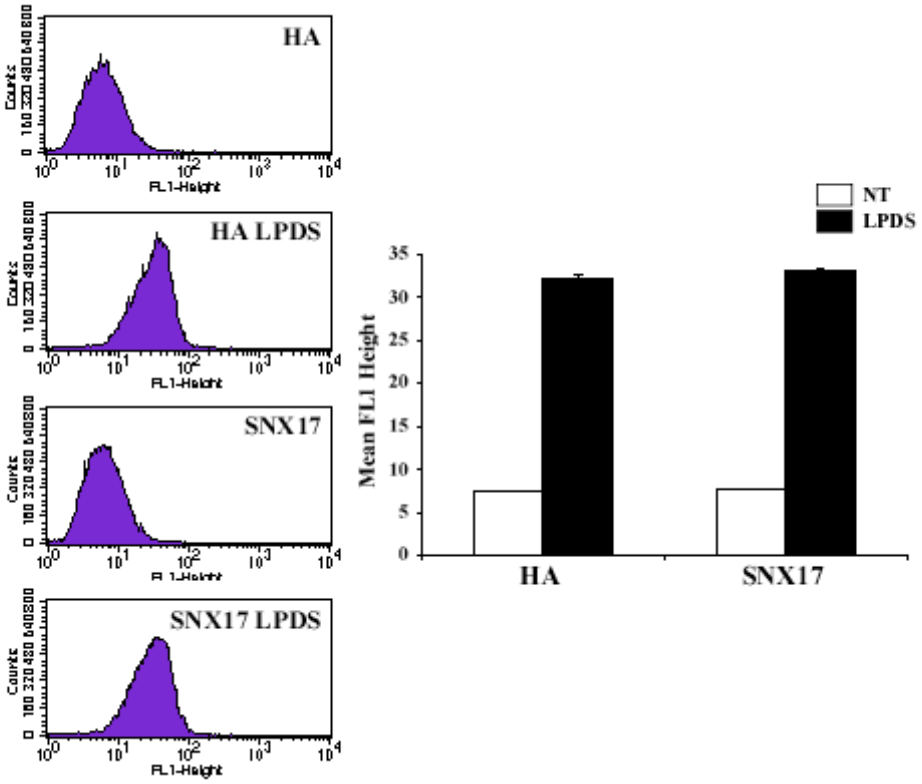

Figure 33. SNX17 overexpression does not affect LDLR cell surface expression. 10^5 HeLa cells were infected with 100 PFU/cell of recombinant HA-SNX17 or control HA adenovirus in normal or lipoprotein-deficient media for 18 hours. The cells were incubated in PBS++ containing 1% BSA and 4.6 μg/ml α-LDLR at 4° C for 1 hour, followed by incubation in secondary α-mouse conjugated to Alexa 488 for 1 hour at 4° C. Labeled cells were detached from the wells using a non-enzymatic reagent as described in *Materials and Methods* and analyzed by FACS. The mean fluorescence intensity of 20,000 cells was recorded. The error bars represent the standard deviation of duplicate samples.

Transferrin Receptor Recycling and Internalization is Unaffected by SNX17 Overexpression.

TfR is internalized and recycled in the same pathway as the LDLR. To determine if SNX17 alters the endocytic recycling pathway or if its effects are specific to LDLR, experiments were performed to assay the effect of overexpression of SNX17 on TfR trafficking. HeLa cells were infected with 2.5 PFU/cell recombinant SNX17 or control HA adenovirus and the recycling assay was executed exactly the same way as the experiment to measure LDLR recycling except the neutra-avidin precipitates were immunoblotted with

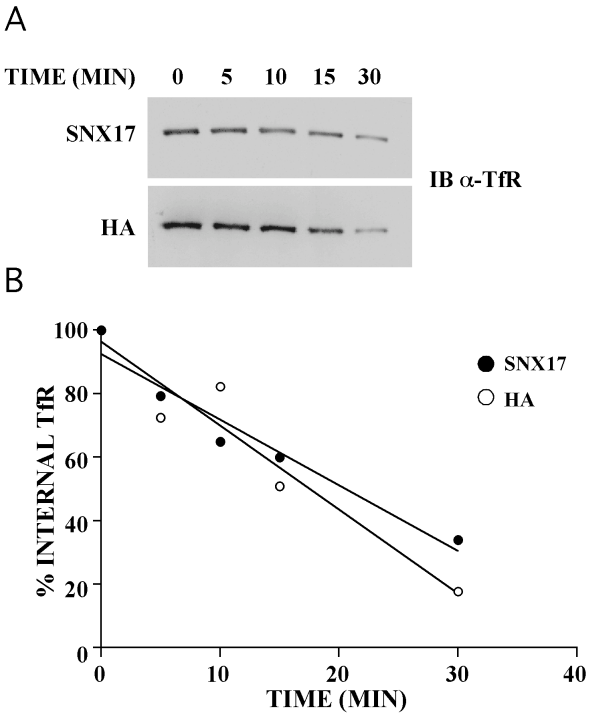

Figure 34. Transferrin receptor recycling is unaffected by SNX17 overepression. (A) HeLa cells infected for 16 hours with 2.5 PFU/cell recombinant HA or SNX17 adenovirus were incubated with Sulfo-NHS-Biotin for 1 hour at 37º C to allow surface proteins to accumulate inside the cell. The cells were incubated at 32º C for 0 to 30 minutes in the presence of MesNa to cleave the external biotin from the proteins, followed by lysis in buffer containing 1% Triton X-100 and 0.1% SDS, and precipitation with neutra-avidin beads. The beads were washed, resolved by SDS-PAGE, immobilized on nitrocellulose, and immunoblotted with α-TfR. (B) Protein bands were analyzed by densitometry and the percentage of internal TfR was calculated relative to the total internal TfR at time zero for each condition. The data was plotted with Graphpad Prism® software and fitted to a linear curve.

antibody specific to transferrin receptor (Figure 34). Transferrin receptor recycling was unaffected by SNX17 overexpression (Figure 34), suggesting that SNX17 does not alter the recycling machinery.

To determine whether SNX17 affects Tf internalization, HeLa cells infected with recombinant HA-SNX17 or control HA adenovirus were incubated with Tf conjugated to Alexa 488 (Molecular Probes) for 0 to 30 minutes at 37° C. The cells were washed with PBS containing magnesium and calcium which was adjusted to pH 5.0 to remove external bound Tf and internal Tf-488 was quantitated by FACS (BD FacsCaliber) (Figure 35). Transferrin internalization in SNX17-overexpressing cells was almost identical to control cells, indicating that SNX17 overexpression did not affect Tf endocytosis. This data, in conjunction with the lack of an effect of SNX17 overexpression on TfR recycling, suggests that SNX17 does not alter the endocytic recycling machinery.

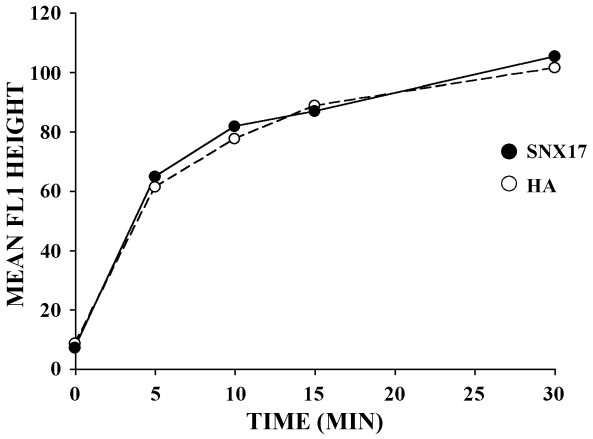

Figure 35. Transferrin internalization is not affected by SNX17 overexpression. 10^5 HeLa cells were infected with 100 PFU/cell recombinant HA-SNX17 or control HA adenovirus for 16-18 hours at 37° C. The cells were incubated at 37° C for 30 minutes in DMEM to allow surface-bound iron to dissociate, followed by incubation for 0 to 30 minutes in PBS++ containing 0.2% BSA and 50 μg/ml Tf-488. Surface Tf-488 was removed by washing with PBS++ adjusted to pH 5.0 and internal fluorescent Tf quantitated by FACS. The mean fluorescent intensity of 20,000 cells was calculated.

CHAPTER FIVE
DISCUSSION

Eleven Amino Acids in the Transmembrane Domain of HA are Required for Apical Sorting and DRM Association

Mutating certain residues in the transmembrane of domain of HA or several other apically sorted proteins significantly affects the ability of the protein to be transported to the apical membrane of epithelial cells and to partition into DRMs (Huang et al., 1997; Lin et al., 1998; Mateus Fernandez et al., 2002; Scheiffele et al., 1997). In this study, we show that at least eleven TM amino acids that would reside in the outer leaflet of the membrane are required for preferential apical sorting. While twelve amino acids are required for both apical sorting and DRM association, thirteen wild-type TM residues are all required for sorting of HA to the apical membrane and partitioning into DRMs with efficiencies similar to wild type HA. The most conserved residues in this region have small, relatively polar side chains of the type that stabilize oligomers of transmembrane helices by promoting the formation of interchain hydrogen bonds (Huang et al., 1997; Senes et al., 2001). Assuming that the three HA monomers cross the membrane as alpha helices and oligomerize with these small residues oriented towards the center of the oligomer, then large hydrophobic residues oriented towards the surrounding lipids as well as side chains that might stabilize the TM structure were all necessary for HA to enter DRMs and be sorted. Mutation of residues that would reside in the inner leaflet had no appreciable effect on ability of the HA mutants to incorporate into DRMs. It is possible that HA could associate with a lipid that is primarily localized to the outer leaflet, such as SM. If this is true, perturbation of the SM association

by affecting the structure of the transmembrane trimer in the outer leaflet could disrupt the ability of HA mutants to be incorporated into DRMs. In the minimum sequences that allowed sorting to the apical surface, TM 11.0 – TM 11.4, changing to leucine any one of four contiguous wild type residues that would sit in one turn of helix had no appreciable affect on sorting, but severely inhibited partitioning into DRMs. Changing additional residues, even when they were not contiguous, prevented sorting. Taken together, the results suggest that the requirements of the TM domain for isolation of HA in DRMs are more stringent than the requirements for sorting.

To determine if the ability to partition into DRMs reflects the ability of HA mutants to enter lipid rafts on the plasma membrane surface of living cells, we investigated the lateral mobility of HA TM 11.0 and HA TM 12.0 on live COS-1 cells. The lateral mobility of wild type HA at the plasma membrane increased when cholesterol levels were lowered, but the mobility of HA 2A520, a mutant that does not enter DRMs and is not sorted apically, is both faster than wild type HA and independent of cholesterol levels. HA TM 12.0, which is sorted slightly more efficiently to the apical surface, behaved like wild type HA. HA TM 11.0, a mutant that is sorted apically but does not partition with Triton-insoluble membranes, showed cholesterol-independent lateral mobility at the surface of live cells. However, when lateral mobility was measured in the presence of an immobilized raft marker, HA TM 11.0 had a cholesterol-dependent lateral diffusion rate. These data suggest that HA TM 11.0 had only a transient association with lipid rafts, which was undetectable by both standard lateral mobility measurements and partitioning into DRMs. I interpret my data to suggest that, for HA, even a transient association with lipid rafts is sufficient for HA to interact with the

apical sorting machinery. Others have observed that some apical proteins do not appear to enter DRMs and have interpreted this as support for a second pathway to the apical surface that is independent of lipid rafts. It is possible that the fraction of HA TM 11.0 that is sorted apically enters a raft-independent pathway to the apical surface different from that taken by wild-type HA. Another possibility is that the DRM assay used to measure lipid raft incorporation is not sufficiently sensitive to detect transient raft associations. The DRM assay is the most common method to operationally define lipid rafts. However, I and other groups have observed that this assay is not sufficient to determine if a protein is associated with lipid rafts (Bacia et al., 2004; Edidin, 2003; Heerklotz, 2002; Heerklotz et al., 2003).

MAL and HA do not Associate in Apical Vesicles Derived from the TGN

The fact that amino acid side chains of the HA TM that would extend towards the lipids in the outer leaflet of the bilayer are also important for the ability of HA to be transported apically indicates that the TM forms a surface that interacts with either lipids or protein. Previously it has been shown that the integral membrane protein MAL is required for transport of many proteins to the apical surface and that HA can be co-precipitated with MAL (Puertollano et al., 1999). I investigated this interaction using several HAs with mutations in the TM. Mutations that inhibited partitioning into DRMs inhibited co-precipitation with MAL and only mutants such as HA TM 13.0 that entered DRMs and were sorted well were able to co-precipitate similar to wild type HA. Under the conditions I employed, at most a few percent of HA was observed to co-precipitate with MAL in Triton X-100. Co-precipitation of HA and MAL was not reciprocal. HA was precipitated by

antibody to the cytoplasmically oriented myc-tag on MAL but MAL was not precipitated by antibody to the external domain of HA. I found that the HA that co-precipitated with MAL was inaccessible to trypsin unless low concentrations of SDS were added to the precipitate, and this was true for cells lysed in Triton X-100 both at 4° C or at 37° C (data not shown). This suggests that HA and MAL co-precipitate only when they are both present in a closed DRM vesicle. Overexpression of MAL in MDCK cells infected with recombinant adenovirus did not increase the fraction of wild-type HA or HA TM 11.0 that associated with DRMs, suggesting that MAL does not recruit HA into DRMs. Taken together, the data suggests that MAL and HA may co-precipitate only when they are both present in a lipid raft, and it is unclear if the two proteins interact directly. HA is transiently associated with lipid rafts, which could explain the low percentage of HA that co-precipitated with MAL. This hypothesis also explains why HA TM 11.4, a mutant that most likely occupies lipid rafts for less time than wild-type HA was not observed to associate with MAL.

The orientation of HA and MAL in DRM vesicles is that expected for a vesicle derived from internal membranes, not fragments of the plasma membrane that vesicularize after homogenization. However, very little HA precipitated with MAL until 80 min after a shift from 20° C to 37° C, although HA reached steady state levels at the plasma membrane after 60 min of chase. In order to determine if MAL and HA co-precipitate in the endocytic pathway, I biotinylated cell surface proteins in MDCK cells and measured the association of HA and MAL 60 minutes after internalization. While proteins that were biotinylated at the cell surface and allowed to internalize co-precipitated with MAL, I did not observe an association between MAL and HA in this time period. HA is internalized less than 1% per

minute (Lazarovits and Roth, 1988), which should allow a sufficient amount of HA to accumulate inside the cell to detect an association between HA and MAL if one occurred. It is possible that MAL and HA are sorted into different pathways subsequent to internalization. The percentage of HA in the same endocytic compartment as MAL at any given time could be very small, which would preclude detection of an association between biotinylated HA and MAL in my assay. It is also possible that the HA that co-precipitates with MAL comes from a surface pool that is difficult to biotinylate, such as HA residing in invaginations of the apical plasma membrane or missorted HA that has been endocytosed from lateral membranes.

If MAL has an active role in the recruitment of HA to rafts at the TGN, it may act transiently or catalytically to form the transport intermediate without incorporating stoichiometrically with cargo into the transport vesicle. In this respect, MAL might behave less like a sorting receptor such as the KDEL receptor or mannose 6-phosphate receptor and more like proteins such as Sar1 and Arf1 that organize the formation of a transport intermediate but do not themselves bind cargo. Although possible, this hypothesis is unlikely given the predominant localization of MAL to vesicular structures separate from the TGN (Puertollano et al., 2001a). In addition, attenuation of MAL in MDCK cells inhibits apical internalization of pIgR and transferrin receptor, two proteins which do not have a detectable association with DRMs and are internalized by a clathrin-mediated mechanism, suggesting that MAL may affect the endocytic pathway (Altschuler et al., 1999; Martin-Belmonte et al., 2003). Basolateral internalization of pIgR is unaffected by MAL reduction (Martin-Belmonte et al., 2003). Apical internalization of folate receptor, a GPI-anchored DRM-associated

protein that is internalized by a clathrin-independent mechanism, is also unaffected by MAL reduction (Martin-Belmonte et al., 2003; Sabharanjak and Mayor, 2004). The two proteins affected by MAL reduction are not detectable in DRMs and most likely do not associate with MAL, suggesting that MAL most likely affects a clathrin-mediated pathway from the apical membrane. Sphingomyelin (SM), a necessary component of lipid rafts and possibly apical transport vesicles, is internalized through both a clathrin-dependent and caveolar mechanism (Puri et al., 2001). Co-immunoprecipitation of MAL and the galactolipid sulfatide from detergent insoluble fractions suggests that MAL could directly bind the lipid (Frank et al., 1998). In addition, depletion of endogenous MAL from MDCK cells significantly diminishes the percentage of HA in DRMs (Puertollano et al., 1999). MAL may recycle SM from the plasma membrane to the TGN, where SM could be incorporated into apical transport vesicles (Figure 36). The hypothesis that MAL is required to recycle a necessary component of apical vesicles from the plasma membrane to the TGN is consistent with the observation of an accumulation of HA in the TGN of cells depleted of endogenous MAL (Cheong et al., 1999). MAL could also act in the apical recycling endosome to sort apical proteins to the correct surface. However, it is unlikely that MAL sorts HA in the recycling endosome, because HA should accumulate in an endosomal compartment instead of the Golgi when MAL is reduced.

Measurement of SM recycling in MAL-depleted MDCK cells could confirm the hypothesis that MAL is required for SM recycling. This experiment is not trivial, since attenuation of MAL by antisense oligonucleotides is not always reproducible (personal communication, M. Alonso) and transfection of MDCK cells with siRNA oligonucleotides is

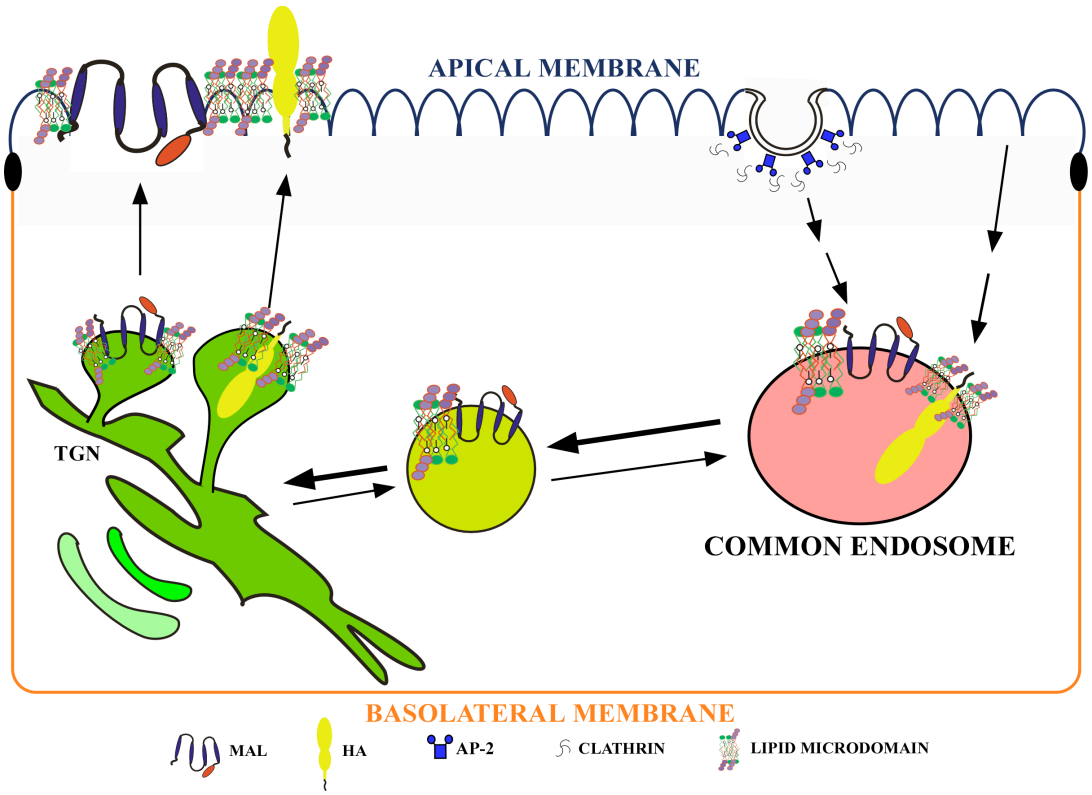

Figure 36. Proposed mechanism of MAL effect on apical sorting. MAL and HA are sorted in the TGN by their ability to associate with lipid rafts. The two integral membrane proteins may transiently associate in apical vesicles or in the endocytic pathway, although a direct association has not been determined. MAL may directly associate with apical vesicle components, such as SM or glycosphingolipids, transporting the sphingolipid to the TGN, where it is incorporated into an apical vesicle.

not efficient (unpublished data). Stable transfection of short hairpin RNA oligonucleotides under the control of a U6 RNA polymerase promoter have been used successfully to deplete a Rho exchange factor in MDCK cells and this method could be used to deplete MAL (Benais-Pont et al., 2003).

The First NPXY Sequence in the Cytoplasmic Domain of Megalin is Required for an Association with Sorting Nexin 17

The stoichiometry and timing of MAL and HA association, combined with the subcellular localization of MAL suggest that MAL does not sort HA apically at the TGN. Therefore, we performed a yeast two-hybrid screen with the cytoplasmic domain of megalin, which has been shown to contain an apical sorting signal, to identify candidates that could biosynthetically sort apical proteins. While the screen identified many novel interaction partners for megalin, none of the proteins were obviously apical sorting proteins. SNX17 was one of the most likely candidates for the regulation of protein sorting. The sorting nexin family of proteins regulates several aspects of the endocytic recycling pathway. SNX17 has been shown to associate with the cytoplasmic domain of all core members of the LDLR family *in vitro* except megalin (Stockinger et al., 2002a). However, it is possible that the megalin GST-fusion construct utilized in those studies to detect an association between SNX17 and megalin was not properly folded, abrogating a SNX17 and megalin interaction. We confirmed the yeast two-hybrid interaction of megalin and SNX17 by co-precipitation of the two proteins from HeLa cells.

While megalin is sorted apically, LDLR and LRP, two other members of the LDLR family are sorted basolaterally. SNX17 associates with all three proteins, suggesting that SNX17 may not function as an apical sorting protein. However, it is possible that LDLR and LRP contain basolateral targeting signals that are stronger than the two apparent basolateral signals, di-leucine and YXXΦ, in the cytoplasmic domain of megalin. While basolateral targeting sequences are usually dominant over apical sequences it is possible that megalin

could have a dominant apical sequence. Megalin floats on density gradients (Marzolo et al., 2003), suggesting that it could be apically sorted through interaction with another protein that is associated with lipid rafts. It is unlikely that SNX17 could sort megalin into lipid rafts at the TGN. SNX17 is localized to sorting and recycling endosomes and does not partition into DRMs (unpublished results). If SNX17 regulates an aspect of apical and/or basolateral sorting, it may do so at the sorting or apical recycling endosome. SNX17 may function like SNX1, a member of the mammalian retromer, which may be involved in formation of budding vesicles from the sorting or recycling endosome. SNX17 could sort LDLR or megalin into recycling vesicles destined for the apical or basolateral membranes.

Megalin has two NPXY domains and a NXXY sequence, and a truncation that removes the second NPXY sequence significantly impairs endocytosis (Takeda et al., 2003b). Mutagenesis of the tyrosine in the first NPXY sequence of megalin disrupted the interaction of the cytoplasmic tail of megalin and SNX17 in the yeast two-hybrid system, suggesting that SNX17 associates with the first NPXY sequence. Dab2, a clathrin adaptor protein, which has been shown to regulate internalization of megalin, binds to the second NPXY sequence in the cytoplasmic domain of megalin (Oleinikov et al., 2000). Dab1, which may also regulate an aspect of LDLR family member endocytosis, does not compete with SNX17 for binding to ApoER2 (Stockinger et al., 2002a). Although the cytoplasmic tails of ApoER2 and megalin do not share many similarities outside of the NPXY sequence, it is possible that Dab1 and SNX17 may also have different binding sites on the tail of megalin. Because SNX17 interacts with the first NPXY sequence, it probably does not regulate internalization of megalin. Analysis of the interaction sites of Dab2 and SNX17 in the LDLR

cytoplasmic domain is complicated by the presence of only one NPXY sequence. Both Dab2 and SNX17 have independently been shown to associate with the FENPXY sequence of LDLR, which is required for internalization of the receptor (Burden et al., 2004b; Chen et al., 1990; Morris and Cooper, 2001). However, it is not known if Dab2 and SNX17 compete for the same binding site on LDLR.

Megalin is a large (~600 kDa) protein that is expressed predominantly in epithelial cells. The large size makes the protein difficult to mutate and transfect. In addition, transfection of short interfering RNA oligonucleotides is not efficient in epithelial cells, such as MDCK cells. Therefore, the remainder of the experiments assayed the regulation of LDLR by SNX17.

I observed a two-fold increase in the rate of LDLR recycling from internal compartments to the plasma membrane when SNX17 was overexpressed in HeLa cells as compared to control cells. In the recycling assay, I biotinylated cell surface proteins at 37º C for 1 hour to allow the proteins to accumulate inside the cell. Internalized proteins were dispersed through several organelles in the endocytic pathway. Recycling was measured by incubating the cells at 37º C in the presence of a reducing agent that cleaves the biotin label. If SNX17 functions like SNX1, which increases ligand-induced downregulation of EGFR when overexpressed, it is possible that SNX17 could regulate LDLR trafficking to the lysosome. In my recycling assay, a loss of biotinylated LDLR signal could be a result of increased targeting to the lysosome. Therefore, I performed the recycling assay in the presence of leupeptin, a lysosomal protease inhibitor. Leupeptin did not affect the increased LDLR recycling caused by SNX17 overexpression, indicating that degradation of LDLR

when SNX17 was overexpressed did not influence the recycling assay. Transferrin receptor internalization and recycling was unaffected by SNX17 overexpression, suggesting that the endocytic recycling pathway was unaffected and the effect on LDLR recycling was specific.

Endocytic recycling requires a few minutes, but sorting to lysosomes occurs much more slowly, on a time scale of hours. To confirm that SNX17 overexpression does not result in increased LDLR lysosomal targeting, I metabolically labeled LDLR with [^{35}S]-amino acids and measured the degradation rate of the receptor in the cells overexpressing SNX17 as compared to control cells. In the first seven hours following synthesis of the mature LDLR, there was no significant difference in the degradation rate of LDLR in cells overexpressing SNX17 as compared to control cells. However, there was two fold less [^{35}S]-labeled LDLR in SNX17-overexpressing versus control cells 30 hours after synthesis of mature LDLR. Approximately 3% of the LDLR is predicted to be sorted to the lysosome every time it passes through the sorting endosome (Straley and Green, 2000). It is possible that the increase in recycling caused by SNX17 overexpression causes more LDLR to cycle through the sorting endosome, which would increase the total LDLR that would be targeted to the lysosome (Figure 37). Therefore, a change in the degradation rate of LDLR in control versus SNX17-overexpressing cells may be too small to observe until many cycles through the sorting endosome.

At steady state, I did not observe a change in LDLR expression until we increased the concentration of recombinant adenovirus expresssing SNX17 to 100 PFUs per cell. Increasing SNX17 overexpression fifty-fold causes a 40% reduction in LDLR expression at steady state, which is rescued by the addition of leupeptin, indicating that very high SNX17

overexpression causes LDLR to be targeted to the lysosome. Attenuation of SNX17 by RNA interference increases LDLR expression by 1.7 fold. These experiments suggest that SNX17 may indirectly target LDLR to the lysosome by increasing the rate of recycling, which causes more LDLR to cycle through the endosome, increasing the probability that the receptor will be targeted to the lysosome (Figure 37).

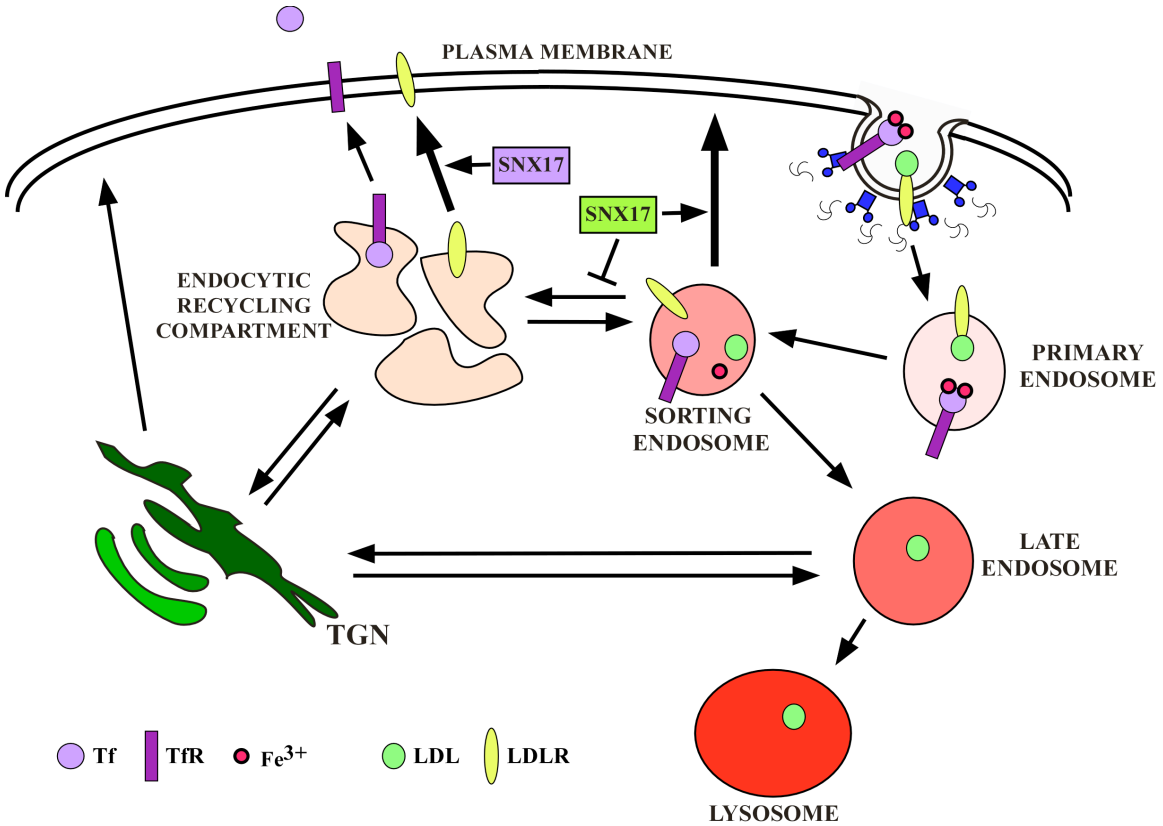

Figure 37. Proposed model for regulation of LDLR trafficking by SNX17. LDLR is internalized through clathrin-coated pits and transported to the sorting endosome. It is possible that SNX17 directs LDLR directly to the plasma membrane from the sorting endosome (green box), avoiding the long pathway through the endocytic recycling compartment, which would increase the rate of recycling if SNX17 is overexpressed. It is also possible that overexpression of SNX17 accelerates release of LDLR from the endocytic recycling compartment to the plasma membrane (purple box).

If LDLR recycling to the cell surface is increased, I would expect to observe an increase in LDLR cell surface expression if the rate of internalization is unchanged. However, I did not observe a significant change in LDLR cell surface expression at steady state, suggesting that the increased LDLR recycling to the plasma membrane is accompanied by an apparent increase in internalization. LDLR is rapidly internalized once it contacts a pre-existing clathrin cluster at the cell surface (Ehrlich et al., 2004). Release of LDLR from the recycling endosome is the rate limiting step in the endocytic recycling pathway (Maxfield and McGraw, 2004). Thus, it is possible that SNX17 acts in the sorting endosome to traffick LDLR directly to the plasma membrane in the short recycling pathway, which would avoid the long recycling pathway through the endocytic recycling compartment. SNX17 may facilitate the ability of LDLR to sort into the rab4-associated vesicles that bud from the sorting endosome. It is also possible that overexpression of SNX17 accelerates recycling out of the recycling endosome. Experiments that attempted to measure the rate of internalization of biotinylated LDLR in SNX17-overexpressing versus control cells were unsuccessful. Therefore, I plan to quantitate LDLR internalization with ^{125}I-LDL in a more sensitive, reproducible assay. I expect to observe an indirect increase in LDLR internalization caused by an increase in the number of receptors delivered to the surface in SNX17-overexpressing versus control cells.

In a preliminary experiment, I observed that SNX17 associates with SynGAP, a ras GTPase activating protein (GAP) in the yeast two-hybrid system (data not shown). Several members of the LDLR family, including LRP and megalin, have been implicated in various signaling pathways by binding to signaling proteins, including ras effectors, in their

cytoplasmic domains (May et al., 2003). It is possible that SynGAP could affect LDLR family member targeting through SNX17. If a cell must rapidly turn off a signaling pathway intiated by a member of the LDLR family, SynGAP may sequester or change the conformation of SNX17, interfering with its ability to recycle the receptor. If receptor recycling is retarded, it may be targeted to the lysosome, which would halt the signaling pathway.

BIBLIOGRAPHY

Agarwala, S., T.A. Sanders, and C.W. Ragsdale. 2001. Sonic hedgehog control of size and shape in midbrain pattern formation. *Science*. 291:2147-50.

Almeida, P.F., W.L. Vaz, and T.E. Thompson. 1993. Percolation and diffusion in three-component lipid bilayers: effect of cholesterol on an equimolar mixture of two phosphatidylcholines. *Biophys J*. 64:399-412.

Alonso, M.A., and S.M. Weissman. 1987. cDNA cloning and sequence of MAL, a hydrophobic protein associated with human T-cell differentiation. *Proc Natl Acad Sci U S A*. 84:1997-2001.

Altschuler, Y., S. Liu, L. Katz, K. Tang, S. Hardy, F. Brodsky, G. Apodaca, and K. Mostov. 1999. ADP-ribosylation factor 6 and endocytosis at the apical surface of Madin-Darby canine kidney cells. *J Cell Biol*. 147:7-12.

Anderson, R.G. 1998. The caveolae membrane system. *Annu Rev Biochem*. 67:199-225.

Anderson, R.G., M.S. Brown, and J.L. Goldstein. 1977. Role of the coated endocytic vesicle in the uptake of receptor-bound low density lipoprotein in human fibroblasts. *Cell*. 10:351-64.

Anderson, R.G., and K. Jacobson. 2002. A role for lipid shells in targeting proteins to caveolae, rafts, and other lipid domains. *Science*. 296:1821-5.

Apodaca, G., L.A. Katz, and K.E. Mostov. 1994. Receptor-mediated transcytosis of IgA in MDCK cells is via apical recycling endosomes. *J Cell Biol*. 125:67-86.

Arighi, C.N., L.M. Hartnell, R.C. Aguilar, C.R. Haft, and J.S. Bonifacino. 2004. Role of the mammalian retromer in sorting of the cation-independent mannose 6-phosphate receptor. *J Cell Biol*. 165:123-33.

Aroeti, B., P.A. Kosen, I.D. Kuntz, F.E. Cohen, and K.E. Mostov. 1993. Mutational and secondary structural analysis of the basolateral sorting signal of the polymeric immunoglobulin receptor. *J Cell Biol*. 123:1149-60.

Bacia, K., D. Scherfeld, N. Kahya, and P. Schwille. 2004. Fluorescence Correlation Spectroscopy Relates Rafts in Model and Native Membranes. *Biophys. J.* 87:1034-1043.

Bello, V., J.W. Goding, V. Greengrass, A. Sali, V. Dubljevic, C. Lenoir, G. Trugnan, and M. Maurice. 2001. Characterization of a di-leucine-based signal in the cytoplasmic tail of the nucleotide-pyrophosphatase NPP1 that mediates basolateral targeting but not endocytosis. *Mol Biol Cell.* 12:3004-15.

Benais-Pont, G., A. Punn, C. Flores-Maldonado, J. Eckert, G. Raposo, T.P. Fleming, M. Cereijido, M.S. Balda, and K. Matter. 2003. Identification of a tight junction-associated guanine nucleotide exchange factor that activates Rho and regulates paracellular permeability. *J Cell Biol.* 160:729-40.

Boll, W., I. Rapoport, C. Brunner, Y. Modis, S. Prehn, and T. Kirchhausen. 2002. The mu2 subunit of the clathrin adaptor AP-2 binds to FDNPVY and YppO sorting signals at distinct sites. *Traffic.* 3:590-600.

Bonifacino, J.S., and B.S. Glick. 2004. The mechanisms of vesicle budding and fusion. *Cell.* 116:153-66.

Bonifacino, J.S., and L.M. Traub. 2003. Signals for sorting of transmembrane proteins to endosomes and lysosomes. *Annu Rev Biochem.* 72:395-447.

Brandli, A.W., R.G. Parton, and K. Simons. 1990. Transcytosis in MDCK cells: identification of glycoproteins transported bidirectionally between both plasma membrane domains. *Journal of Cell Biology.* 111:2909-21.

Bravo, J., D. Karathanassis, C.M. Pacold, M.E. Pacold, C.D. Ellson, K.E. Anderson, P.J. Butler, I. Lavenir, O. Perisic, P.T. Hawkins, L. Stephens, and R.L. Williams. 2001. The crystal structure of the PX domain from p40(phox) bound to phosphatidylinositol 3-phosphate. *Mol Cell.* 8:829-39.

Bretscher, M.S. 1972. Asymmetrical lipid bilayer structure for biological membranes. *Nat New Biol.* 236:11-2.

Brewer, C.B., and M.G. Roth. 1991. A single amino acid change in the cytoplasmic domain alters the polarized delivery of influenza virus hemagglutinin. *Journal of Cell Biology*. 114:413-21.

Brown, D.A., B. Crise, and J.K. Rose. 1989. Mechanism of membrane anchoring affects polarized expression of two proteins in MDCK cells. *Science*. 245:1499-501.

Brown, D.A., and E. London. 2000. Structure and function of sphingolipid- and cholesterol-rich membrane rafts. *J Biol Chem*. 275:17221-4.

Brown, D.A., and J.K. Rose. 1992. Sorting of GPI-anchored proteins to glycolipid-enriched membrane subdomains during transport to the apical cell surface. *Cell*. 68:533-44.

Brown, M.S., R.G. Anderson, S.K. Basu, and J.L. Goldstein. 1982. Recycling of cell-surface receptors: observations from the LDL receptor system. *Cold Spring Harb Symp Quant Biol*. 46 Pt 2:713-21.

Brown, M.S., R.G. Anderson, and J.L. Goldstein. 1983. Recycling receptors: the round-trip itinerary of migrant membrane proteins. *Cell*. 32:663-7.

Brown, M.S., J.R. Faust, and J.L. Goldstein. 1978. Induction of 3-hydroxy-3-methylglutaryl coenzyme A reductase activity in human fibroblasts incubated with compactin (ML-236B), a competitive inhibitor of the reductase. *J Biol Chem*. 253:1121-8.

Brown, M.S., and J.L. Goldstein. 1984. How LDL receptors influence cholesterol and atherosclerosis. *Sci Am*. 251:58-66.

Brugger, B., R. Sandhoff, S. Wegehingel, K. Gorgas, J. Malsam, J.B. Helms, W.D. Lehmann, W. Nickel, and F.T. Wieland. 2000. Evidence for segregation of sphingomyelin and cholesterol during formation of COPI-coated vesicles. *J Cell Biol*. 151:507-18.

Burden, J.J., X.M. Sun, A.B. Garcia Garcia, and A.K. Soutar. 2004b. Sorting motifs in the intracellular domain of the low density lipoprotein (LDL) receptor interact with a novel domain of sorting nexin-17. *J Biol Chem*. 279:16237-45.

Cao, T.T., H.W. Deacon, D. Reczek, A. Bretscher, and M. von Zastrow. 1999. A kinase-regulated PDZ-domain interaction controls endocytic sorting of the beta2-adrenergic receptor. *Nature*. 401:286-90.

Carlton, J., M. Bujny, B.J. Peter, V.M. Oorschot, A. Rutherford, H. Mellor, J. Klumperman, H.T. McMahon, and P.J. Cullen. 2004. Sorting Nexin-1 Mediates Tubular Endosome-to-TGN Transport through Coincidence Sensing of High- Curvature Membranes and 3-Phosphoinositides. *Curr Biol*. 14:1791-800.

Carter, L.L., T.E. Redelmeier, L.A. Woollenweber, and S.L. Schmid. 1993. Multiple GTP-binding proteins participate in clathrin-coated vesicle-mediated endocytosis. *J Cell Biol*. 120:37-45.

Casanova, J.E., G. Apodaca, and K.E. Mostov. 1991. An autonomous signal for basolateral sorting in the cytoplasmic domain of the polymeric immunoglobulin receptor. *Cell*. 66:65-75.

Chen, W.J., J.L. Goldstein, and M.S. Brown. 1990. NPXY, a sequence often found in cytoplasmic tails, is required for coated pit-mediated internalization of the low density lipoprotein receptor. *J Biol Chem*. 265:3116-23.

Cheong, K.H., D. Zacchetti, E.E. Schneeberger, and K. Simons. 1999. VIP17/MAL, a lipid raft-associated protein, is involved in apical transport in MDCK cells. *Proceedings of the National Academy of Sciences of the United States of America*. 96:6241-8.

Choi, J.H., W.-P. Hong, M.J. Kim, J.H. Kim, S.H. Ryu, and P.-G. Suh. 2004. Sorting nexin 16 regulates EGF receptor trafficking by phosphatidylinositol-3-phosphate interaction with the Phox domain. *J Cell Sci*:jcs.01233.

Chuang, J.Z., and C.H. Sung. 1998. The cytoplasmic tail of rhodopsin acts as a novel apical sorting signal in polarized MDCK cells. *Journal of Cell Biology*. 142:1245-56.

Collins, B.M., A.J. McCoy, H.M. Kent, P.R. Evans, and D.J. Owen. 2002. Molecular architecture and functional model of the endocytic AP2 complex. *Cell*. 109:523-35.

Compans, R.W., and N.J. Dimmock. 1969. An electron microscopic study of single-cycle infection of chick embryo fibroblasts by influenza virus. *Virology*. 39:499-515.

Cooper, A.A., and T.H. Stevens. 1996. Vps10p cycles between the late-Golgi and prevacuolar compartments in its function as the sorting receptor for multiple yeast vacuolar hydrolases. *J Cell Biol*. 133:529-41.

Copeland, C.S., R.W. Doms, E.M. Bolzau, R.G. Webster, and A. Helenius. 1986. Assembly of influenza hemagglutinin trimers and its role in intracellular transport. *Journal of Cell Biology*. 103:1179-91.

Cozier, G.E., J. Carlton, A.H. McGregor, P.A. Gleeson, R.D. Teasdale, H. Mellor, and P.J. Cullen. 2002. The phox homology (PX) domain-dependent, 3-phosphoinositide-mediated association of sorting nexin-1 with an early sorting endosomal compartment is required for its ability to regulate epidermal growth factor receptor degradation. *J Biol Chem*. 277:48730-6.

Crane, J.M., and L.K. Tamm. 2004. Role of Cholesterol in the Formation and Nature of Lipid Rafts in Planar and Spherical Model Membranes. *Biophys. J*. 86:2965-2979.

Davis, C.G., M.A. Lehrman, D.W. Russell, R.G. Anderson, M.S. Brown, and J.L. Goldstein. 1986. The J.D. mutation in familial hypercholesterolemia: amino acid substitution in cytoplasmic domain impedes internalization of LDL receptors. *Cell*. 45:15-24.

Dawson, J.P., J.S. Weinger, and D.M. Engelman. 2002. Motifs of serine and threonine can drive association of transmembrane helices. *Journal of Molecular Biology*. 316:799-805.

Degroote, S., J. Wolthoorn, and G. van Meer. 2004. The cell biology of glycosphingolipids. *Semin Cell Dev Biol*. 15:375-87.

Devaux, P.F. 1991. Static and dynamic lipid asymmetry in cell membranes. *Biochemistry*. 30:1163-73.

Devaux, P.F., and R. Morris. 2004. Transmembrane asymmetry and lateral domains in biological membranes. *Traffic*. 5:241-6.

Diamond, J.M. 1977. Twenty-first Bowditch lecture. The epithelial junction: bridge, gate, and fence. *Physiologist*. 20:10-8.

Dietrich, C., B. Yang, T. Fujiwara, A. Kusumi, and K. Jacobson. 2002. Relationship of Lipid Rafts to Transient Confinement Zones Detected by Single Particle Tracking. *Biophys. J.* 82:274-284.

Doms, R.W., and A. Helenius. 1986. Quaternary structure of influenza virus hemagglutinin after acid treatment. *Journal of Virology*. 60:833-9.

Dunn, K.W., and F.R. Maxfield. 1992. Delivery of ligands from sorting endosomes to late endosomes occurs by maturation of sorting endosomes. *J Cell Biol*. 117:301-10.

Dunn, K.W., T.E. McGraw, and F.R. Maxfield. 1989. Iterative fractionation of recycling receptors from lysosomally destined ligands in an early sorting endosome. *J Cell Biol*. 109:3303-14.

Edidin, M. 2003. The state of lipid rafts: from model membranes to cells. *Annu Rev Biophys Biomol Struct*. 32:257-83.

Ehrlich, M., W. Boll, A. Van Oijen, R. Hariharan, K. Chandran, M.L. Nibert, and T. Kirchhausen. 2004. Endocytosis by random initiation and stabilization of clathrin-coated pits. *Cell*. 118:591-605.

Fields, S., and O. Song. 1989. A novel genetic system to detect protein-protein interactions. *Nature*. 340:245-6.

Florian, V., T. Schluter, and R. Bohnensack. 2001. A new member of the sorting nexin family interacts with the C-terminus of P-selectin. *Biochem Biophys Res Commun*. 281:1045-50.

Folsch, H., H. Ohno, J.S. Bonifacino, and I. Mellman. 1999. A novel clathrin adaptor complex mediates basolateral targeting in polarized epithelial cells. *Cell*. 99:189-98.

Folsch, H., M. Pypaert, S. Maday, L. Pelletier, and I. Mellman. 2003. The AP-1A and AP-1B clathrin adaptor complexes define biochemically and functionally distinct membrane domains. *J Cell Biol*. 163:351-62.

Frank, M., N. Schaeren-Wiemers, R. Schneider, and M.E. Schwab. 1999. Developmental expression pattern of the myelin proteolipid MAL indicates different functions of MAL for immature Schwann cells and in a late step of CNS myelinogenesis. *J Neurochem*. 73:587-97.

Frank, M., M.E. van der Haar, N. Schaeren-Wiemers, and M.E. Schwab. 1998. rMAL is a glycosphingolipid-associated protein of myelin and apical membranes of epithelial cells in kidney and stomach. *J Neurosci*. 18:4901-13.

Futerman, A.H., B. Stieger, A.L. Hubbard, and R.E. Pagano. 1990. Sphingomyelin synthesis in rat liver occurs predominantly at the cis and medial cisternae of the Golgi apparatus. *J Biol Chem*. 265:8650-7.

Gage, R.M., K.A. Kim, T.T. Cao, and M. von Zastrow. 2001. A transplantable sorting signal that is sufficient to mediate rapid recycling of G protein-coupled receptors. *J Biol Chem*. 276:44712-20.

Gan, Y., T.E. McGraw, and E. Rodriguez-Boulan. 2002. The epithelial-specific adaptor AP1B mediates post-endocytic recycling to the basolateral membrane. *Nat Cell Biol*. 4:605-9.

Garcia, C.K., K. Wilund, M. Arca, G. Zuliani, R. Fellin, M. Maioli, S. Calandra, S. Bertolini, F. Cossu, N. Grishin, R. Barnes, J.C. Cohen, and H.H. Hobbs. 2001. Autosomal recessive hypercholesterolemia caused by mutations in a putative LDL receptor adaptor protein. *Science*. 292:1394-8.

Ghersi, E., C. Noviello, and L. D'Adamio. 2004. AIDA-1 proteins bind to A{beta}PP and modulates its processing in an isoform specific manner. *J Biol Chem*. Epub ahead of print.

Goldstein, J.L., M.S. Brown, R.G. Anderson, D.W. Russell, and W.J. Schneider. 1985. Receptor-mediated endocytosis: concepts emerging from the LDL receptor system. *Annu Rev Cell Biol*. 1:1-39.

Gorvel, J.P., P. Chavrier, M. Zerial, and J. Gruenberg. 1991. rab5 controls early endosome fusion in vitro. *Cell*. 64:915-25.

Gotthardt, M., M. Trommsdorff, M.F. Nevitt, J. Shelton, J.A. Richardson, W. Stockinger, J. Nimpf, and J. Herz. 2000. Interactions of the Low Density Lipoprotein Receptor Gene Family with Cytosolic Adaptor and Scaffold Proteins Suggest Diverse Biological Functions in Cellular Communication and Signal Transduction. *J. Biol. Chem*. 275:25616-25624.

Griffiths, G., and K. Simons. 1986. The trans Golgi network: sorting at the exit site of the Golgi complex. *Science*. 234:438-43.

Gullapalli, A., T.A. Garrett, M.M. Paing, C.T. Griffin, Y. Yang, and J. Trejo. 2004. A role for sorting nexin 2 in epidermal growth factor receptor down-regulation: evidence for distinct functions of sorting nexin 1 and 2 in protein trafficking. *Mol Biol Cell*. 15:2143-55.

Habermann, B. 2004. The BAR-domain family of proteins: a case of bending and binding? *EMBO Rep*. 5:250-5.

Haft, C.R., M. de la Luz Sierra, V.A. Barr, D.H. Haft, and S.I. Taylor. 1998. Identification of a family of sorting nexin molecules and characterization of their association with receptors. *Mol Cell Biol*. 18:7278-87.

Hama, H., G.G. Tall, and B.F. Horazdovsky. 1999. Vps9p is a guanine nucleotide exchange factor involved in vesicle-mediated vacuolar protein transport. *J Biol Chem*. 274:15284-91.

Hanada, K., K. Kumagai, S. Yasuda, Y. Miura, M. Kawano, M. Fukasawa, and M. Nishijima. 2003. Molecular machinery for non-vesicular trafficking of ceramide. *Nature*. 426:803-9.

Hao, M., and F.R. Maxfield. 2000. Characterization of rapid membrane internalization and recycling. *J Biol Chem*. 275:15279-86.

Harder, T., P. Scheiffele, P. Verkade, and K. Simons. 1998. Lipid Domain Structure of the Plasma Membrane Revealed by Patching of Membrane Components. *J. Cell Biol*. 141:929-942.

He, G., S. Gupta, M. Yi, P. Michaely, H.H. Hobbs, and J.C. Cohen. 2002. ARH is a modular adaptor protein that interacts with the LDL receptor, clathrin, and AP-2. *J Biol Chem*. 277:44044-9.

He, T.C., S. Zhou, L.T. da Costa, J. Yu, K.W. Kinzler, and B. Vogelstein. 1998. A simplified system for generating recombinant adenoviruses. *Proceedings of the National Academy of Sciences of the United States of America*. 95:2509-14.

Heerklotz, H. 2002. Triton Promotes Domain Formation in Lipid Raft Mixtures. *Biophys. J*. 83:2693-2701.

Heerklotz, H., H. Szadkowska, T. Anderson, and J. Seelig. 2003. The Sensitivity of Lipid Domains to Small Perturbations Demonstrated by the Effect of Triton. *Journal of Molecular Biology*. 329:793-799.

Herz, J., and H.H. Bock. 2002. Lipoprotein receptors in the nervous system. *Annu Rev Biochem*. 71:405-34.

Herzlinger, D.A., T.G. Easton, and G.K. Ojakian. 1982. The MDCK epithelial cell line expresses a cell surface antigen of the kidney distal tubule. *J Cell Biol*. 93:269-77.

Hoekstra, D., O. Maier, J.M. van der Wouden, T.A. Slimane, and S.C.D. van IJzendoorn. 2003. Membrane dynamics and cell polarity: the role of sphingolipids. *J. Lipid Res*. 44:869-877.

Holopainen, J.M., A.J. Metso, J.P. Mattila, A. Jutila, and P.K. Kinnunen. 2004. Evidence for the lack of a specific interaction between cholesterol and sphingomyelin. *Biophys J*. 86:1510-20.

Holthuis, J.C., T. Pomorski, R.J. Raggers, H. Sprong, and G. Van Meer. 2001. The organizing potential of sphingolipids in intracellular membrane transport. *Physiol Rev*. 81:1689-723.

Honing, S., I.V. Sandoval, and K. von Figura. 1998. A di-leucine-based motif in the cytoplasmic tail of LIMP-II and tyrosinase mediates selective binding of AP-3. *Embo J*. 17:1304-14.

Horazdovsky, B.F., B.A. Davies, M.N. Seaman, S.A. McLaughlin, S. Yoon, and S.D. Emr. 1997. A sorting nexin-1 homologue, Vps5p, forms a complex with Vps17p and is required for recycling the vacuolar protein-sorting receptor. *Mol Biol Cell*. 8:1529-41.

Hortin, G., and I. Boime. 1981. Transport of an uncleaved preprotein into the endoplasmic reticulum of rat pituitary cells. *Journal of Biological Chemistry*. 256:1491-4.

Hua, X., J. Sakai, M.S. Brown, and J.L. Goldstein. 1996. Regulated cleavage of sterol regulatory element binding proteins requires sequences on both sides of the endoplasmic reticulum membrane. *J Biol Chem*. 271:10379-84.

Huang, J., and G.W. Feigenson. 1999. A microscopic interaction model of maximum solubility of cholesterol in lipid bilayers. *Biophys J*. 76:2142-57.

Huang, X.F., R.W. Compans, S. Chen, R.A. Lamb, and P. Arvan. 1997. Polarized apical targeting directed by the signal/anchor region of simian virus 5 hemagglutinin-neuraminidase. *Journal of Biological Chemistry*. 272:27598-604.

Huitema, K., J. van den Dikkenberg, J.F. Brouwers, and J.C. Holthuis. 2004. Identification of a family of animal sphingomyelin synthases. *Embo J*. 23:33-44.

Hunziker, W., and C. Fumey. 1994. A di-leucine motif mediates endocytosis and basolateral sorting of macrophage IgG Fc receptors in MDCK cells. *Embo J*. 13:2963-9.

Inukai, K., A.M. Shewan, W.S. Pascoe, S. Katayama, D.E. James, and Y. Oka. 2003. Carboxy Terminus of Glucose Transporter GLUT3 Contains an Apical Membrane Targeting Domain. *Mol Endocrinol*:me.2003-0089.

Jacob, R., and H.Y. Naim. 2001. Apical membrane proteins are transported in distinct vesicular carriers. *Curr Biol*. 11:1444-50.

Jia, Y.J., M. Kai, I. Wada, F. Sakane, and H. Kanoh. 2003. Differential localization of lipid phosphate phosphatases 1 and 3 to cell surface subdomains in polarized MDCK cells. *FEBS Lett*. 552:240-6.

Jing, S.Q., T. Spencer, K. Miller, C. Hopkins, and I.S. Trowbridge. 1990. Role of the human transferrin receptor cytoplasmic domain in endocytosis: localization of a specific signal sequence for internalization. *J Cell Biol*. 110:283-94.

Karathanassis, D., R.V. Stahelin, J. Bravo, O. Perisic, C.M. Pacold, W. Cho, and R.L. Williams. 2002. Binding of the PX domain of p47(phox) to phosphatidylinositol 3,4-bisphosphate and phosphatidic acid is masked by an intramolecular interaction. *Embo J*. 21:5057-68.

Karlsson, K.A. 1970. Sphingolipid long chain bases. *Lipids*. 5:878-91.

Keller, P., and K. Simons. 1998. Cholesterol is required for surface transport of influenza virus hemagglutinin. *J Cell Biol*. 140:1357-67.

Keller, P., D. Toomre, E. Diaz, J. White, and K. Simons. 2001. Multicolour imaging of post-Golgi sorting and trafficking in live cells. *Nat Cell Biol*. 3:140-9.

Kemble, G.W., T. Danieli, and J.M. White. 1994. Lipid-anchored influenza hemagglutinin promotes hemifusion, not complete fusion. *Cell*. 76:383-91.

Kenworthy, A.K., N. Petranova, and M. Edidin. 2000. High-Resolution FRET Microscopy of Cholera Toxin B-Subunit and GPI-anchored Proteins in Cell Plasma Membranes. *Mol. Biol. Cell*. 11:1645-1655.

Keyel, P.A., S.C. Watkins, and L.M. Traub. 2004. Endocytic adaptor molecules reveal an endosomal population of clathrin by total internal reflection fluorescence microscopy. *J Biol Chem*. 279:13190-204.

Kibbey, R.G., J. Rizo, L.M. Gierasch, and R.G. Anderson. 1998. The LDL receptor clustering motif interacts with the clathrin terminal domain in a reverse turn conformation. *J Cell Biol*. 142:59-67.

Kim, T., and S.E. Pfeiffer. 2002. Subcellular localization and detergent solubility of MVP17/rMAL, a lipid raft-associated protein in oligodendrocytes and myelin. *J Neurosci Res*. 69:217-26.

Kirchhausen, T. 2000. Three ways to make a vesicle. *Nat Rev Mol Cell Biol.* 1:187-98.

Kirchhausen, T. 2002. Clathrin adaptors really adapt. *Cell*. 109:413-6.

Koivisto, U.-M., A.L. Hubbard, and I. Mellman. 2001. A Novel Cellular Phenotype for Familial Hypercholesterolemia due to a Defect in Polarized Targeting of LDL Receptor. *Cell.* 105:575-585.

Kounnas, M.Z., C.C. Haudenschild, D.K. Strickland, and W.S. Argraves. 1994. Immunological localization of glycoprotein 330, low density lipoprotein receptor related protein and 39 kDa receptor associated protein in embryonic mouse tissues. *In Vivo*. 8:343-51.

Kroschewski, R., A. Hall, and I. Mellman. 1999. Cdc42 controls secretory and endocytic transport to the basolateral plasma membrane of MDCK cells. *Nat Cell Biol.* 1:8-13.

Kundu, A., R.T. Avalos, C.M. Sanderson, and D.P. Nayak. 1996. Transmembrane domain of influenza virus neuraminidase, a type II protein, possesses an apical sorting signal in polarized MDCK cells. *J Virol*. 70:6508-15.

Kurten, R.C., D.L. Cadena, and G.N. Gill. 1996. Enhanced degradation of EGF receptors by a sorting nexin, SNX1. *Science*. 272:1008-10.

Kurzchalia, T.V., P. Dupree, R.G. Parton, R. Kellner, H. Virta, M. Lehnert, and K. Simons. 1992. VIP21, a 21-kD membrane protein is an integral component of trans-Golgi-network-derived transport vesicles. *J Cell Biol*. 118:1003-14.

Kusumi, A., I. Koyama-Honda, and K. Suzuki. 2004. Molecular Dynamics and Interactions for Creation of Stimulation-Induced Stabilized Rafts from Small Unstable Steady-State Rafts. *Traffic*. 5:213-230.

Larsson, M., G. Hjalm, A.M. Sakwe, A. Engstrom, A.S. Hoglund, E. Larsson, R.C. Robinson, C. Sundberg, and L. Rask. 2003. Selective interaction of megalin with postsynaptic density-95 (PSD-95)-like membrane-associated guanylate kinase (MAGUK) proteins. *Biochem J*. 373:381-91.

Latham, T., and J.M. Galarza. 2001. Formation of wild-type and chimeric influenza virus-like particles following simultaneous expression of only four structural proteins. *J Virol*. 75:6154-65.

Lazarovits, J., and M. Roth. 1988. A single amino acid change in the cytoplasmic domain allows the influenza virus hemagglutinin to be endocytosed through coated pits. *Cell*. 53:743-52.

Lazarovits, J., S.P. Shia, N. Ktistakis, M.S. Lee, C. Bird, and M.G. Roth. 1990. The effects of foreign transmembrane domains on the biosynthesis of the influenza virus hemagglutinin. *J Biol Chem*. 265:4760-7.

Le Borgne, R., and B. Hoflack. 1998. Protein transport from the secretory to the endocytic pathway in mammalian cells. *Biochim Biophys Acta*. 1404:195-209.

Leheste, J.R., F. Melsen, M. Wellner, P. Jansen, U. Schlichting, I. Renner-Muller, T.T. Andreassen, E. Wolf, S. Bachmann, A. Nykjaer, and T.E. Willnow. 2003. Hypocalcemia and osteopathy in mice with kidney-specific megalin gene defect. *Faseb J*. 17:247-9.

Lehrman, M.A., J.L. Goldstein, M.S. Brown, D.W. Russell, and W.J. Schneider. 1985. Internalization-defective LDL receptors produced by genes with nonsense and frameshift mutations that truncate the cytoplasmic domain. *Cell*. 41:735-43.

Lin, S., H.Y. Naim, A.C. Rodriguez, and M.G. Roth. 1998. Mutations in the middle of the transmembrane domain reverse the polarity of transport of the influenza virus hemagglutinin in MDCK epithelial cells. *Journal of Cell Biology*. 142:51-7.

Lin, S., H.Y. Naim, and M.G. Roth. 1997. Tyrosine-dependent basolateral sorting signals are distinct from tyrosine-dependent internalization signals. *Journal of Biological Chemistry*. 272:26300-5.

Lisanti, M.P., I.W. Caras, M.A. Davitz, and E. Rodriguez-Boulan. 1989. A glycophospholipid membrane anchor acts as an apical targeting signal in polarized epithelial cells. *J Cell Biol*. 109:2145-56.

Liscum, L., and N.J. Munn. 1999. Intracellular cholesterol transport. *Biochim Biophys Acta*. 1438:19-37.

Lou, X., T. McQuistan, R.A. Orlando, and M.G. Farquhar. 2002. GAIP, GIPC and G{alpha}i3 are Concentrated in Endocytic Compartments of Proximal Tubule Cells: Putative Role in Regulating Megalin's Function. *J Am Soc Nephrol*. 13:918-927.

Lundmark, R., and S.R. Carlsson. 2003. Sorting nexin 9 participates in clathrin-mediated endocytosis through interactions with the core components. *J Biol Chem*. 278:46772-81.

Maccioni, H.J., J.L. Daniotti, and J.A. Martina. 1999. Organization of ganglioside synthesis in the Golgi apparatus. *Biochim Biophys Acta*. 1437:101-18.

Marks, M.S., L. Woodruff, H. Ohno, and J.S. Bonifacino. 1996. Protein targeting by tyrosine- and di-leucine-based signals: evidence for distinct saturable components. *J Cell Biol*. 135:341-54.

Martin-Belmonte, F., P. Arvan, and M.A. Alonso. 2001. MAL Mediates Apical Transport of Secretory Proteins in Polarized Epithelial Madin-Darby Canine Kidney Cells. *J. Biol. Chem*. 276:49337-49342.

Martin-Belmonte, F., J.A. Martinez-Menarguez, J.F. Aranda, J. Ballesta, M.C. de Marco, and M.A. Alonso. 2003. MAL regulates clathrin-mediated endocytosis at the apical surface of Madin-Darby canine kidney cells. *J Cell Biol*. 163:155-64.

Martin-Belmonte, F., R. Puertollano, J. Millan, and M.A. Alonso. 2000. The MAL Proteolipid Is Necessary for the Overall Apical Delivery of Membrane Proteins in the Polarized Epithelial Madin-Darby Canine Kidney and Fischer Rat Thyroid Cell Lines. *Mol. Biol. Cell*. 11:2033-2045.

Marzolo, M.P., M.I. Yuseff, C. Retamal, M. Donoso, F. Ezquer, P. Farfan, Y. Li, and G. Bu. 2003. Differential Distribution of Low-Density Lipoprotein-Receptor-Related Protein (LRP) and Megalin in Polarized Epithelial Cells is Determined by Their Cytoplasmic Domains. *Traffic*. 4:273-288.

Mateus Fernandez, S.B., Z. Hollo, A. Kern, E. Bakos, P.A. Fischer, P. Borst, and R. Evers. 2002. Role of the N-terminal transmembrane region of the multidrug resistance protein MRP2 in routing to the apical membrane in MDCKII cells. *J Biol Chem*. 11:11.

Matlin, K., and K. Simons. 1984. Sorting of an apical plasma membrane glycoprotein occurs before it reaches the cell surface in cultured epithelial cells. *J. Cell Biol*. 99:2131-2139.

Matter, K., W. Hunziker, and I. Mellman. 1992. Basolateral sorting of LDL receptor in MDCK cells: the cytoplasmic domain contains two tyrosine-dependent targeting determinants. *Cell*. 71:741-53.

Mattson, M.P. 1999. Establishment and plasticity of neuronal polarity. *J Neurosci Res*. 57:577-89.

Maxfield, F.R., and T.E. McGraw. 2004. Endocytic recycling. *Nat Rev Mol Cell Biol*. 5:121-32.

May, P., H.H. Bock, and J. Herz. 2003. Integration of endocytosis and signal transduction by lipoprotein receptors. *Sci STKE*. 2003:PE12.

Mayor, S., J.F. Presley, and F.R. Maxfield. 1993. Sorting of membrane components from endosomes and subsequent recycling to the cell surface occurs by a bulk flow process. *J Cell Biol*. 121:1257-69.

McCarthy, R.A., J.L. Barth, M.R. Chintalapudi, C. Knaak, and W.S. Argraves. 2002. Megalin Functions as an Endocytic Sonic Hedgehog Receptor. *J. Biol. Chem*. 277:25660-25667.

McConnell, H.M., and A. Radhakrishnan. 2003. Condensed complexes of cholesterol and phospholipids. *Biochim Biophys Acta*. 1610:159-73.

McIntosh, T.J., A. Vidal, and S.A. Simon. 2003. Sorting of lipids and transmembrane peptides between detergent-soluble bilayers and detergent-resistant rafts. *Biophys J*. 85:1656-66.

Melikyan, G.B., S. Lin, M.G. Roth, and F.S. Cohen. 1999. Amino acid sequence requirements of the transmembrane and cytoplasmic domains of influenza virus hemagglutinin for viable membrane fusion. *Mol Biol Cell.* 10:1821-36.

Melman, L., H.J. Geuze, Y. Li, L.M. McCormick, P. Van Kerkhof, G.J. Strous, A.L. Schwartz, and G. Bu. 2002. Proteasome regulates the delivery of LDL receptor-related protein into the degradation pathway. *Mol Biol Cell.* 13:3325-35.

Michaely, P., W.P. Li, R.G. Anderson, J.C. Cohen, and H.H. Hobbs. 2004. The modular adaptor protein ARH is required for low density lipoprotein (LDL) binding and internalization but not for LDL receptor clustering in coated pits. *J Biol Chem.* 279:34023-31.

Millan, J., R. Puertollano, L. Fan, and M.A. Alonso. 1997. Caveolin and MAL, two protein components of internal detergent-insoluble membranes, are in distinct lipid microenvironments in MDCK cells. *Biochemical & Biophysical Research Communications*. 233:707-12.

Mishra, S.K., P.A. Keyel, M.J. Hawryluk, N.R. Agostinelli, S.C. Watkins, and L.M. Traub. 2002a. Disabled-2 exhibits the properties of a cargo-selective endocytic clathrin adaptor. *EMBO J*. 21:4915-4926.

Mishra, S.K., S.C. Watkins, and L.M. Traub. 2002b. The autosomal recessive hypercholesterolemia (ARH) protein interfaces directly with the clathrin-coat machinery. *Proc Natl Acad Sci U S A*. 99:16099-104.

Morris, S.M., and J.A. Cooper. 2001. Disabled-2 colocalizes with the LDLR in clathrin-coated pits and interacts with AP-2. *Traffic*. 2:111-23.

Morris, S.M., M.D. Tallquist, C.O. Rock, and J.A. Cooper. 2002. Dual roles for the Dab2 adaptor protein in embryonic development and kidney transport. *Embo J*. 21:1555-64.

Morton, C.J., and I.D. Campbell. 1994. SH3 domains. Molecular 'Velcro'. *Curr Biol*. 4:615-7.

Mostov, K.E., A. de Bruyn Kops, and D.L. Deitcher. 1986. Deletion of the cytoplasmic domain of the polymeric immunoglobulin receptor prevents basolateral localization and endocytosis. *Cell*. 47:359-64.

Mostov, K.E., and D.L. Deitcher. 1986. Polymeric immunoglobulin receptor expressed in MDCK cells transcytoses IgA. *Cell*. 46:613-21.

Mostov, K.E., M. Verges, and Y. Altschuler. 2000. Membrane traffic in polarized epithelial cells. *Current Opinion in Cell Biology*. 12:483-490.

Motley, A., N.A. Bright, M.N.J. Seaman, and M.S. Robinson. 2003. Clathrin-mediated endocytosis in AP-2-depleted cells. *J. Cell Biol*. 162:909-918.

Moyer, B.D., J. Denton, K.H. Karlson, D. Reynolds, S. Wang, J.E. Mickle, M. Milewski, G.R. Cutting, W.B. Guggino, M. Li, and B.A. Stanton. 1999. A PDZ-interacting domain in CFTR is an apical membrane polarization signal. *J Clin Invest*. 104:1353-61.

Muller, D., A. Nykjaer, and T.E. Willnow. 2003. From holoprosencephaly to osteopathology: role of multifunctional endocytic receptors in absorptive epithelia. *Ann Med*. 35:290-9.

Munro, S. 1995. An investigation of the role of transmembrane domains in Golgi protein retention. *Embo J*. 14:4695-704.

Murata, M., J. Peranen, R. Schreiner, F. Wieland, T.V. Kurzchalia, and K. Simons. 1995. VIP21/caveolin is a cholesterol-binding protein. *Proc Natl Acad Sci U S A*. 92:10339-43.

Musil, L.S., and J.U. Baenziger. 1987. Cleavage of membrane secretory component to soluble secretory component occurs on the cell surface of rat hepatocyte monolayers. *J Cell Biol*. 104:1725-33.

Nagai, M., T. Meerloo, T. Takeda, and M.G. Farquhar. 2003. The Adaptor Protein ARH Escorts Megalin to and through Endosomes. *Mol. Biol. Cell*. 14:4984-4996.

Naim, H.Y., and M.G. Roth. 1994. Characteristics of the internalization signal in the Y543 influenza virus hemagglutinin suggest a model for recognition of internalization signals containing tyrosine. *J Biol Chem*. 269:3928-33.

Nayak, D.P., E.K.-W. Hui, and S. Barman. 2004. Assembly and budding of influenza virus. *Virus Research*. In Press, Corrected Proof.

Nicolaissen, B., Jr., B.E. Nicolaissen, K. Beraki, A. Kolstad, K. Arnesen, and D. Armstrong. 1982. Monolayered explants in the study of retinal pigment epithelial behavior in culture. *Acta Ophthalmol (Copenh)*. 60:873-80.

Ohno, H., J. Stewart, M.C. Fournier, H. Bosshart, I. Rhee, S. Miyatake, T. Saito, A. Gallusser, T. Kirchhausen, and J.S. Bonifacino. 1995. Interaction of tyrosine-based sorting signals with clathrin-associated proteins. *Science*. 269:1872-5.

Oleinikov, A.V., J. Zhao, and S.P. Makker. 2000. Cytosolic adaptor protein Dab2 is an intracellular ligand of endocytic receptor gp600/megalin. *Biochem J*. 347 Pt 3:613-21.

Orzech, E., K. Schlessinger, A. Weiss, C.T. Okamoto, and B. Aroeti. 1999. Interactions of the AP-1 Golgi Adaptor with the Polymeric Immunoglobulin Receptor and Their Possible Role in Mediating Brefeldin A-sensitive Basolateral Targeting from the trans-Golgi Network. *J. Biol. Chem*. 274:2201-2215.

Owen, D.J., and P.R. Evans. 1998. A structural explanation for the recognition of tyrosine-based endocytotic signals. *Science*. 282:1327-32.

Pagano, A., P. Crottet, C. Prescianotto-Baschong, and M. Spiess. 2004. In vitro formation of recycling vesicles from endosomes requires adaptor protein-1/clathrin and is regulated by rab4 and the connector rabaptin-5. *Mol Biol Cell*. 15:4990-5000.

Palade, G. 1975. Intracellular aspects of the process of protein synthesis. *Science*. 189:347-58.

Parton, R.G., K. Prydz, M. Bomsel, K. Simons, and G. Griffiths. 1989. Meeting of the apical and basolateral endocytic pathways of the Madin-Darby canine kidney cell in late endosomes. *Journal of Cell Biology*. 109:3259-72.

Parton, R.G., and A.A. Richards. 2003. Lipid rafts and caveolae as portals for endocytosis: new insights and common mechanisms. *Traffic*. 4:724-38.

Pasqualato, S., F. Senic-Matuglia, L. Renault, B. Goud, J. Salamero, and J. Cherfils. 2004. The structural GDP/GTP cycle of Rab11 reveals a novel interface involved in the dynamics of recycling endosomes. *J Biol Chem*. 279:11480-8.

Petersen, H.H., J. Hilpert, D. Militz, V. Zandler, C. Jacobsen, A.J. Roebroek, and T.E. Willnow. 2003. Functional interaction of megalin with the megalinbinding protein (MegBP), a novel tetratrico peptide repeat-containing adaptor molecule. *J Cell Sci*. 116:453-61.

Pietrzik, C.U., I.-S. Yoon, S. Jaeger, T. Busse, S. Weggen, and E.H. Koo. 2004. FE65 Constitutes the Functional Link between the Low-Density Lipoprotein Receptor-Related Protein and the Amyloid Precursor Protein. *J. Neurosci*. 24:4259-4265.

Polishchuk, E.V., A. Di Pentima, A. Luini, and R.S. Polishchuk. 2003. Mechanism of constitutive export from the golgi: bulk flow via the formation, protrusion, and en bloc cleavage of large trans-golgi network tubular domains. *Mol Biol Cell*. 14:4470-85.

Polishchuk, R., A.D. Pentima, and J. Lippincott-Schwartz. 2004. Delivery of raft-associated, GPI-anchored proteins to the apical surface of polarized MDCK cells by a transcytotic pathway. *Nature Cell Biology*. 6:297-307.

Pralle, A., P. Keller, E.L. Florin, K. Simons, and J.K. Horber. 2000. Sphingolipid-cholesterol rafts diffuse as small entities in the plasma membrane of mammalian cells. *J Cell Biol*. 148:997-1008.

Presley, J.F., S. Mayor, T.E. McGraw, K.W. Dunn, and F.R. Maxfield. 1997. Bafilomycin A1 treatment retards transferrin receptor recycling more than bulk membrane recycling. *J Biol Chem*. 272:13929-36.

Puertollano, R., and M.A. Alonso. 1999. Substitution of the two carboxyl-terminal serines by alanine causes retention of MAL, a component of the apical sorting machinery, in the endoplasmic reticulum. *Biochemical & Biophysical Research Communications*. 260:188-92.

Puertollano, R., F. Martin-Belmonte, J. Millan, M.C. de Marco, J.P. Albar, L. Kremer, and M.A. Alonso. 1999. The MAL proteolipid is necessary for normal apical transport and accurate sorting of the influenza virus hemagglutinin in Madin-Darby canine kidney cells. *Journal of Cell Biology*. 145:141-51.

Puertollano, R., J.A. Martinez-Menarguez, A. Batista, J. Ballesta, and M.A. Alonso. 2001a. An intact dilysine-like motif in the carboxyl terminus of MAL is required for normal apical transport of the influenza virus hemagglutinin cargo protein in epithelial Madin-Darby canine kidney cells. *Molecular Biology of the Cell*. 12:1869-83.

Puertollano, R., P.A. Randazzo, J.F. Presley, L.M. Hartnell, and J.S. Bonifacino. 2001b. The GGAs promote ARF-dependent recruitment of clathrin to the TGN. *Cell*. 105:93-102.

Puri, V., R. Watanabe, R.D. Singh, M. Dominguez, J.C. Brown, C.L. Wheatley, D.L. Marks, and R.E. Pagano. 2001. Clathrin-dependent and -independent internalization of plasma membrane sphingolipids initiates two Golgi targeting pathways. *J Cell Biol*. 154:535-47.

Radhakrishnan, A., X.M. Li, R.E. Brown, and H.M. McConnell. 2001. Stoichiometry of cholesterol-sphingomyelin condensed complexes in monolayers. *Biochim Biophys Acta*. 1511:1-6.

Rapoport, I., Y.C. Chen, P. Cupers, S.E. Shoelson, and T. Kirchhausen. 1998. Dileucine-based sorting signals bind to the beta chain of AP-1 at a site distinct and regulated differently from the tyrosine-based motif-binding site. *Embo J*. 17:2148-55.

Ren, X., A.G. Ostermeyer, L.T. Ramcharan, Y. Zeng, D.M. Lublin, and D.A. Brown. 2004. Conformational defects slow Golgi exit, block oligomerization, and reduce raft affinity of caveolin-1 mutant proteins. *Mol Biol Cell*. 15:4556-67.

Rindler, M.J., I.E. Ivanov, H. Plesken, E. Rodriguez-Boulan, and D.D. Sabatini. 1984. Viral glycoproteins destined for apical or basolateral plasma membrane domains traverse the same Golgi apparatus during their intracellular transport in doubly infected Madin-Darby canine kidney cells. *Journal of Cell Biology*. 98:1304-19.

Robinson, M.S., and J.S. Bonifacino. 2001. Adaptor-related proteins. *Curr Opin Cell Biol*. 13:444-53.

Rock, C.O., V. Fitzgerald, and F. Snyder. 1977. Properties of dihydroxyacetone phosphate acyltransferase in the harderian gland. *Journal of Biological Chemistry*. 252:6363-6.

Rodriguez-Boulan, E. 1983. Polarized assembly of enveloped viruses from cultured epithelial cells. *Methods Enzymol*. 98:486-501.

Rodriguez-Boulan, E., and A. Gonzalez. 1999. Glycans in post-Golgi apical targeting: sorting signals or structural props? *Trends Cell Biol*. 9:291-4.

Rodriguez-Boulan, E., A. Musch, and A. Le Bivic. 2004. Epithelial trafficking: new routes to familiar places. *Curr Opin Cell Biol*. 16:436-42.

Rodriguez-Boulan, E., and W.J. Nelson. 1989. Morphogenesis of the polarized epithelial cell phenotype. *Science*. 245:718-25.

Rog, T., and M. Pasenkiewicz-Gierula. 2004. Non-polar interactions between cholesterol and phospholipids: a molecular dynamics simulation study. *Biophys Chem*. 107:151-64.

Roth, M.G. 2004. Phosphoinositides in constitutive membrane traffic. *Physiol Rev*. 84:699-730.

Roth, M.G., R.W. Compans, L. Giusti, A.R. Davis, D.P. Nayak, M.J. Gething, and J. Sambrook. 1983. Influenza virus hemagglutinin expression is polarized in cells infected with recombinant SV40 viruses carrying cloned hemagglutinin DNA. *Cell*. 33:435-43.

Rothberg, K.G., J.E. Heuser, W.C. Donzell, Y.S. Ying, J.R. Glenney, and R.G. Anderson. 1992. Caveolin, a protein component of caveolae membrane coats. *Cell*. 68:673-82.

Rothman, J.E. 1994. Mechanisms of intracellular protein transport. *Nature*. 372:55-63.

Roush, D.L., C.J. Gottardi, H.Y. Naim, M.G. Roth, and M.J. Caplan. 1998. Tyrosine-based membrane protein sorting signals are differentially interpreted by polarized Madin-Darby canine kidney and LLC-PK1 epithelial cells. *J Biol Chem*. 273:26862-9.

Sabharanjak, S., and S. Mayor. 2004. Folate receptor endocytosis and trafficking. *Adv Drug Deliv Rev*. 56:1099-109.

Sankaram, M.B., and T.E. Thompson. 1990. Interaction of cholesterol with various glycerophospholipids and sphingomyelin. *Biochemistry*. 29:10670-5.

Schaeren-Wiemers, N., A. Bonnet, M. Erb, B. Erne, U. Bartsch, F. Kern, N. Mantei, D. Sherman, and U. Suter. 2004. The raft-associated protein MAL is required for maintenance of proper axon-glia interactions in the central nervous system. *J. Cell Biol*. 166:731-742.

Scheiffele, P., A. Rietveld, T. Wilk, and K. Simons. 1999. Influenza viruses select ordered lipid domains during budding from the plasma membrane. *J Biol Chem*. 274:2038-44.

Scheiffele, P., M.G. Roth, and K. Simons. 1997. Interaction of influenza virus haemagglutinin with sphingolipid-cholesterol membrane domains via its transmembrane domain. *EMBO J*. 16:5501-5508.

Scheiffele, P., P. Verkade, A.M. Fra, H. Virta, K. Simons, and E. Ikonen. 1998. Caveolin-1 and -2 in the exocytic pathway of MDCK cells. *J Cell Biol*. 140:795-806.

Scheinfeld, M.H., S. Matsuda, and L. D'Adamio. 2003. JNK-interacting protein-1 promotes transcription of Abeta protein precursor but not Abeta precursor-like proteins, mechanistically different than Fe65. *PNAS*. 100:1729-1734.

Schroeder, R.J., S.N. Ahmed, Y. Zhu, E. London, and D.A. Brown. 1998. Cholesterol and sphingolipid enhance the Triton X-100 insolubility of glycosylphosphatidylinositol-anchored proteins by promoting the formation of detergent-insoluble ordered membrane domains. *J Biol Chem*. 273:1150-7.

Schuck, S., M. Honsho, K. Ekroos, A. Shevchenko, and K. Simons. 2003. Resistance of cell membranes to different detergents. *PNAS*. 100:5795-5800.

Schulte, S., and W. Stoffel. 1993. Ceramide UDPgalactosyltransferase from myelinating rat brain: purification, cloning, and expression. *Proc Natl Acad Sci U S A*. 90:10265-9.

Schwarz, D.G., C.T. Griffin, E.A. Schneider, D. Yee, and T. Magnuson. 2002. Genetic Analysis of Sorting Nexins 1 and 2 Reveals a Redundant and Essential Function in Mice. *Mol. Biol. Cell.* 13:3588-3600.

Seaman, M.N., E.G. Marcusson, J.L. Cereghino, and S.D. Emr. 1997. Endosome to Golgi retrieval of the vacuolar protein sorting receptor, Vps10p, requires the function of the VPS29, VPS30, and VPS35 gene products. *J Cell Biol.* 137:79-92.

Seaman, M.N., J.M. McCaffery, and S.D. Emr. 1998. A membrane coat complex essential for endosome-to-Golgi retrograde transport in yeast. *J Cell Biol.* 142:665-81.

Seaman, M.N., and H.P. Williams. 2002. Identification of the functional domains of yeast sorting nexins Vps5p and Vps17p. *Mol Biol Cell.* 13:2826-40.

Senes, A., I. Ubarretxena-Belandia, and D.M. Engelman. 2001. The Calpha ---H...O hydrogen bond: a determinant of stability and specificity in transmembrane helix interactions. *Proceedings of the National Academy of Sciences of the United States of America*. 98:9056-61.

Sheets, E.D., G.M. Lee, R. Simson, and K. Jacobson. 1997. Transient confinement of a glycosylphosphatidylinositol-anchored protein in the plasma membrane. *Biochemistry*. 36:12449-58.

Shelly, M., Y. Mosesson, A. Citri, S. Lavi, Y. Zwang, N. Melamed-Book, B. Aroeti, and Y. Yarden. 2003. Polar expression of ErbB-2/HER2 in epithelia. Bimodal regulation by Lin-7. *Dev Cell.* 5:475-86.

Shvartsman, D.E., M. Kotler, R.D. Tall, M.G. Roth, and Y.I. Henis. 2003. Differently anchored influenza hemagglutinin mutants display distinct interaction dynamics with mutual rafts. *J. Cell Biol.* 163:879-888.

Simmen, T., S. Honing, A. Icking, R. Tikkanen, and W. Hunziker. 2002. AP-4 binds basolateral signals and participates in basolateral sorting in epithelial MDCK cells. *Nat Cell Biol.* 4:154-9.

Simons, K., and E. Ikonen. 1997. Functional rafts in cell membranes. *Nature*. 387:569-72.

Simons, K., and G. van Meer. 1988. Lipid sorting in epithelial cells. *Biochemistry*. 27:6197-202.

Simons, K., and W.L. Vaz. 2004. Model systems, lipid rafts, and cell membranes. *Annu Rev Biophys Biomol Struct*. 33:269-95.

Skibbens, J.E., M.G. Roth, and K.S. Matlin. 1989. Differential extractability of influenza virus hemagglutinin during intracellular transport in polarized epithelial cells and nonpolar fibroblasts. *Journal of Cell Biology*. 108:821-32.

Smart, E.J., Y.S. Ying, C. Mineo, and R.G. Anderson. 1995. A detergent-free method for purifying caveolae membrane from tissue culture cells. *Proc Natl Acad Sci U S A*. 92:10104-8.

Stegmann, T. 2000. Membrane fusion mechanisms: the influenza hemagglutinin paradigm and its implications for intracellular fusion. *Traffic*. 1:598-604.

Stein, M.-P., A. Wandinger-Ness, and T. Roitbak. 2002. Altered trafficking and epithelial cell polarity in disease. *Trends in Cell Biology*. 12:374-381.

Stockinger, W., B. Sailler, V. Strasser, B. Recheis, D. Fasching, L. Kahr, W.J. Schneider, and J. Nimpf. 2002a. The PX-domain protein SNX17 interacts with members of the LDL receptor family and modulates endocytosis of the LDL receptor. *EMBO J*. 21:4259-4267.

Stockinger, W., B. Sailler, V. Strasser, B. Recheis, D. Fasching, L. Kahr, W.J. Schneider, and J. Nimpf. 2002b. The PX-domain protein SNX17 interacts with members of the LDL receptor family and modulates endocytosis of the LDL receptor. *Embo J*. 21:4259-67.

Straley, K.S., and S.A. Green. 2000. Rapid transport of internalized P-selectin to late endosomes and the TGN: roles in regulating cell surface expression and recycling to secretory granules. *J Cell Biol*. 151:107-16.

Subczynski, W.K., and A. Kusumi. 2003. Dynamics of raft molecules in the cell and artificial membranes: approaches by pulse EPR spin labeling and single molecule optical microscopy. *Biochim Biophys Acta*. 1610:231-43.

Swanton, E., and N.J. Bulleid. 2003. Protein folding and translocation across the endoplasmic reticulum membrane. *Mol Membr Biol*. 20:99-104.

Takeda, M., G.P. Leser, C.J. Russell, and R.A. Lamb. 2003a. Influenza virus hemagglutinin concentrates in lipid raft microdomains for efficient viral fusion. *Proc Natl Acad Sci U S A*. 100:14610-7.

Takeda, T., H. Yamazaki, and M.G. Farquhar. 2003b. Identification of an apical sorting determinant in the cytoplasmic tail of megalin. *Am J Physiol Cell Physiol*. 284:C1105-13.

Tall, R.D., M.A. Alonso, and M.G. Roth. 2003. Features of influenza HA required for apical sorting differ from those required for association with DRMs or MAL. *Traffic*. 4:838-49.

Tatulian, S.A., and L.K. Tamm. 2000. Secondary structure, orientation, oligomerization, and lipid interactions of the transmembrane domain of influenza hemagglutinin. *Biochemistry*. 39:496-507.

Taylor, C.M., T. Coetzee, and S.E. Pfeiffer. 2002. Detergent-insoluble glycosphingolipid/cholesterol microdomains of the myelin membrane. *J Neurochem*. 81:993-1004.

Teasdale, R.D., D. Loci, F. Houghton, L. Karlsson, and P.A. Gleeson. 2001. A large family of endosome-localized proteins related to sorting nexin 1. *Biochem J*. 358:7-16.

Thomas, D.C., and M.G. Roth. 1994. The basolateral targeting signal in the cytoplasmic domain of glycoprotein G from vesicular stomatitis virus resembles a variety of intracellular targeting motifs related by primary sequence but having diverse targeting activities. *J Biol Chem*. 269:15732-9.

Trommsdorff, M., J.-P. Borg, B. Margolis, and J. Herz. 1998. Interaction of Cytosolic Adaptor Proteins with Neuronal Apolipoprotein E Receptors and the Amyloid Precursor Protein. *J. Biol. Chem*. 273:33556-33560.

Tycko, B., and F.R. Maxfield. 1982. Rapid acidification of endocytic vesicles containing alpha 2-macroglobulin. *Cell*. 28:643-51.

Ullrich, O., S. Reinsch, S. Urbe, M. Zerial, and R.G. Parton. 1996. Rab11 regulates recycling through the pericentriolar recycling endosome. *J Cell Biol*. 135:913-24.

van Balkom, B.W., M.P. Graat, M. van Raak, E. Hofman, P. van der Sluijs, and P.M. Deen. 2004. Role of cytoplasmic termini in sorting and shuttling of the aquaporin-2 water channel. *Am J Physiol Cell Physiol*. 286:C372-9.

van der Sluijs, P., M. Hull, P. Webster, P. Male, B. Goud, and I. Mellman. 1992. The small GTP-binding protein rab4 controls an early sorting event on the endocytic pathway. *Cell*. 70:729-40.

Van, I.S.C., O. Maier, J.M. Van Der Wouden, and D. Hoekstra. 2000. The subapical compartment and its role in intracellular trafficking and cell polarity. *J Cell Physiol*. 184:151-60.

van Meer, G. 1998. Lipids of the Golgi membrane. *Trends Cell Biol*. 8:29-33.

van Meer, G., and K. Simons. 1986. The function of tight junctions in maintaining differences in lipid composition between the apical and the basolateral cell surface domains of MDCK cells. *EMBO Journal*. 5:1455-64.

van Meer, G., and K. Simons. 1988. Lipid polarity and sorting in epithelial cells. *Journal of Cellular Biochemistry*. 36:51-8.

van Meer, G., E.H. Stelzer, R.W. Wijnaendts-van-Resandt, and K. Simons. 1987. Sorting of sphingolipids in epithelial (Madin-Darby canine kidney) cells. *Journal of Cell Biology*. 105:1623-35.

Vargas, G.A., and M. Von Zastrow. 2004. Identification of a novel endocytic recycling signal in the D1 dopamine receptor. *J Biol Chem*. 279:37461-9.

Verges, M., F. Luton, C. Gruber, F. Tiemann, L.G. Reinders, L. Huang, A.L. Burlingame, C.R. Haft, and K.E. Mostov. 2004. The mammalian retromer regulates transcytosis of the polymeric immunoglobulin receptor. *Nat Cell Biol*. 6:763-9.

Wandinger-Ness, A., M.K. Bennett, C. Antony, and K. Simons. 1990. Distinct transport vesicles mediate the delivery of plasma membrane proteins to the apical and basolateral domains of MDCK cells. *Journal of Cell Biology*. 111:987-1000.

Wang, E., P.S. Brown, B. Aroeti, S.J. Chapin, K.E. Mostov, and K.W. Dunn. 2000. Apical and basolateral endocytic pathways of MDCK cells meet in acidic common endosomes distinct from a nearly-neutral apical recycling endosome. *Traffic*. 1:480-93.

Warren, R.A., F.A. Green, and C.A. Enns. 1997. Saturation of the endocytic pathway for the transferrin receptor does not affect the endocytosis of the epidermal growth factor receptor. *J Biol Chem*. 272:2116-21.

Wiley, H.S., and P.M. Burke. 2001. Regulation of receptor tyrosine kinase signaling by endocytic trafficking. *Traffic*. 2:12-8.

Williams, R., T. Schluter, M.S. Roberts, P. Knauth, R. Bohnensack, D.F. Cutler. 2004. Sorting nexin 17 accelerates internalization yet retards degradation of P-selectin. *Mol Biol Cell*. 15:3095-105.

Willnow, T.E., J. Hilpert, S.A. Armstrong, A. Rohlmann, R.E. Hammer, D.K. Burns, and J. Herz. 1996. Defective forebrain development in mice lacking gp330/megalin. *Proc Natl Acad Sci U S A*. 93:8460-4.

Wilson, B.S., S.L. Steinberg, K. Liederman, J.R. Pfeiffer, Z. Surviladze, J. Zhang, L.E. Samelson, L.-h. Yang, P.G. Kotula, and J.M. Oliver. 2004. Markers for Detergent-resistant Lipid Rafts Occupy Distinct and Dynamic Domains in Native Membranes. *Mol. Biol. Cell*. 15:2580-2592.

Worby, C.A., and J.E. Dixon. 2002. Sorting out the cellular functions of sorting nexins. *Nat Rev Mol Cell Biol*. 3:919-31.

Zacchetti, D., J. Peranen, M. Murata, K. Fiedler, and K. Simons. 1995. VIP17/MAL, a proteolipid in apical transport vesicles. *FEBS Letters*. 377:465-9.

Zheng, G., D.R. Bachinsky, I. Stamenkovic, D.K. Strickland, D. Brown, G. Andres, and R.T. McCluskey. 1994. Organ distribution in rats of two members of the low-density

lipoprotein receptor gene family, gp330 and LRP/alpa 2MR, and the receptor-associated protein (RAP). *J Histochem Cytochem*. 42:531-42.

Zhong, Q., C.S. Lazar, H. Tronchere, T. Sato, T. Meerloo, M. Yeo, Z. Songyang, S.D. Emr, and G.N. Gill. 2002. Endosomal localization and function of sorting nexin 1. *Proc Natl Acad Sci U S A*. 99:6767-72.

Zhou, C.Z., I.L. de La Sierra-Gallay, S. Quevillon-Cheruel, B. Collinet, P. Minard, K. Blondeau, G. Henckes, R. Aufrere, N. Leulliot, M. Graille, I. Sorel, P. Savarin, F. de la Torre, A. Poupon, J. Janin, and H. van Tilbeurgh. 2003. Crystal structure of the yeast Phox homology (PX) domain protein Grd19p complexed to phosphatidylinositol-3-phosphate. *J Biol Chem*. 278:50371-6.

Zhou, F.X., H.J. Merianos, A.T. Brunger, and D.M. Engelman. 2001. Polar residues drive association of polyleucine transmembrane helices. *Proceedings of the National Academy of Sciences of the United States of America*. 98:2250-5.

Zhou, Q., J. Zhao, J.G. Stout, R.A. Luhm, T. Wiedmer, and P.J. Sims. 1997. Molecular cloning of human plasma membrane phospholipid scramblase. A protein mediating transbilayer movement of plasma membrane phospholipids. *J Biol Chem*. 272:18240-4.

Zurzolo, C., M.P. Lisanti, I.W. Caras, L. Nitsch, and E. Rodriguez-Boulan. 1993. Glycosylphosphatidylinositol-anchored proteins are preferentially targeted to the basolateral surface in Fischer rat thyroid epithelial cells. *J Cell Biol*. 121:1031-9.

VITAE

Renee Danielle Tall was born in Merrimack, New Hampshire, on June 6, 1974, the daughter of Carmine and Lucille Esposito. She attended Merrimack High School prior to obtaining her Bachelor of Science in Microbiology from the University of New Hampshire. Renee was a technical sales specialist at Active Organics in Lewisville, Texas before she attended the University of Texas Southwestern Medical Center at Dallas.

Permanent Address: 4205 North Hall Street, Number 205
Dallas, Texas 75219